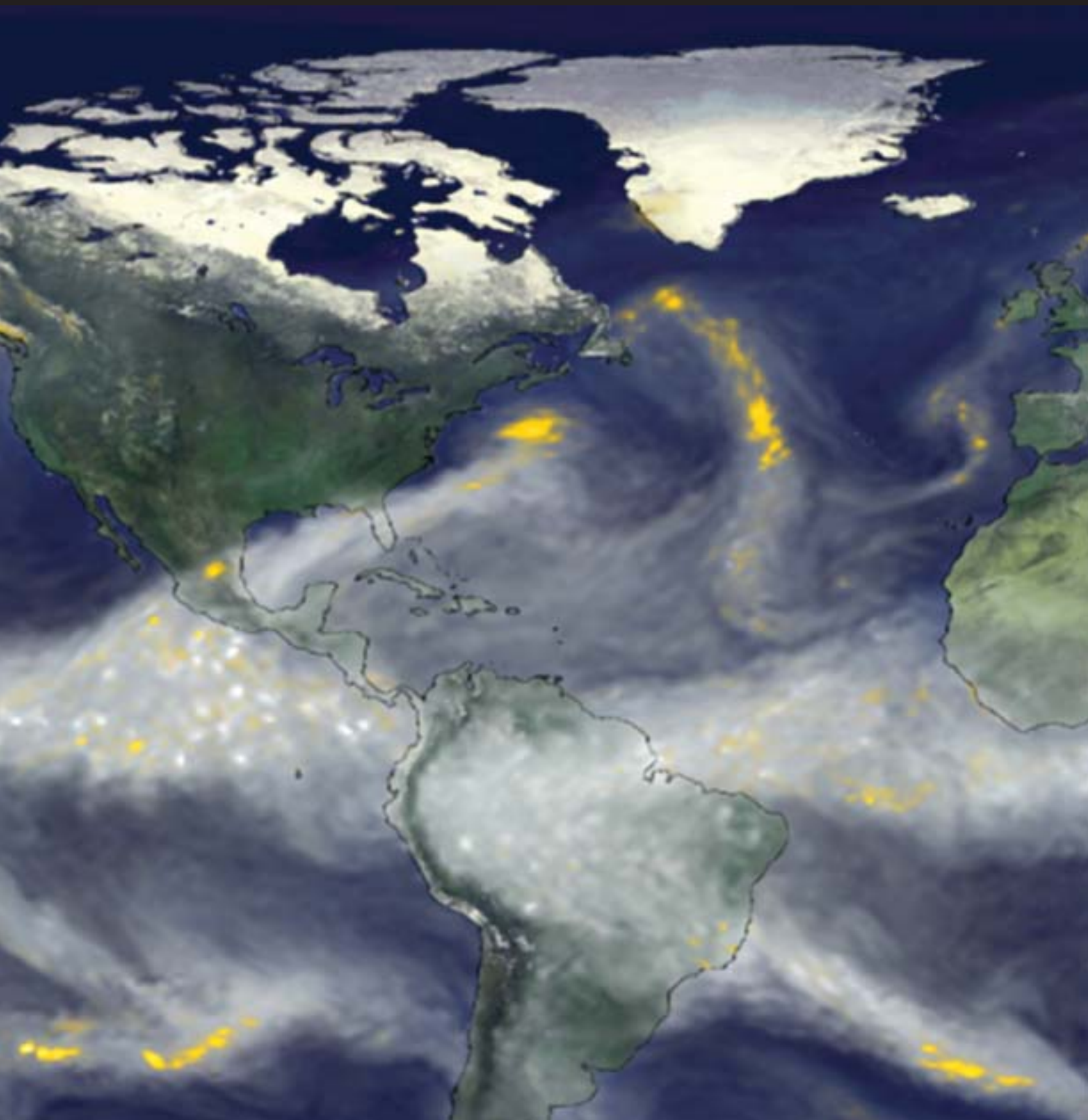
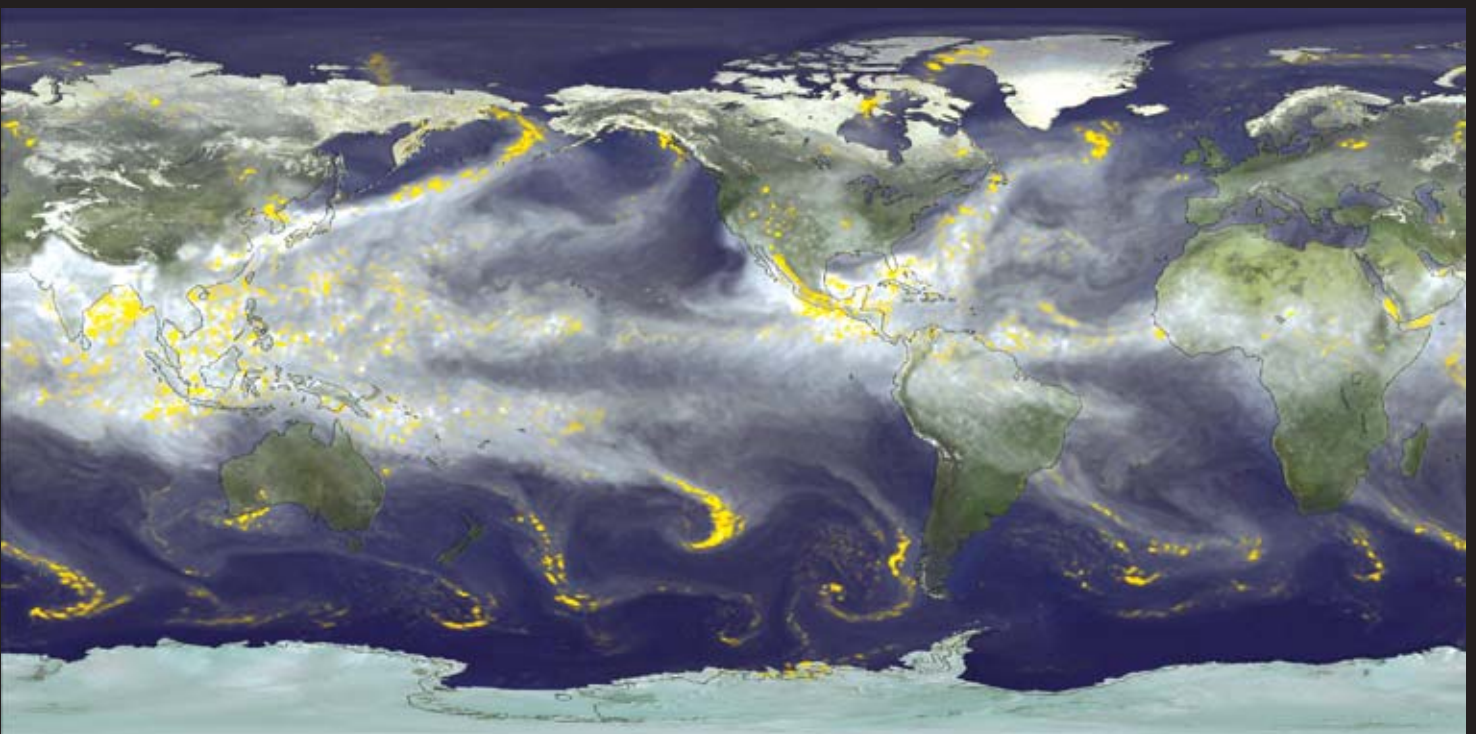
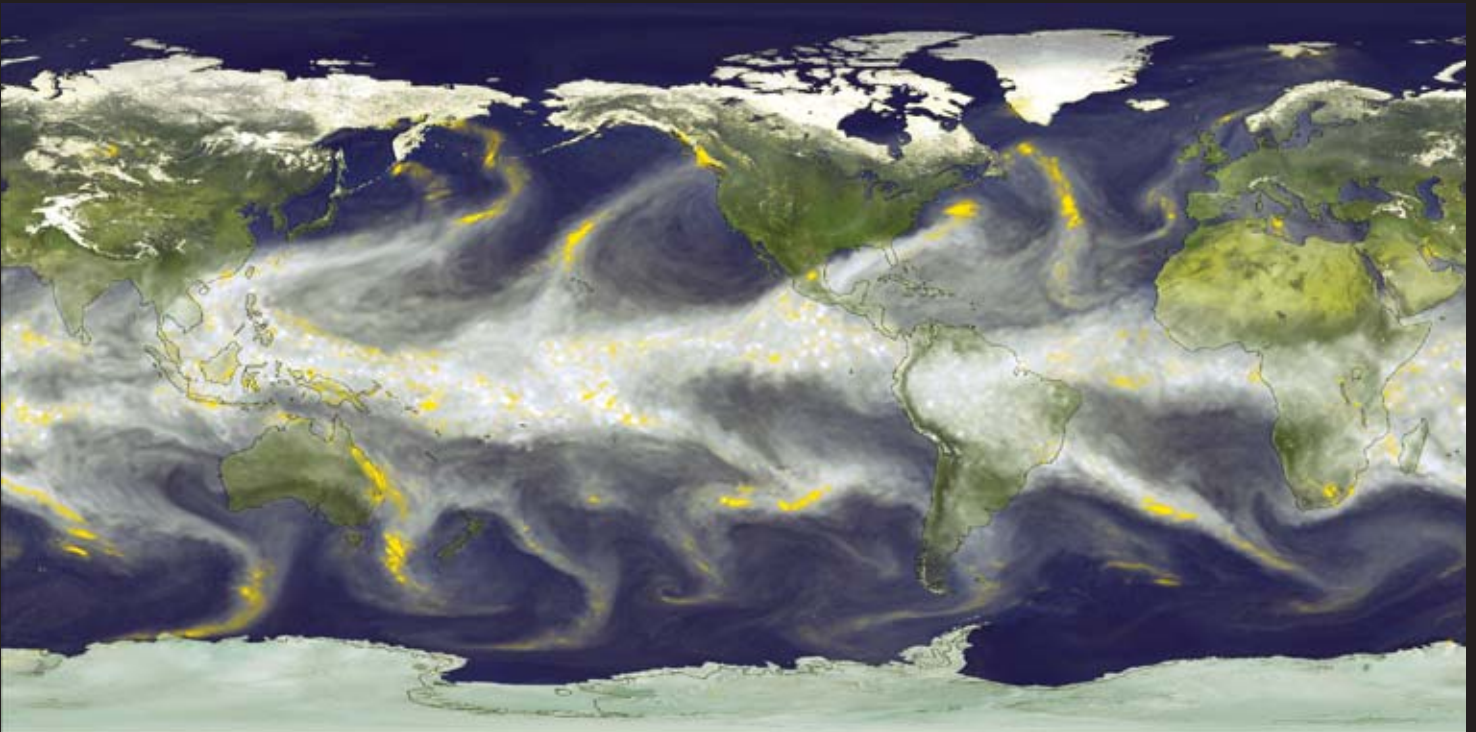


NASA Center for Computational Sciences



NCCS Highlights-FY 2000

Enabling NASA Earth and Space Science



The NASA Seasonal-to-Interannual Prediction Project (NSIPP) combined atmosphere and land system models to calculate the amount of precipitable water in the atmosphere as well as actual global precipitation. These water vapor maps depict precipitation results based on ocean temperature changes recorded during the 1997 El Niño (top) and 1998 La Niña (bottom).

Water vapor is plotted in the cloud-like structure; rainfall is plotted in yellow. Note that the central equatorial Pacific region features a great amount of water vapor during the El Niño phase and much less during La Niña. This decrease is the result of the drop in equatorial Pacific temperatures between the phases.



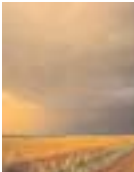

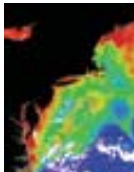
To produce the visualizations, NSIPP's coupled model system was run at four times its normal resolution. This configuration increased the required computational resources by a factor of 64.

NCCS Highlights FY 2000

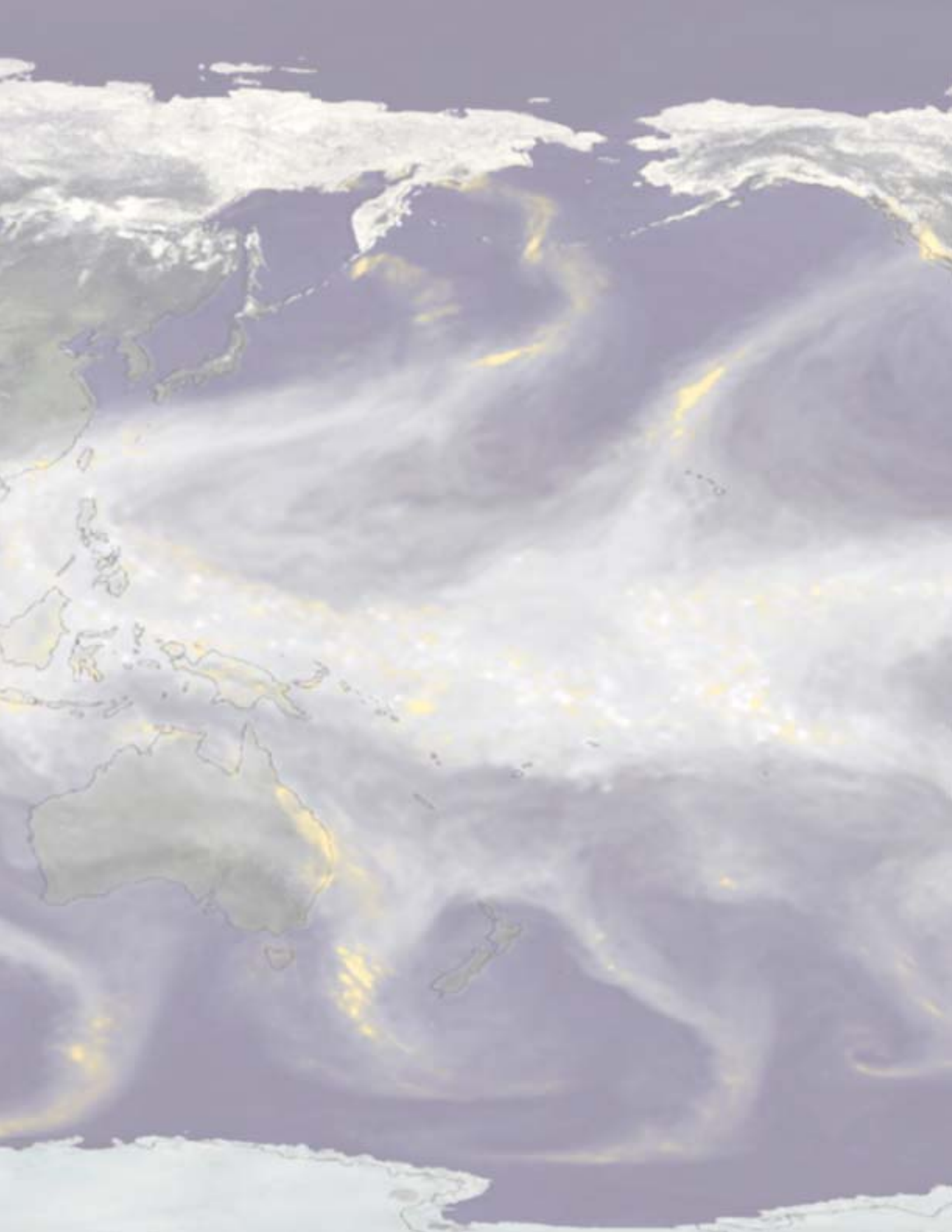
Enabling NASA Earth and Space Sciences

NASA Center for Computational Sciences

Contents

	Introduction	1
	NASA Center for Computational Sciences History and Resources	2
	The Finer Details Climate Modeling	12
	The Child's Tantrum El Niño Research Profile: The Origin of the El Niño-Southern Oscillation Joel Picaut, Eric Hackert, Antonio Busalacchi, Ragu Murtugudde, and Gary Lagerloef	18
	The Breath of Planet Earth Atmospheric Circulation Research Profile: Assimilation of Surface Wind Observations Robert Atlas, Stephen Bloom, and Joseph Otterman	26
	Slow and Steady Ocean Circulation Research Profile: The Influence of Sea Surface Height on Ocean Currents Sirpa Häkkinen	32
	Dust in the Sky Atmospheric Composition Research Profile: Modeling of Aerosol Optical Thickness Mian Chin, Paul Ginoux, Stefan Kinne, Omar Torres, Brent Holben, Bryan Duncan, Randall Martin, Jennifer Logan, Akiko Higurashi, and Teruyuki Nakajima	38

	The Ocean's Carbon Factory Ocean Composition Research Profile: The Growth Patterns of Phytoplankton Species Watson Gregg	46
	Rainfall Across the Globe Precipitation Research Profile: The Role of Landmass in Monsoon Development Winston Chao Research Profile: The Relationship Between Precipitation and Sea Surface Temperature on Decadal Time Scales Siegfried Schubert, Max Suarez, and Philip Pegion	56
	Under the Weather Space Weather Research Profile: The Magnetic Field of the Heliosphere Aaron Roberts and Melvyn Goldstein	66
	Burning in Outer Space Microgravity Research Profile: Simulation of Combustion in a Microgravity Environment Bernard Matkowsky and Anatoly Aldushin	72
	Feeling Gravity's Pull Gravity Modeling Research Profile: The Gravity Field of Mars Frank Lemoine, David Rowlands, Maria Zuber, G. Neumann, Douglas Chinn, and D. Pavlis	76
	NCCS FY2000 Research Projects and Principal Investigators	82
	Acronym List	90





Introduction

NASA has long recognized the close relationship between scientific research and advanced computational support. World-class research requires world-class computing capabilities. The NASA Center for Computational Sciences (NCCS) at Goddard Space Flight Center houses state-of-the-art computing technology and is a powerful resource for the scientific community.

The NCCS supports large-scale computing requirements of NASA Earth and space science research efforts, both at Goddard and across the NASA/university community. These research efforts span nearly the entire spectrum of Earth and space science research disciplines, including global weather, climate, geodynamics, upper atmospheres, oceans and ice, astrophysics, plasma physics, mesoscale processes, solar-terrestrial physics, planetary research, and microgravity. The diversity and complexity of these research efforts make access to advanced computing technology critical.

Modeling is a central component of Earth and space science research. Improved models mean improved results. Computational resources are the limiting factor for improving the resolution and extending the time evolution and realism of existing models. Accompanying the need for computational power to support these advances is the need to merge vast quantities of space data with numerical models to improve accuracy and extend overall scientific understanding.

This document highlights the NCCS computational resources and how their use enabled exciting advances in Earth and space science research in FY2000.





The NCCS has been a leading capacity computing facility, providing a production environment and support resources to address the challenges facing the Earth and space sciences research community.

Hardware resources

The year 2000 marks a transition as the NCCS prepares to acquire next-generation systems that will significantly enhance the computing capacity. The NCCS mass storage capacity has continued to increase rapidly as we have migrated to denser and faster media.

Computing

The NCCS primarily provides two types of computing architectures: vector and parallel supercomputing.

Vector supercomputing allows a single computer to process a large amount of data (vector) with a single instruction. The NCCS is committed to

maintaining and supplying some of the fastest vector machines possible for its users. The NCCS maintains a pair of 24-processor Cray SV1 supercomputers, each of which can perform up to 24 billion floating-point operations per second (GigaFLOPS). Most of the smaller research projects that use NCCS resources are assigned to these systems. Long-standing software that has not been modified to take advantage of parallel computing is best suited for these computers, which provide large shared-memories. However, the SV1 systems provide for modest processing capability.

Specifications: Cray SV1 systems

- 8 gigabytes (GB) of main memory
- 7.6 terabytes (TB) of compressed disk storage (5 TB uncompressed)
- 24 GigaFLOPS
- A pair of StorageTek (STK) Automated Cartridge System tape drive silos

HISTORY

1960s and 1970s



Goddard has a long history of providing the most powerful computing available to its science community. This computing power began with the introduction of Goddard's first scientific processor, an IBM 7090, in 1960. The IBM 7090 was followed by its successor, the IBM 360/91, in the late 1960s. As the computer hardware evolved, so did the operating environment. Terminals ushered in a shift from boxes of cards to batch file systems.



- Eight STK Timberline 9490 cartridge tape drivers
- A Powderhorn Robot and a Wolfcreek Robot
- UNICOS 10.0.0.7 operating system
- Compilers for C, C++, and Fortran 90
- Libraries: BLAS, EISPACK, FISHPACK, HDF, IMSL, NAG, ODEPACK, and SLATEC
- Utilities: FLINT, prof, perfrace, hpm, atexpert, and TotalView

Parallel computing architectures connect multiple processors within a single computer system. These processors collectively work on the same calculating task. The NCCS maintains a parallel-processing SGI Origin 2000, which primarily supports research at the Data Assimilation Office (DAO). The Origin 2000 allows programs to use all 64 processors and the entire memory to work on a single problem. The memory appears similar to the shared memory of the Cray.

Specifications: SGI Origin 2000

- 64 R12000 processors
- Cache-coherent Non Uniform Memory Access (ccNUMA) architecture
- 32 GB of main memory
- 1,559 GB of disk storage
- SGI Irix 6.5 operating system
- Compilers for C, C++, Fortran 77, and Fortran 90

In addition, the NCCS operates a large Cray T3E. The T3E is one of the world's most powerful parallel supercomputers. It can perform a staggering 778 billion floating-point calculations in a single second. Software that is designed to take full advantage of many processors and the short-term memory storage of a computer's cache can perform very well on the T3E.

The T3E is the workhorse of the NASA Seasonal-to-Interannual Prediction Project (NSIPP). The

HISTORY

Early 1980s

An IBM 3081 replaced the IBM 360/91. The interactive processing capabilities of the IBM 3081K literally added a new dimension to scientific investigations. By providing a full range of graphics tools and the means to access large databases, the computing center enabled scientists to analyze their data at individual terminals and workstations. Although a more convenient method for the scientists, this new technology required storage for larger volumes of on-line data.





NSIPP uses 1,000 of the T3E's 1,360 processors. The Grand Challenge Investigations program of NASA's Earth and Space Sciences Project uses the remaining processors.

Specifications: Cray T3E

- 1,360 processors
- 778 GigaFLOPS
- 170 GB of main memory
- 2,205 GB of disk storage

Mass data storage and delivery

Mass storage is the natural complement to performance computing because the output from some computer model simulations can be as large as a terabyte (TB), that is, 1 trillion bytes. Output of that size is routinely broken down into more manageable units for ease of retrieval, creating even more files.

Accommodating today's growing data storage needs is a top priority of the NCCS. Never

before has the science world produced such massive quantities of data. In FY 2000, more than 6 million files containing more than 150 TB of user data are under the control of the NCCS mass storage system. The mass storage system operates under a Sun E10000 server. Information stored on this system is organized by the UniTree Central File Manager.

UniTree is an intelligent hierarchical data archival system. It assigns data to one of several levels of storage media, depending on how often a particular piece of information is required. Initially, all data is recorded onto both magnetic disk and tape cartridge storage. Because of its quick loading speed, magnetic disk space is prioritized for information that is frequently accessed or updated. UniTree's disk cache has been expanded more than three times over, from 1.5 TB to 5 TB capacity. When space is needed on the magnetic disks, UniTree automatically erases information that has not been used recently. The information remains intact on tape cartridge, from which it can be retrieved when needed. To reduce the risk of data loss from tape cartridge

HISTORY

Mid to late 1980s



With the formation of a new directorate focusing on research in the Earth sciences, Goddard acquired a Control Data Corporation CYBER 205 vector supercomputer. This system supported more sophisticated, computationally intensive global models to simulate physical processes more realistically than ever before. The acquisition of the CYBER 205 marked a major shift from scalar computing into vector supercomputing. The center augmented the CYBER 205 with an ETA10 supercomputer in 1988.



failure, the NCCS provides duplicate data storage at a remote location.

Specifications: Sun E10000 server

- Disk cache of 5 TB
- 8 GB of memory
- 12 GB of system disk storage
- UniTree Central File Manager

Specifications: Tape Libraries

- 7 STK 9310 Powderhorn robotic storage silos
- An IBM 3494 robotic tape library

NCCS support services

The NCCS remains committed to staffing its support groups with highly qualified personnel who have backgrounds in information technology and scientific computing. During FY 2000, the NCCS made a significant effort to enhance the services it provides to the scientific user

community through user support, applications support, and systems support. The NCCS changed contractors, reorganized the support services, and increased the number of professionals experienced in high-end computing, numerical modeling, and system administration. The NCCS also extended the hours that customer service is available to users.

User support

The User Support Group functions include the user administration, technical assistance, and system accounting. The primary functions of this group are establishing user accounts on the

NCCS systems, providing general support on effective use of the systems, and tracking system utilization by the user community. User Support Group members work closely with the application and system support groups to respond to user requirements and problems.

NCCS users can contact the Technical Assistance Group (TAG) through e-mail, telephone, phone

HISTORY

Early 1990s

Acquisition of the Cray Research Cray Y-MP marked the next major increase in computational capability and the first time that direct access to the supercomputer was available. As computational power increased, the need for mass storage increased even more rapidly. This storage requirement led to the implementation of a separate mass storage subsystem.





mail, and the World Wide Web (WWW) to send questions and problem reports to the Help Desk. In FY 2000, the TAG received more than 650 requests for help-desk support. Typical questions concerned debugging and optimizing Fortran programs, using systems and applications software, solving input/output and media-related problems, backing up and restoring files, and using other installed utilities and NCCS facilities. When necessary, the TAG also develops new tools to provide the user community with improved or more efficient access to NCCS resources. Although the TAG team resolves most user issues, it can also refer user requests and reports to the applications support or system administration groups for resolution.

Most NCCS documentation is available to the user community through the NCCS WWW documentation server. This site provides general information about the NCCS and its resources, technical information about NCCS systems, system status information, news articles, and minutes of Computer Users Committee (CUC) meetings. Ensuring that this information remains

up-to-date and accurate is a major task for the TAG. The TAG has made significant improvements to both the navigation and content for the site and is committed to providing the best possible interface for the user community.

The NCCS User Administrator is often the first point of contact for outside users, providing assistance to NCCS division representatives, sponsors, and new users with questions, problems, comments, and suggestions. The User Administrator also processes requests from NASA Headquarters funding managers and from GSFC Directorate or Division funding personnel. Funding for a scientific research effort comes from NASA Headquarters or through a GSFC Directorate or Division, which authorizes the computing time. We are reviewing the user administration process to find ever more efficient ways to handle requests for NCCS resources, and we are beginning to develop a new web interface for adding and changing user information.

HISTORY

Early 1990s



A CONVEX mini-supercomputer and STK storage silos, each holding a TB of data, replaced the old mass storage units. This near-line storage was essential for holding the large amounts of data required for coupled land-ocean-atmosphere models.



The NCCS has also begun a total rewrite of the user accounting system to provide improved access to resource utilization information by users, sponsors, and the NCCS management. The new system will provide the potential for user and sponsor access to daily updates to the accounting information through the web, and the monthly accounting reports will be available electronically earlier than through the current hardcopy system. The new system can also adapt to new computing systems and business models quickly as the NCCS adds or upgrades resources or makes other changes that affect resource accounting.

Advanced software technology

Members of the Advanced Software Technology Group (ASTG) have advanced degrees in mathematics, physics, engineering, meteorology, or computer science. This expanded range of expertise is necessary because of the wide range of programming needs of today's NCCS user community. One of the biggest challenges in large-scale computing is optimizing the software

as major codes have migrated from the traditional vector supercomputing environment to scalable-parallel systems to take advantage of the newer architectures. The expert ASTG staff helps users convert vector codes to parallel codes, thereby improving the algorithm execution to make the best use of the NCCS systems. The ASTG has demonstrated the ability to adapt legacy code to newer algorithms and programming practices in use today.

The ASTG works collaboratively with the users to improve understanding of the requirements and to ensure that code improvements and optimizations are incorporated into production models, allowing users to accomplish more in less time. The NCCS offers one-on-one consulting through the ASTG to help major users optimize codes to run on either the NCCS vector systems or scalable-parallel systems. The goal is to allow scientists to complete their studies more rapidly than before and to increase the size of problems they can tackle. Over the past year, the ASTG has optimized and parallelized atmospheric, ocean, and space science codes and

HISTORY

Mid 1990s

The NCCS replaced the Cray Y-MP with a Cray C98. Installation of the Cray C98 marked the first time that the performance of 1 GigaFLOPS per processor was available. In 1995, the NCCS installed its first Cray J90 supercomputer.





has assisted with the conversion of Fortran 77 code to Fortran 90 to take advantage of the features and benefits of the newer Fortran standard.

In addition to working directly on codes, the ASTG enables users to enhance their skills and improve their own codes through participation in classes taught by the resident experts in the technology. The NCCS tailors its training services to support NCCS users during transitions to new hardware and software systems and to help them use NCCS resources most effectively. NCCS personnel regularly teach short classes on Fortran 90, OpenMP or MPI, and basic optimization. The NCCS has also offered other classes, such as awk and Regular Expressions, in response to the user community's needs. New classes are planned to address new systems, including "bring-your-own-code" classes with vendor experts.

The ASTG started a new initiative to develop a powerful software engineering tool (called qDoc) to aid users in the documentation of legacy Fortran code through "reverse engineering"

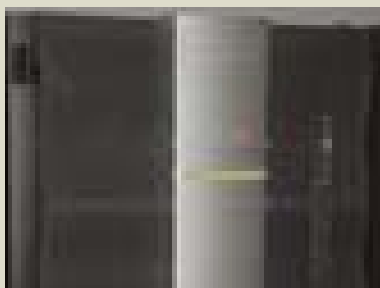
technology. The technology will provide the original source code, augmented with comments describing major functionality and made available in hypertext markup language (HTML) format with links to the documentation; a pop-up data dictionary describing the functions of variables, arrays, structures, and other major code objects; and a documentation-linked entity-relationship diagram. The NCCS is developing the qDoc tool for initial use on a major meteorological code. After demonstration of the tool's capability, qDoc will be made available for broader use.

System support

System support staff serve as administrators for the various machines, keeping them on-line and installing system upgrades when necessary. During the past year, the system administrators have completed several major operating system upgrades and have been actively involved in bringing new computing resources on-line in a stable operating configuration.

HISTORY

Mid 1990s



Even though the J90 processors were less powerful than the C98, the increased number of processors provided substantially more computing capacity. The NCCS mass storage subsystem was the largest such system in the world, with a data storage capacity of 38 TB.



Another significant function of the systems administrators is maintaining security. The focus of the NCCS security team is on the organizations and projects within the domain of the computing center and of related projects and facilities. The security team is part of a Goddard Center-wide security organization that benefits users and administrators in the NCCS and elsewhere. The NCCS makes its security experts available for consultation to other organizations within Goddard. The security team's chief challenge is finding a way to balance the need to build and maintain effective security with the need to provide public services to the users. An open Goddard network environment is essential to the productivity of the scientific community; however, protecting NCCS computing resources in this type of environment requires significant effort. The security team is continually evaluating and enhancing the NCCS network topology,

proactively monitoring the network, and maintaining intrusion detection efforts.

Computer Users Committee

The NCCS constantly strives to address the changing needs of its users and provide the best services and facilities. The NCCS CUC provides a forum for discussion of computer hardware and software, the way the computing and support services are being delivered, and plans for the future. The bimonthly meeting serves as a forum to obtain input from customers, promote communication between the NCCS staff and the user community, announce changes, and work to improve the facilities and their operation. The CUC meetings provide opportunities to address specific issues associated with the NCCS.

HISTORY

Late 1990s

The acquisition of the Cray T3E marked the next major shift from vector supercomputing to large-scale parallel computing. By using commodity processors with a high speed interconnect, this system provided the user community with both significant capability and capacity. The T3E was the platform for research in high-performance computing methods.





Preparing for the Future

The NCCS's commitment to provide exceptional computing resources to the scientific community will remain steadfast. We recognize that dependence on computational power for advances in scientific research is expected to increase dramatically in the 21st century. The NCCS continues to explore effective utilization of both scalable microprocessors and vector supercomputers. The era of the great observatories for both space and Earth sciences will increase the volume of observational data sets by orders of magnitude within the next decade. The NCCS is evaluating new technologies for mass storage to meet these demanding requirements.

As technology continues to change at a rapid pace, we will explore innovative ways to manage these changes effectively for our users. The combined modeling, data analysis, and data assimilation requirements for this era represent a formidable challenge to all aspects of NCCS support. The NCCS is prepared to meet this challenge and will continue its critical role in enabling cutting-edge science research well into the future.

HISTORY

Late 1990s



An SGI Origin 2000 provided a small parallel system with a shared memory architecture that is easier to program than the distributed memory architecture of the T3E. At the end of the 1990s, the J90s were upgraded to Cray SV1s, which returned performance to 1 GigaFLOPS per processor.

A satellite image of Earth from space, showing the Americas and surrounding oceans. The image is a curved view of the planet, with the Americas in the center. The oceans are a deep blue, and the landmasses are green and brown. White clouds are scattered across the scene. The title 'The Finer Details' is overlaid in white text.

The Finer Details

Climate
modeling
techniques
can increase
accuracy and
speed up
processing time



If you want to know whether you will need sunscreen or an umbrella for tomorrow's picnic, you can simply read the local weather report.

However, if you are calculating the impact of gas combustion on global temperatures, or anticipating next year's rainfall levels to set water conservation policy, you must conduct a more comprehensive investigation. Such complex matters require long-range modeling techniques that predict broad trends in climate development rather than day-to-day details.

Climate models are built from equations that calculate the progression of weather-related conditions over time. Based on the laws of physics, climate model equations have been developed to predict a number of environmental factors, for example:

- Amount of solar radiation that hits the Earth
- Varying proportions of gases that make up the air
- Temperature at the Earth's surface
- Circulation of ocean and wind currents
- Development of cloud cover

Numerical modeling of the climate can improve our understanding of both the past and the future. A model can confirm the accuracy of

environmental measurements taken in the past and can even fill in gaps in those records. In

Efficient and accurate climate modeling requires powerful computers that can process billions of mathematical calculations in a single second.

addition, by quantifying the relationship between different aspects of climate, scientists can estimate how a future change in one aspect may alter the rest of the world. For example, could an increase in the temperature of the Pacific Ocean somehow set off a drought on the other side of

the world? A computer simulation could lead to an answer for this and other questions.

Quantifying the chaotic, nonlinear activities that shape our climate is no easy matter. You cannot run these simulations on your desktop computer and expect results by the time you have finished checking your morning e-mail. Efficient and accurate climate modeling requires powerful computers that can process billions of mathematical calculations in a single second. The NCCS exists to provide this degree of vast computing capability.

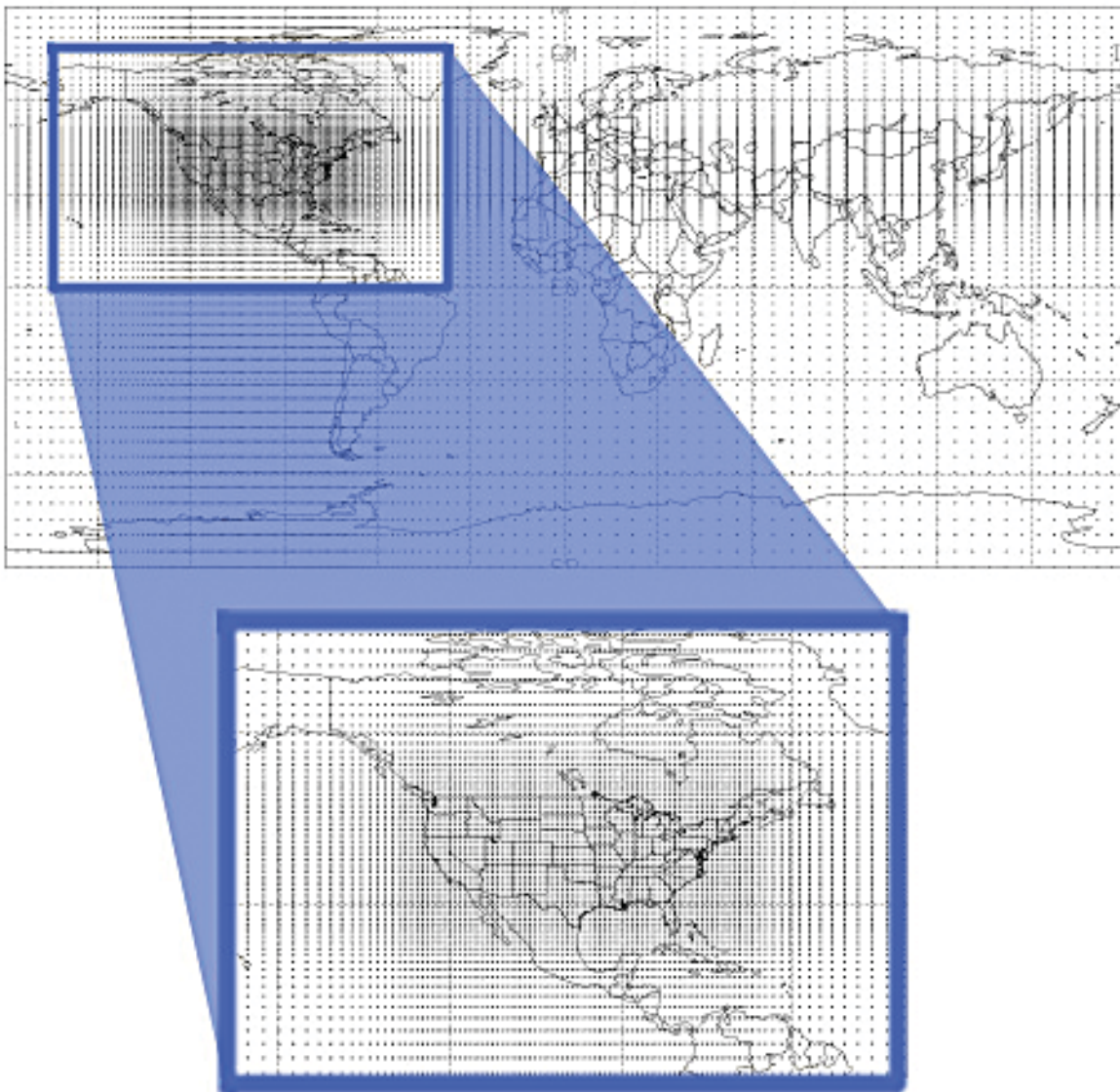
The challenge of accuracy

Why does a climate model need so much processing power? The answer lies not only in the sheer complexity of the equations but also in the number of times that the equations are performed to produce results that are as accurate as possible.



First, the model calculates each equation for numerous points throughout the physical area that it is designed to cover. An investigator defines a three-dimensional area in a grid of

points for the physical space that the climate model will cover. The grid is divided into layers for various altitudes within its vertical scale. It may cover an altitude as high as 60 kilometers



A stretched grid concentrates a climate model's calculation points in a specific area, reducing the amount of computation time spent outside that area. *Image credit: Michael Fox-Rabinovitz, NASA Goddard Space Flight Center, Data Assimilation Office*



Regional Modeling

Sometimes, a researcher wants to focus on a particular region, but a high-resolution global climate model would require extensive work for areas in which the researcher is not necessarily interested. If researchers could reduce or even eliminate this extra work, they could use the processing time they saved to increase the resolution for the area of interest.

Would it be possible to calculate only for the selected region and cut out the rest of the model? Perhaps, but doing so would ignore the interconnected nature of the world-wide global climate system. Therefore, the goal is to reduce unneeded processing and still record the influence of the entire environment on the selected region.

A nested grid can accomplish this goal. A *nested grid* is a low-resolution global model that contains another smaller, high-resolution grid. At each time step, the computer calculates first for the global grid. Because its resolution is low, it runs relatively quickly and provides just enough data to initialize the high-resolution grid that covers the smaller focus area.

One problem with the nested grid approach is that the connection between the two grids is not always perfect. Because of the difference in resolution, inaccuracies in the results, or *noise*, may result for the boundary layer where the grids meet. The noise can be “turned down” by adding special formulae, or *boundary schemes*, to the model equations. These schemes are designed to ease the sharp differences that may appear between grids that are drastically different in resolution.

On the other hand, a variable-resolution model does not require boundary schemes because it contains only a single stretched grid. Many of the calculation points are concentrated in a selected area, and the remaining points are stretched over the rest of the globe. This distribution reduces resolution and, thus, computing time for areas in which fine climate details are not required.



and divide the distance over dozens of *strata*, or layers.

Each level in the vertical scale contains points that vary in location by 1 to 3 degrees in latitude and longitude. The *resolution*, or number of calculation points, determines a model's accuracy. If the resolution is too low, some factors that influence the climate, such as cloud cover, may slip through the grid points and not be taken into account.

Researchers can increase the accuracy of a model by coupling it with models of other climate factors. This process employs algorithms to use one model's calculations as input to another model. A coupled climate model is more accurate because it takes into account the interrelated nature of our environment. For instance, warm sea surface temperatures (SSTs) can heat low-lying air and strengthen the flow of nearby wind currents. Depending on the extra models, coupling additional climate components may

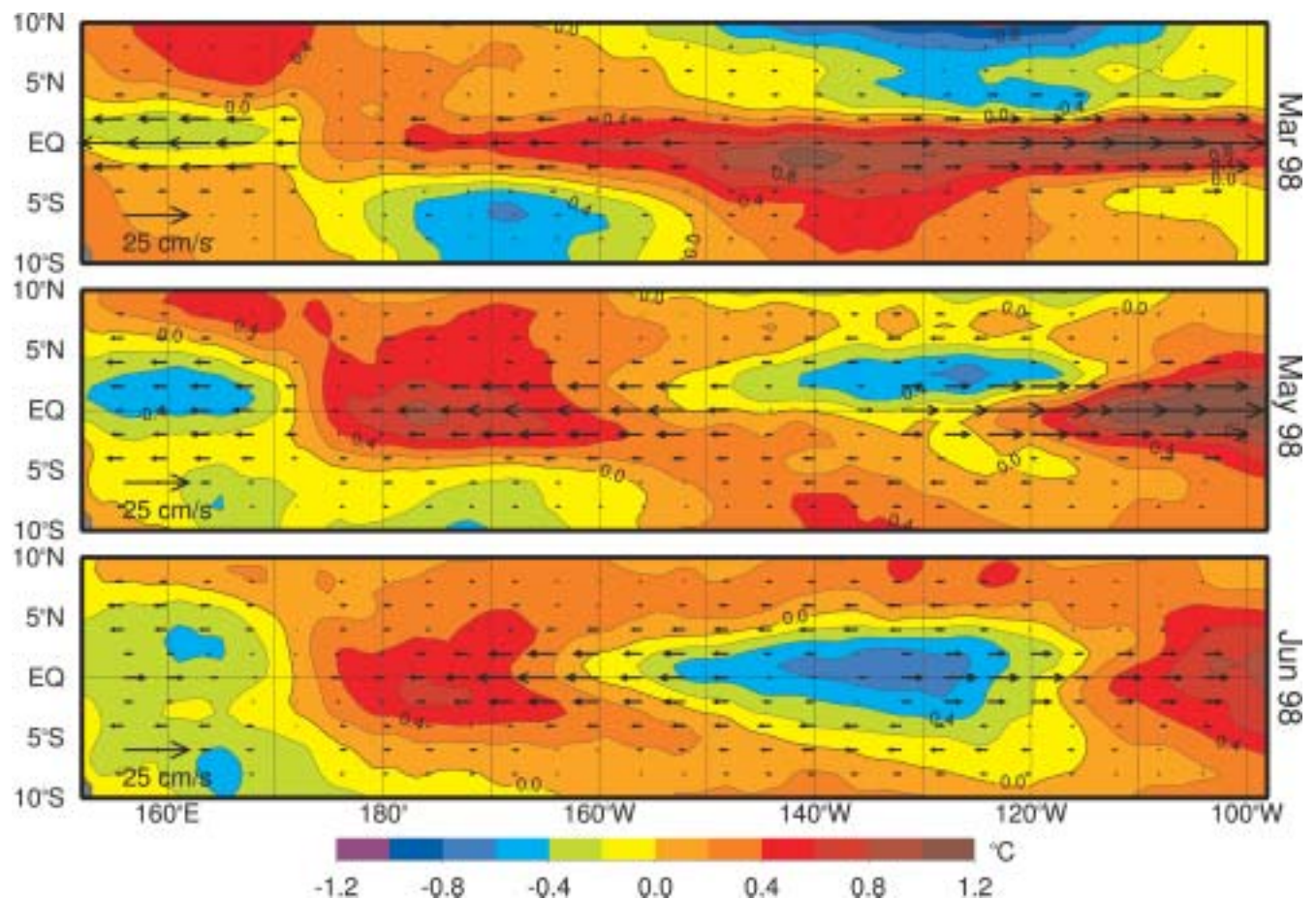
Obtaining a reliable climate solution at any particular moment in time may require many thousands of calculations.

increase the computational load by up to 10 times.

Data assimilation is another modeling task that typically requires powerful mathematical calculating capability. Assimilation entails the periodic input of observed climate measurement values into a sim-

ulation. Recordings such as SSTs taken on boats and remote sensing data from satellite readings can be assimilated into a climate model. The measurements provide a reality check for the simulation, and the new calculations can fill in any missing spots in the measurement data set.

Obtaining a reliable climate solution at any particular moment in time may require many thousands of calculations, and that is only the beginning. Results are generated for numerous time steps in a single run that can cover decades of time. Furthermore, an investigator will often repeat the entire run multiple times to verify the results.



A major challenge in studying climate progression is making sense of huge amounts of observational data. Through a complex series of mathematical operations known as a *multivariate empirical orthogonal function* (MEOF) analysis, major patterns of variation in the data can be isolated. This graph shows MEOF results for the movement of equatorial currents and ocean temperature changes during the 1998 La Niña phenomenon. Image credit: University of Maryland, Earth System Science Interdisciplinary Center (ESSIC)

The Child's Tantrum

El Niño brought the world's attention to climate modeling





In 1997, a child's tantrums caught the world's attention. These tantrums took the form not of crying and foot stamping, but of droughts and floods. Obviously, this was no ordinary child. It was, in fact, The Child, or *El Niño*, as it was named in the late 1800s by South American observers, who noted that its timing coincided with the Christmas holiday.

El Niño is a reversal in sea surface temperature (SST) distributions that occurs once every few years in the tropical Pacific. When it coincides with a cyclical shift in air pressure, known as the *Southern Oscillation*, normal weather patterns are drastically altered. The combined phenomenon is known as *El Niño-Southern Oscillation* (ENSO).

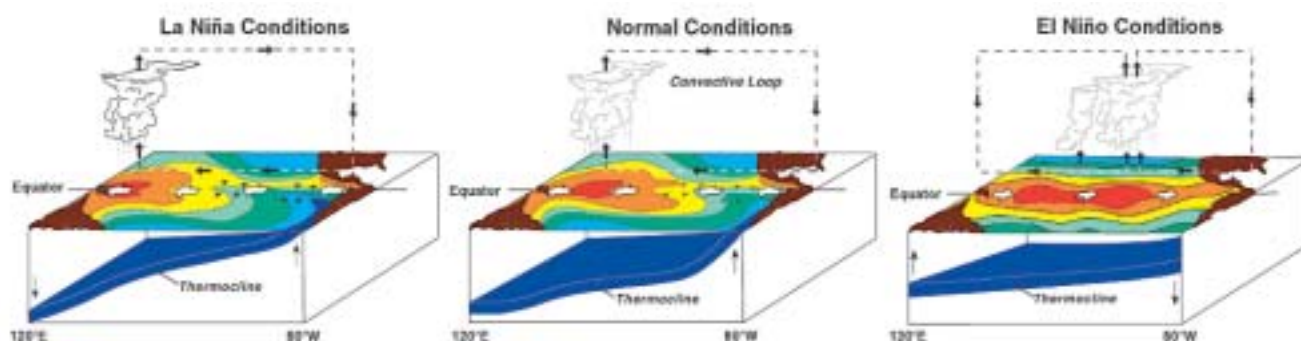
Although ENSO is a regular phenomenon, it was unusually strong in 1997. It produced heavy rainfall and floods in California and bestowed spring-like temperatures on the Midwest during the winter. These drastic changes in normal

weather patterns captured the public's imagination, from news reports to jokes on late-night talk shows.

Naturally, people wanted to know as much about El Niño as possible. Fortunately, scientists had at their disposal new satellites and ocean sensors that provided an unprecedented level of information. Consequently, not only was the 1997 ENSO the strongest in recent memory, but it was also the most thoroughly studied. Prominent groups such as the NASA Seasonal-to-Interannual Prediction Project (NSIPP) combined numerous aspects of climate modeling into a single, predictive endeavor.

What happens during El Niño?

Ocean surface temperatures rise and fall throughout the year. Normally, the Pacific waters remain warmer in the west than in the east. Heavier amounts of rainfall are associated with



The El Niño phenomenon pushes cold ocean water away from the surface in the eastern Pacific. In contrast, the La Niña phase brings the cold water up farther than usual near the South American coastline. These changes are evident in the shifting of the thermocline, the depth at which ocean water reaches its maximum temperature gradient. Image credit: National Oceanic and Atmospheric Administration (NOAA)/Pacific Marine Environmental Laboratory (PMEL)/Tropical Atmosphere Ocean (TAO) Project



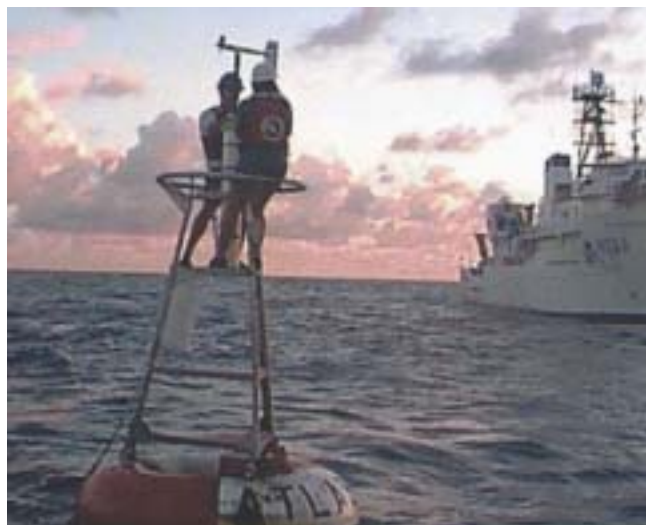
higher SSTs. Furthermore, air pressure over the eastern Pacific is normally higher than it is over the other side of the ocean during the winter months. This increased pressure keeps easterly winds (which start in the east and move west) close to the surface. The low air currents help push warm surface waters toward the west.

An upwelling of cold water from the eastern depths rises in response to this displacement. Meanwhile, the accumulation of heated waters in the west warms the atmosphere above. This heat affects the major jet streams that influence global weather.

Once every few years, however, air pressure decreases over the eastern Pacific and increases over the western Pacific. This change in air pressure reverses the direction of the Pacific winds, and warm water that normally would migrate westward remains near the coast of South America. Consequently, SSTs in the eastern Pacific are higher than usual. This reversal is the El Niño effect, and it normally lasts throughout the winter months.

During El Niño, heavy rainfall shifts from the Indian Ocean to the Atlantic. As a result, weather in Australia and Indonesia is drier than usual, whereas South America and the Gulf Coast of the United States get drenched.

A few years after the El Niño warming period, a cyclical cooling of the eastern Pacific waters follows. This event, known as *La Niña*, brings the



Sensors located on the buoys of the TAO array help keep track of the ocean's temperature. *Image credit: NOAA/PMEL/TAO Project*

SST of the eastern Pacific down below its normal levels. The combined El Niño/La Niña cycle typically spans 2 to 4 years.

How do we study El Niño?

The Tropical Ocean Global Atmosphere (TOGA) program has provided much of our ability to study El Niño. Begun in 1985, TOGA was an international effort to create instant observations and models of the ocean and atmosphere. TOGA used satellites to record the speed and direction of ocean and wind currents, the level of the ocean, and SSTs.

Another important component of TOGA was the Tropical Atmosphere Ocean (TAO) array, a set of 70 moorings that were positioned along the Equator across much of the Pacific. These moorings provided *in situ* (at-the-site) tempera-



ture recordings from the ocean surface to a depth of 500 meters. With these instruments, scientists were better able to detect the onset of El Niño.

Once scientists have collected the measurement data on the El Niño phenomenon, they must study and analyze this vast amount of information to make sense of it. NSIPP, a leader in this effort, focuses on studying climate patterns that span several months to a few years, such as ENSO.

NSIPP developed the Poseidon ocean general circulation model (GCM) as well as a number of ocean data assimilation systems. By combining these with an atmospheric GCM, NSIPP can use ocean measurement data to forecast future movement of warm and cool waters in the Pacific.

The NCCS has provided critical support that enabled NSIPP to piece together the El Niño puzzle. In 1997, the NCCS purchased a Cray T3E supercomputer and dedicated it to NSIPP's use. "Working with the NCCS to configure the T3E has really helped us," said Michele Rienecker, NSIPP's principal investigator.

References

Battisti, D. S., "Dynamics and thermodynamics of a warming event in a coupled tropical atmosphere-ocean model," *Journal of Atmospheric Sciences*, Vol. 45, 2889-2919, 1988

Changnon, S. A. (Ed.), *El Niño 1997-1998*, Oxford University Press, 2000

Neelin, J. D., "The slow-sea surface temperature mode and the fast-wave limit: Analytic theory for tropical interannual oscillations and experiments in a hybrid coupled model," *Journal of Atmospheric Sciences*, Vol. 48, 584-606, 1991

Picaut, J., Hackert, E., Busalacchi, A., Murtuguude, R., and Lagerloef, G., "Mechanisms of the 1997-1998 El Niño-La Niña, as inferred from space-based observations," *Journal of Geophysical Research*, Vol. 107, 2002

Picaut, J., Masia, F., and du Penhoat, Y., "An advective-reflective conceptual model for the oscillatory nature of the ENSO," *Science*, Vol. 277, 663-667, 1997

Schopf, P. S., and Suarez, M. J., "Vacillations in a coupled ocean-atmosphere model," *Journal of Atmospheric Sciences*, Vol. 45, 549-566, 1988

Weisberg, R. H., and Wang, Chunzai, "A western Pacific oscillator paradigm for the El Niño-Southern Oscillation," *Geophysical Research Letters*, Vol. 24, 779-782, 1997

Wilks, D. S., *Statistical Methods in the Atmospheric Sciences*, Academic Press, 1995

Wyrtki, K., "Water displacements in the Pacific and the genesis of El Niño cycles," *Journal of Geophysical Research*, Vol. 90, 7129-7132, 1985



Research Profile: The Origin of the El Niño-Southern Oscillation

Investigators:

Joel Picaut, Institute for Research and Development (IRD), Laboratory for the Space-Based Study of Geophysics and Oceanography (LEGOS); Eric Hackert, Antonio Busalacchi, and Ragu Murtugudde, Earth System Science Interdisciplinary Center (ESSIC), University of Maryland; Gary Lagerloef, Earth and Space Research

Using the resources of the NCCS, this cooperative research project analyzed data sets for the 1997-1998 El Niño event. The NCCS computers performed complex calculations in single-processor mode to draw recognizable patterns from an enormous amount of data. From this examination, the researchers described the preconditioning, onset, and growth of the El Niño event, as well as its faster-than-usual transition to the La Niña phase. By comparing these observations with current theories on the origin and operation of ENSO, the researchers produced new insight into this global weather phenomenon.

Gary Lagerloef, from the Earth and Space Research organization, provided the statistical model that calculated the ocean currents. Lagerloef's model used wind data from satellite-based microwave sensors as well as ocean-level recordings from the TOPEX/POSEIDON satellite array to determine how the sea level and winds shape the movement of the seas.

The movement of an imaginary marker called a *hypothetical drifter* is tracked through the use of currents. The drifter highlights strong Pacific currents that pushed the eastern end of the

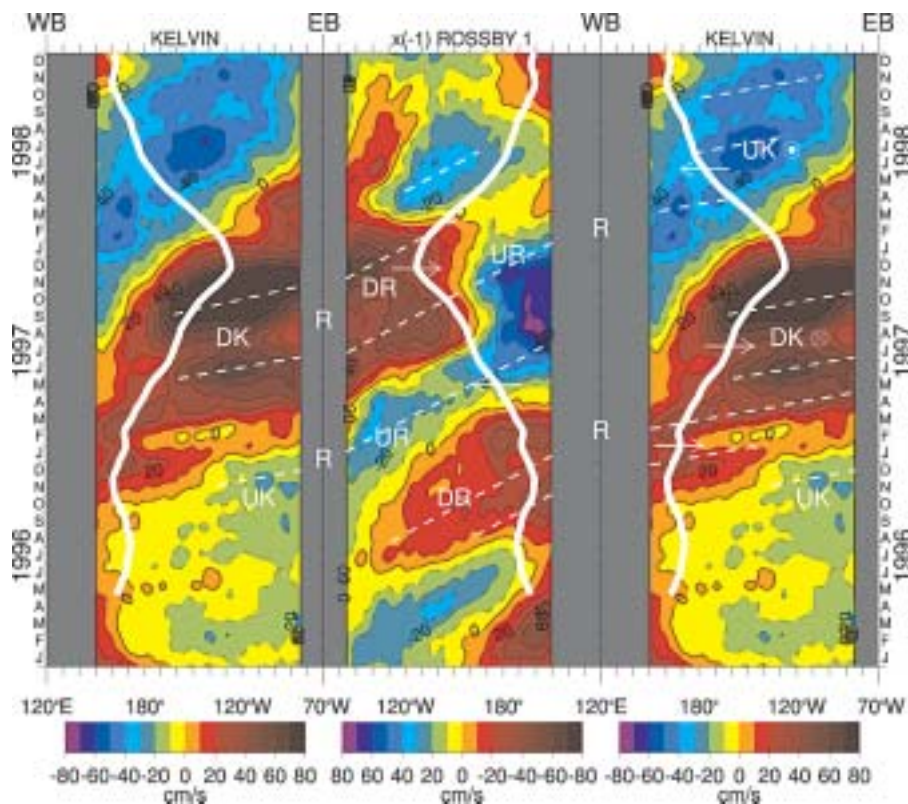
warm pool during the 1997 El Niño. Tracing these temperature disparities enables researchers to see the influence of El Niño on the Pacific.

Once the research team determined the movement of wind and water, their next task was to detect patterns out of that massive collection of data. They accomplished this task through a *multivariate empirical orthogonal function* (MEOF), a complex mathematical analysis.

The first MEOF analysis grouped 19 percent of total data variance in a pattern that corresponded with the mature phase of ENSO. The second MEOF analysis drew out the onset of ENSO and accounted for 17 percent of total data variance. With these patterns of related data, the study shed light on several theories about how El Niño emerges and develops into La Niña.

The *recharge theory* states that for El Niño to start, warm water must accumulate in the western Pacific equatorial basin. The study confirmed this prerequisite feature.

Convergence zone theory explains that the shift between ENSO's warm and cold phases is related to the movement of the eastern edge of the western Pacific warm pool. As this edge



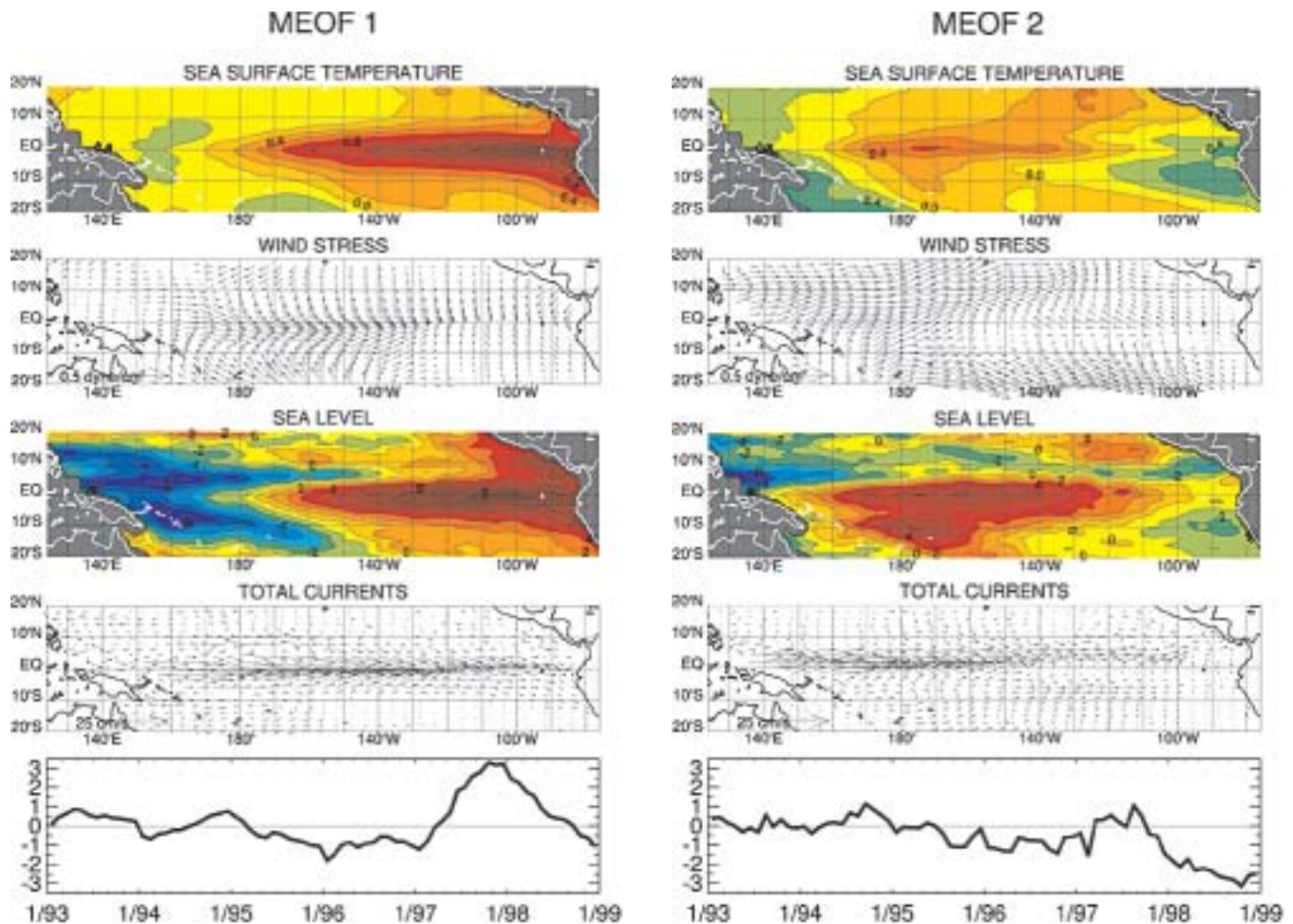
The speed of ocean currents is mapped out for the equatorial region (2 degrees N - 2 degrees S). The currents are divided into Kelvin and Rossby wave components. The path of a hypothetical drifter (shown in white) traces the shifting of the eastern edge of the warm ocean pool.

travels eastward and then westward, El Niño shifts into La Niña.

Although this theory was demonstrated at the beginning of the 1997 ENSO cycle, the return of the warm pool to the west did not seem to change the Pacific SST. Because of the strength of the 1997 El Niño, the SST along the Equator was already nearly constant. An additional source of cold water was required to initiate the move into La Niña.

The *delayed action oscillator theory* can explain this source of cold water. According to this theory, the rise of cold waters from the depths erodes El Niño warming in the east and moves the ENSO cycle into the La Niña phase. Equatorial Rossby waves and Kelvin waves, which are created by wind forcing and wave reflection, provide the mechanism for this transition.

Using space-based data alone, researchers identified the mechanism for the sudden transition of the El Niño to the La Niña. Results of a complex

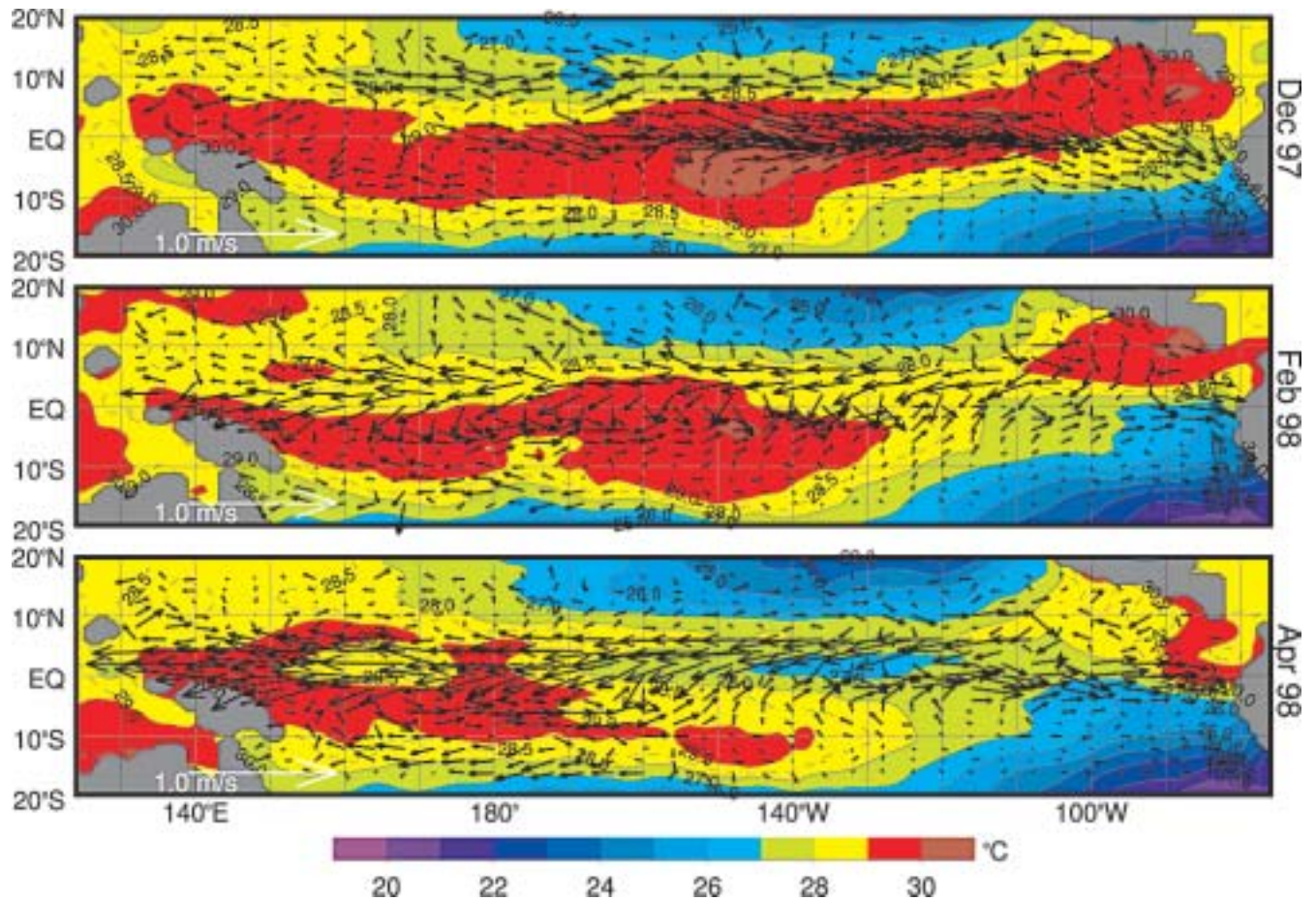


Two MEOF analyses extracted the main trends in the progression of the ENSO. Scientists follow these trends through measurements of SST, wind stress, sea surface height, and currents. The first analysis (left) shows the characteristic peak of the El Niño phase, which accounts for 19 percent of data variance. The second analysis (right) depicts the transition into La Niña, which accounts for 17.4 percent of data variance.

MEOF analysis show how Rossby waves pull currents to the east and Kelvin waves draw surface waters to the west, effectively separating warm surface waters and allowing cold water from below to surface.

This analysis confirmed the western Pacific oscillator conceptual model. This theory attributes

the beginning of La Niña to the lowering of the SST in the off-equatorial western Pacific during El Niño. This cold SST anomaly raises sea-level pressure, which, in turn, produces the easterly winds that slow El Niño and turn it into La Niña.



This map shows SST between December 1997 and April 1998. During the peak of El Niño in December, the warm pool stretches across the basin. By April, it mostly returns to the western Pacific Ocean. Some warm water remains in the east, providing the mechanism for a sudden shift to La Niña.

A satellite image of Earth showing a large, swirling hurricane over the ocean. The hurricane has a distinct eye and is surrounded by dense, white clouds. The ocean is a deep blue, and the surrounding landmasses are green. The text "The Breath of Planet Earth" is overlaid in large, bold, black letters. Below it, in smaller green letters, is the text "Aspects of climate drive the movement of wind across our planet".

The Breath of Planet Earth

Aspects of
climate drive
the movement
of wind across
our planet



Differences in air pressure are a major cause of atmospheric circulation. Because heat excites the movement of atoms, warm temperatures cause air molecules to expand. Because those molecules now occupy a larger space, the pressure that their weight exerts is decreased. Air from surrounding high-pressure areas is pushed toward the low-pressure areas, creating circulation.

This process causes a major pattern of global atmosphere movement known as *meridional circulation*. In this form of *convection*, or vertical air movement, heated equatorial air rises and travels through the upper atmosphere toward higher latitudes. Air just above the equator heads toward the North Pole, and air just below the equator moves southward. This air movement fills the gap created where increased air pressure pushes down cold air. The cold air moves along the surface back toward the equator, replacing the air masses that rise there.

Another influence on atmospheric circulation is the Coriolis force. Because of the Earth's rotation, large-scale wind currents move in the direction of this axial spin around low-pressure areas. Wind rotates counterclockwise in the Northern Hemisphere and clockwise in the Southern Hemisphere.

Just as the Earth's rotation affects airflow, so too does its surface. In the phenomenon of orographic lifting, elevated topographic features

such as mountain ranges lift air as it moves up their surface.

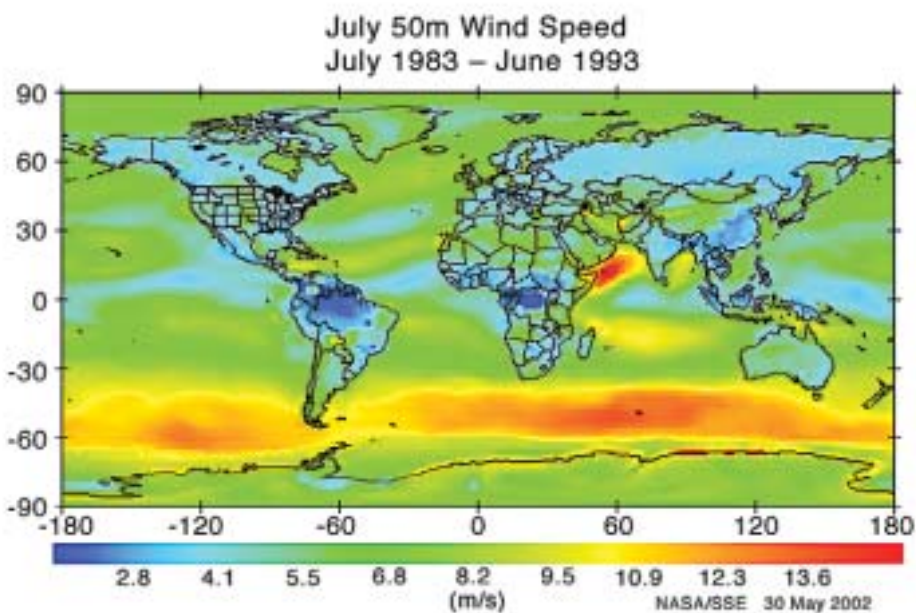
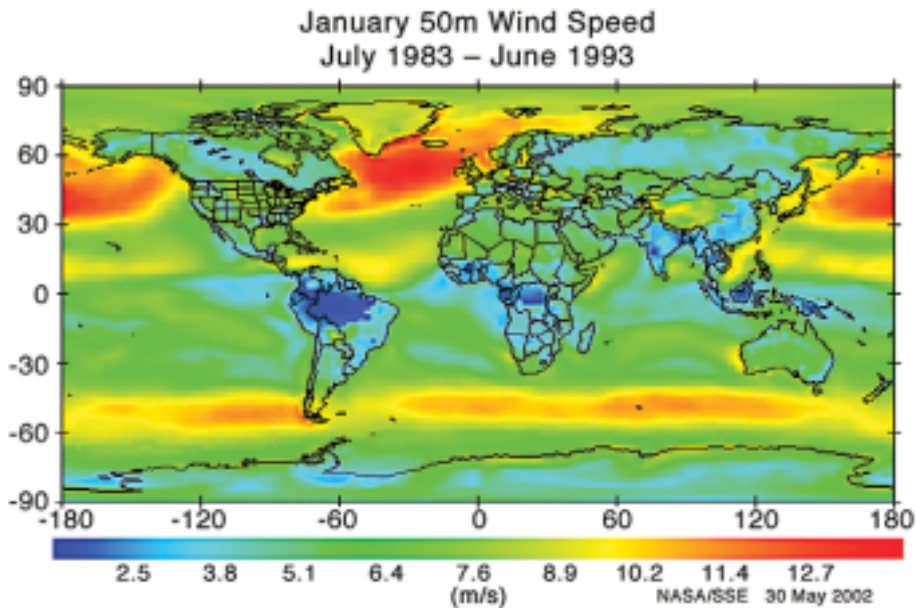
Atmospheric modeling

Scientists have developed numerical systems to quantify and predict the behavior of atmospheric winds. These systems are called *atmospheric general circulation models* (AGCMs). An AGCM has three major components:

- Equations that calculate the speed and direction of wind currents
- Parameterizations that estimate the values of other climate factors that can affect wind currents
- Boundary data that defines the physical grid points at which the model calculates atmospheric circulation



Clouds swirl around the high peaks of the Canary Islands. The influence of a land feature on atmospheric circulation is called an *orographic effect*. Image credit: SeaWiFS Project, NASA Goddard Space Flight Center, and ORBIMAGE



The measurements of satellite-borne sensors can be assimilated into records of monthly averaged wind speed. *Image credit: NASA Surface Meteorology and Solar Energy Project*

After calculating initial values for wind speed and direction at each grid point, an AGCM determines whether any condensation or clouds

are present. The presence of water or cloud cover is important because these things influence atmospheric temperature. For example, clouds



reflect sunlight away from the Earth, and raindrops scatter solar energy that passes through them.

Next, the AGCM produces temperature values for the grid points. As noted earlier, temperature affects air pressure, and air pressure differences drive circulation.

Finally, the model accounts for factors that may reduce the kinetic energy of wind movement. One such factor is the orographic effect of land topography, which creates a drag on surface winds.

Atmospheric observation

For years, scientists relied on weather balloons to carry the instruments that recorded wind speed and direction. Today, observations from orbiting satellites help scientists keep a direct eye on atmospheric circulation.

For example, an altimeter bounces radar pulses off the ocean surface. By analyzing the signal that is reflected back, an altimeter can determine various physical properties. Among those properties are the speed and direction of the wind that moves over the ocean. Generally, a smaller signal feedback indicates that the radar pulse was scattered in multiple directions. This result hints at a choppy sea surface and, therefore, high winds over the ocean.

A radiometer can derive information on wind near the ocean surface by recording the microwave emission of sunlight reflecting off the oceans. This measurement indicates the ocean's brightness temperature, or *apparent temperature*. The temperature is merely apparent because different factors can actually alter a microwave reading. For example, sea foam, which is likely to be caused by high winds, can increase a brightness temperature measurement.

In this process, multiple recordings must be taken over the same area at different angles. Atmospheric interference and other geophysical factors that can affect an ocean surface microwave reading must be taken out. For example, rain interferes with microwave readings and makes an ocean appear warmer than it actually is.

References

- Ikeda, M., and Dobson, F. W. (Eds.), *Oceanographic Applications of Remote Sensing*, CRC Press, 1995
- Trenberth, K. E. (Ed.), *Climate System Modeling*, Cambridge University Press, 1992
- Wentz, F. J., "Measurement of oceanic wind vector using satellite microwave radiometers," *IEEE Transactions on Geoscience and Remote Sensing*, Vol. 30, 960-972, 1992



Research Profile: Assimilation of Surface Wind Observations

Investigators:

Robert Atlas, Stephen Bloom, and Joseph Otterman, NASA Goddard Space Flight Center, Data Assimilation Office

The Data Assimilation Office (DAO) developed and tested several methods of assimilating microwave observations from satellites into high-resolution global grids of ocean surface wind data. These data sets were released for public use, and several scientific articles have made use of them.

This project used measurements from the Special Sensor Microwave/Imager (SSM/I) instrument, a satellite-based radiometer that records the microwave emission of sunlight as it is reflected off the ocean surface. The SSM/I indicates the ocean's brightness temperature, or apparent temperature. Brightness temperature is merely apparent because the roughness of the ocean surface can alter a microwave reading. This is how surface wind speed can be derived from microwave readings.

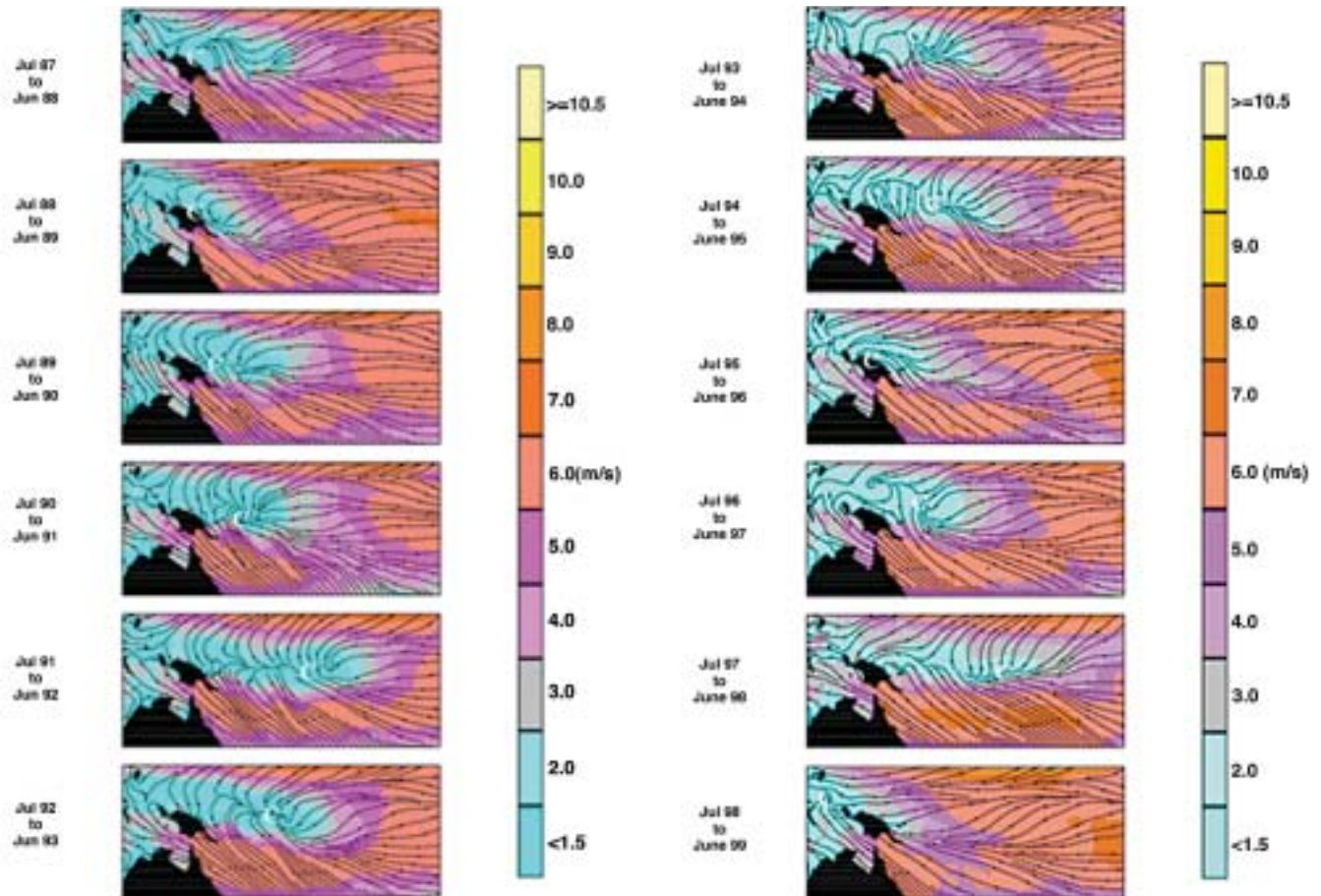
On their own, the SSM/I recordings indicate surface wind speed but not direction. To fill in the blanks, the DAO combined, or *assimilated*, the SSM/I data set with surface observations and analyses from the European Centre for Medium-Range Weather Forecasts (ECMWF).

The DAO researchers devised six different methods to filter together these measurement sets and generate wind direction vectors. They tested the results for each method using in situ

measurements, simulated surface winds, and the Seasat Scatterometer wind vector data set. Ultimately, the tests showed that a variational analysis method was the most accurate.

Once the DAO researchers had selected a filtering method, they applied it to process wind direction vectors for the SSM/I data set. For the period of July 1987 through December 1999, analyses were performed at 6-hour intervals. This amounted to more than 10,000 time steps for a 1-degree latitude by 1-degree longitude global grid. This data set is now available to the public through the Distributed Active Archive Center at the NASA Jet Propulsion Laboratory.

The DAO researchers then created more global grids of wind speed and direction by assimilating the SSM/I measurements with other data sets. One of these data sets was *gdas1*, in which the National Centers for Environmental Prediction (NCEP) merged climate recordings from numerous sources into a single set of meteorological fields. The final product of this effort was a global set of wind information that runs from July 1999 to the present. It is available via anonymous ftp to NASA investigators. Also in 2000, work began on the assimilation of wind speed data from the NCEP Reanalyses recordings into a climatological record for the years 1987-1999.

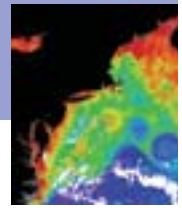


The SSM/I data set is used to map out the annual average streamline patterns over the surface of the western tropical Pacific region. The depicted area is an *intertropical convergence zone*, where trade winds from the Northern and Southern Hemispheres meet. The “C” represents the convergent vortex. It moves eastward during the warm phase of the ENSO cycle and then back west as the warm phase decays. To produce the SSM/I data set, the Data Assimilation Office used surface wind information from the ECMWF.



Slow and Steady

The ocean's natural resistance to changes in motion presents a unique modeling challenge



The study of ocean circulation is vital to understanding how our climate works. The movement of the ocean is closely linked to the progression of atmospheric motion. Winds close to sea level add momentum to ocean surface currents. At the same time, heat that is stored and transported by the ocean warms the atmosphere above and alters air pressure distribution. Therefore, any attempt to model climate variation accurately must include reliable calculations of ocean circulation.

Unlike movement of the atmosphere, movement of the ocean's waters takes place mostly near the surface. The major patterns of surface circulation form gigantic circular cells known as *gyres*. They are categorized according to their general location—equatorial, subtropical, subpolar, and polar—and may run across an entire ocean. The smaller-scale cell of ocean circulation is known as an *eddy*. Eddies are much more common than gyres and much more difficult to track in computer simulations of ocean currents.

What moves the ocean?

As mentioned earlier, atmospheric circulation and ocean circulation are closely linked. Both are governed by the distribution of momentum, heat, and moisture. For example, just as differences in air pressure push atmospheric circulation, differences in ocean density move water currents. Low temperatures and high *salinity* (the amount of salt in the water) increase the density

of a body of water, making cold, salty water sink below warmer water. Movement that is driven by density is called *thermohaline circulation*.

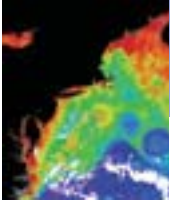
Despite some basic similarities in atmosphere and ocean movement, ocean circulation generally changes much more slowly than atmospheric circulation. Because water has a higher density than air, beginning or altering a current takes more momentum. Furthermore, the effect of heat lasts longer in ocean circulation than in atmospheric movement because water can contain far more thermal energy than air. In effect, the ocean has a longer “memory” of the climate’s influence on circulation than air does.

Modeling the ocean

Because observational data of ocean circulation is scarce, developing accurate ocean general circulation models (OGCMs) is important.

Unfortunately, the scarcity of measurements that can be assimilated into a model is a challenge to ocean modeling. Most measurements are limited to the surface and the Northern Hemisphere.

The complex characteristics of ocean flow present other modeling challenges as well. First, the small size of eddy currents makes their effect difficult to capture. In addition, an OGCM must incorporate salinity in its calculations. Furthermore, an OGCM must account for the slower rate of temperature changes in the deep ocean. One way to adjust a model for this phenomenon



Sea Surface Height

Another important aspect of ocean movement is sea surface height (SSH). SSH is a measure of the deviation of the vertical position of the sea surface relative to a known reference surface. Tracking the height of the ocean can provide an early warning of dramatic climate changes, such as the melting of polar ice sheets. Moreover, measuring SSH helps track other ocean characteristics, such as current velocity, because violently strong ocean currents create waves that change SSH.

Causes of sea-level variation include the following:

- Barotropic response to wind stress
- Changes as a result of heating and cooling (water expands when heated)
- Internal fluctuations of water density as a result of ocean currents
- Variations in geostrophic velocities caused by the Earth's rotation
- Melting ice from the polar caps

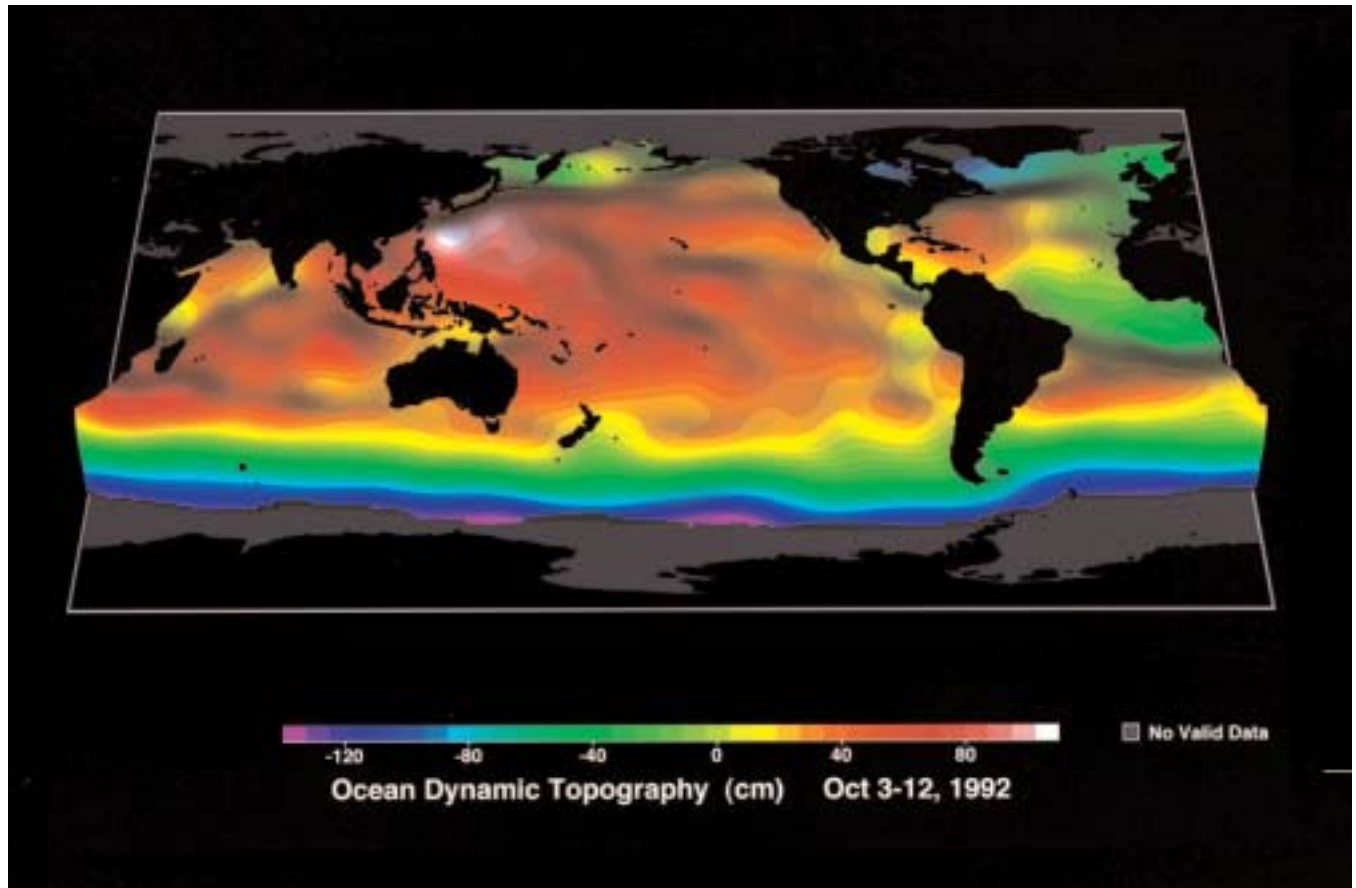
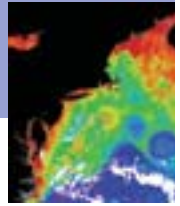
Satellite altimeters can make measurements of SSH. These measurements are compared to a reference surface such as the *oceanic geoid*, the shape of the Earth's surface under normal conditions.

is to alter the time step numerically for deep ocean calculations.

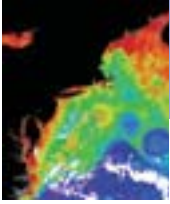
Trenberth, K. (Ed.), *Climate System Modeling*, University Press, 1992

References

Olson, D., "Ocean Circulation," *Encyclopedia of Earth System Science*, Vol. 3, Academic Press, 1992



Ocean topography data from satellite recordings can provide information on ocean circulation. *Image credit: NASA Jet Propulsion Laboratory*



Research Profile: The Influence of Sea Surface Height on Ocean Currents

Investigator:

Sirpa Häkkinen, NASA Goddard Space Flight Center, Oceans and Ice Branch

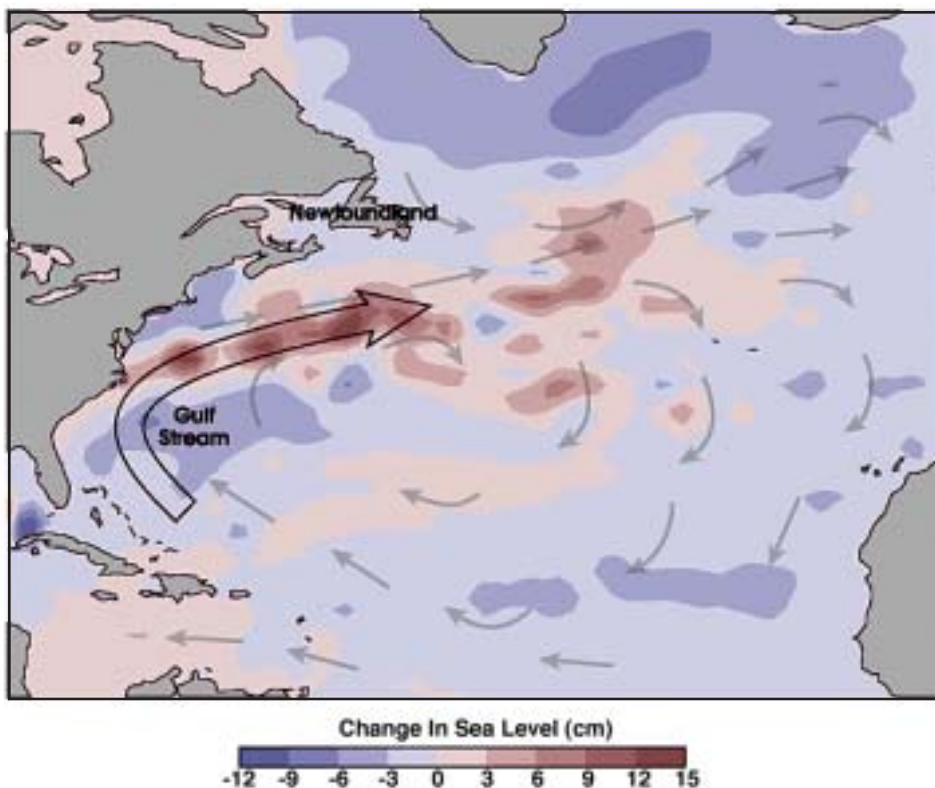
Häkkinen used the computing resources of the NCCS to study the connection between SSH and ocean circulation in the North Atlantic. She sought to determine which held the greater influence on SSH: basin-scale temperature changes or wind-driven currents.

In this research project, Häkkinen ran three simulations of SSH variation between the years 1951 and 1993 and one simulation between 1958 and 2000. The numerical grid covered the Arctic and

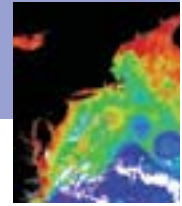
North Atlantic oceans, with a resolution of 0.7 by 0.9 degrees and 20 different coordinate levels.

“Clearly, simulation of 50 years...is not exactly nontrivial,” says Häkkinen. “Also, the (data) storage requirements are rather large because the analysis of this data has to be on-line always.”

The model computed the movement of heat through the oceans based on sea surface temperatures (SSTs), saturation humidity, air



Sirpa Häkkinen, a scientist at NASA Goddard Space Flight Center, ran computer models of SSH variation on an NCCS supercomputer. The results revealed a close association between SSH and the strength of overturning currents in the North Atlantic. The models also recorded a 12-centimeter drop in SSH between the winters of 1995 and 1996. “People have not wanted to believe that you can have these kinds of changes over a decadal time scale” said Häkkinen, “But in fact, very large changes can occur over decadal time scales.”



temperatures, and atmospheric humidity. Monthly climatology averages estimated the amount of cloud cover that influenced SST, as well as the effects of precipitation, evaporation, and river runoff on ocean height.

Each simulation assimilated different sets of actual SSH recordings to study the effects of different anomalies:

- Experiment 1 used anomalies in wind speed and temperature, as recorded by the Comprehensive Ocean Atmosphere Data Set (COADS).
- Experiment 2 used only the temperature anomalies from COADS.
- Experiment 3 used only the wind speed anomalies from COADS.
- Experiment 4 used anomalies in wind speed and temperature, as recorded by the National Centers for Environmental Prediction (NCEP)/National Center for Atmospheric Research (NCAR) Reanalysis data set.

Removing a type of anomaly from an experiment run and replacing it with monthly climatological averages enables the experimenter to observe closely the influence of the remaining anomaly type. Complete removal of an anomaly's effect is not possible, but the relative strength of one compared to the other is still evident.

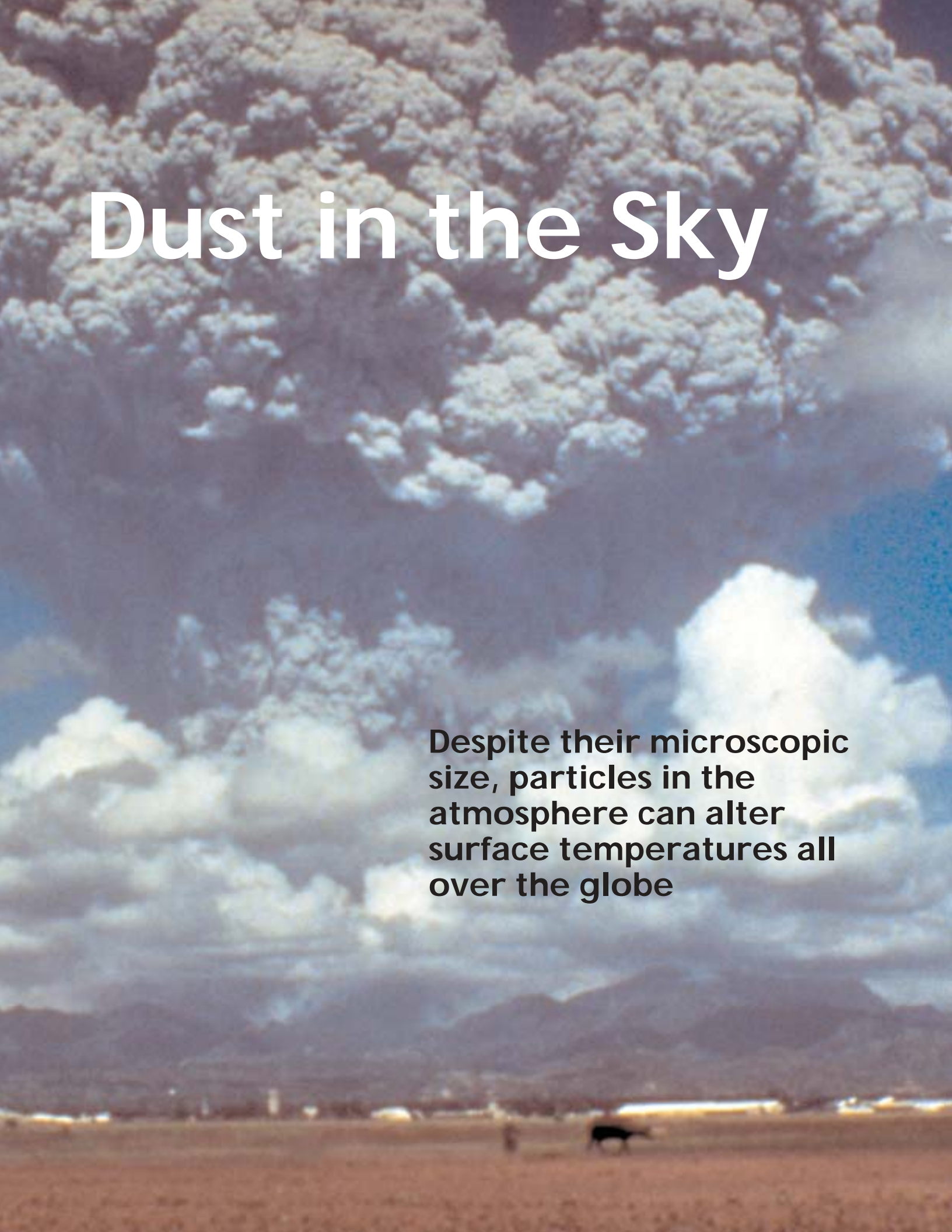
Häkkinen performed an empirical orthogonal function (EOF) analysis on the results of these SSH simulations. The EOF analysis organized the vast calculations of SSH change into recognizable trends, or orthogonal modes. Most of the simulated variation occurred along the Gulf Stream and North Atlantic Current. The main orthogonal mode also contained an opposing variation in SSH along the U.S. eastern seaboard and in the subpolar gyre.

According to the EOF analysis, the main cause of decadal variation in SSH and gyre circulation in the North Atlantic was basin-scale temperature changes rather than wind currents. The results from Experiment 2, in which only thermal recording anomalies were included in calculations, showed the strongest evidence of a decadal pattern of variation. The two orthogonal modes from Experiment 2, which was influenced by anomalies in ocean temperature, also had the most correlation when compared to the other simulation runs.

Next, this research effort determined the effect of meridional overturning. Meridional overturning is a major circulation pattern in which water flows either north or south away from the Equator, sinks when it cools, returns to the equatorial region, and then rises back to the ocean surface. This project determined whether meridional overturning in the Atlantic followed the same decadal pattern attached to the temperature variation in the Gulf Stream. In fact, heat changes in the Gulf Stream follow within 2 years of current speed changes in the meridional overturning at a latitude of 25° N.

Dust in the Sky

Despite their microscopic size, particles in the atmosphere can alter surface temperatures all over the globe





An *aerosol* is any small particle of matter that rests suspended in the atmosphere. Natural sources, such as deserts, create some aerosols; consumption of fossil fuels and industrial activity create other aerosols. All the microscopic aerosol particles add up to a large amount of material floating in the atmosphere. You can see the particles in the haze that floats over polluted cities.

Beyond this visible effect, aerosols can actually lower temperatures. They do this by blocking, or *scattering*, a portion of the sun's energy from reaching the surface. Because of this influence, scientists study the physical properties of atmospheric aerosols. Reliable numerical models for atmospheric aerosols play an important role in research.

Aerosol basics

For the most part, aerosols that scientists study reside in the *troposphere*, the portion of our atmosphere that lies between 15 and 45 kilometers above the surface. Particles remain at this altitude until they absorb enough moisture from the atmosphere and gain enough mass to sink back to the surface.

The following are the major types of aerosols:

- *Sulfate* is produced mostly from fuel combustion and industrial activity. Volcanic eruptions and the burning of biomass also produce sulfate.

- *Dust* is carried into the air from deserts and other dry plains.
- *Sea-salt*, like dust, is lifted from the ocean by wind. It does not remain in the air long before absorbing enough moisture to sink back down to the surface.
- *Organic carbon* (OC) and *black carbon* (BC) are created mostly from the burning of vegetation.

The distribution of aerosols varies by both location and season. For example, dust is usually the predominant aerosol type over the deserts of northern Africa. However, carbon aerosols are more common in this area during the winter months, when biomass burning is more common.

Aerosol optical thickness (AOT) is the primary measurement by which scientists determine the amount of aerosol material in the skies. It quantifies the amount of light, at a particular wavelength, that the aerosol is blocking at a specific location. The types of aerosols produced in an area, the ability of those aerosol particles to grow by absorbing moisture from the air, and the wind currents that carry aerosols are all factors that determine AOT.

Measurement of aerosols

Over the past 20 years, a number of space-based and ground-based monitoring programs have



The volcanic eruption of Mount Pinatubo hurled a tremendous amount of ash and other particles into the atmosphere over the Philippines. This aerosol layer is visible in the sunset photo (top), taken in August 1991, 1 month after Pinatubo's eruption. In comparison, a similar photo taken in August 1984 shows much less material in the sky. *Image credit: NASA Johnson Space Center*





monitored the level of aerosol material in the atmosphere:

- The Total Ozone Mapping Spectrometer (TOMS) program observes atmospheric aerosols, ozone, solar radiation reflected from the Earth, and ultraviolet radiation. The Atmospheric Chemistry and Dynamics Branch at the NASA Goddard Space Flight Center manages the TOMS program.
- The Advanced Very High Resolution Radiometer (AVHRR) scans the visible, infrared, and near-infrared spectrums. AVHRR is carried aboard the Television and Infrared Observation Satellite (TIROS)-N and operated by the National Ocean and Atmospheric Administration. Two methods are used to extract AOT from the AVHRR's radiation measurements.

- Unlike the previous satellite observing systems, the Aerosol Robotic Network (AERONET) is ground based. Sunphotometers record light at more than 100 locations around the world. The AERONET data collections are made of single-point recordings rather than global-scale ones.

Each of these measurement systems has limitations. Ground systems are limited to covering only areas where stations are located. Satellite systems can maintain a global range, but they do not provide as many details about specific aerosol types. Furthermore, light that is reflected off land may interfere with readings. Nevertheless, these measurement systems are useful for verifying the accuracy of numerical models.

Reference

Singh, H. B. (Ed.), *Composition, Chemistry, and Climate of the Atmosphere*, John Wiley & Sons, 1995



Research Profile: Modeling of Aerosol Optical Thickness

Investigators:

Mian Chin, Paul Ginoux, Stefan Kinne, Omar Torres, and Brent Holben, NASA Goddard Space Flight Center; Bryan Duncan, Randall Martin, and Jennifer Logan, Harvard University, Department of Earth and Planetary Studies; Akiko Higurashi, National Institute for Environmental Studies; and Teruyuki Nakajima, University of Tokyo, Center for Climate System Research

These researchers tested the accuracy of the Georgia Tech/Goddard Global Ozone Chemistry Aerosol Radiation and Transport (GOCART) model against observation records.

GOCART simulates AOT at the 500-nanometer (nm) wavelength for major types of tropospheric aerosols. These global calculations include a breakdown of AOT by altitude and aerosol type. The resolution grid of this model provided 8 to 10 times the detail of previous modeling attempts. Only supercomputing centers such as the NCCS can provide such fine detail in numerical simulations.

GOCART calculates AOT from the mass of aerosol material in a particular location, as well as from the aerosol's *mass extinction efficiency*, that is, a measurement of the ability of the aerosol to absorb or scatter light. Mass extinction efficiency depends on the type and size of the aerosol, as well as the amount of moisture that the aerosol has absorbed.

The scientists fed meteorological data on wind, temperature, pressure, humidity, cloud flux, and precipitation from 1990, 1996, and 1997 into the model. Scientists also used data on fuel

combustion from the Emission Database for Global Atmospheric Research (EDGAR).

The GOCART results noted that AOT was highest over northern Africa, where dust is normally the predominant aerosol type. A large plume of dust that blows over the Atlantic Ocean from Africa stands out in the graphs that depict AOT totals. Sulfate predominated over high-pollution areas such as eastern North America, Europe, and eastern Asia. Biomass burning made carbon the primary aerosol over Brazil, Africa, and southern Asia.

To identify the areas from which dust aerosols originate in the model, scientists used a new approach. The basic premise of this approach is that the depth of a nonflat, bare surface increases the likelihood of dust accumulation that wind can carry into the atmosphere. The new method has successfully located major dust sources in deserts and dried lake basins around the world.

A new biomass burning database was used to estimate the emission of black carbon, organic carbon, and other tracers from biomass burning activities. This new database was based on the location of fires recorded in satellite



observations. Therefore, the location, time, and amount of material released from biomass burning can be estimated much more effectively than ever before.

The scientists compared GOCART's results against measurement records from TOMS, AVHRR, and AERONET. Overall, the scientists report agreement within a factor of two. The correlation is closest in areas with high AOT and areas where a single aerosol type dominates.

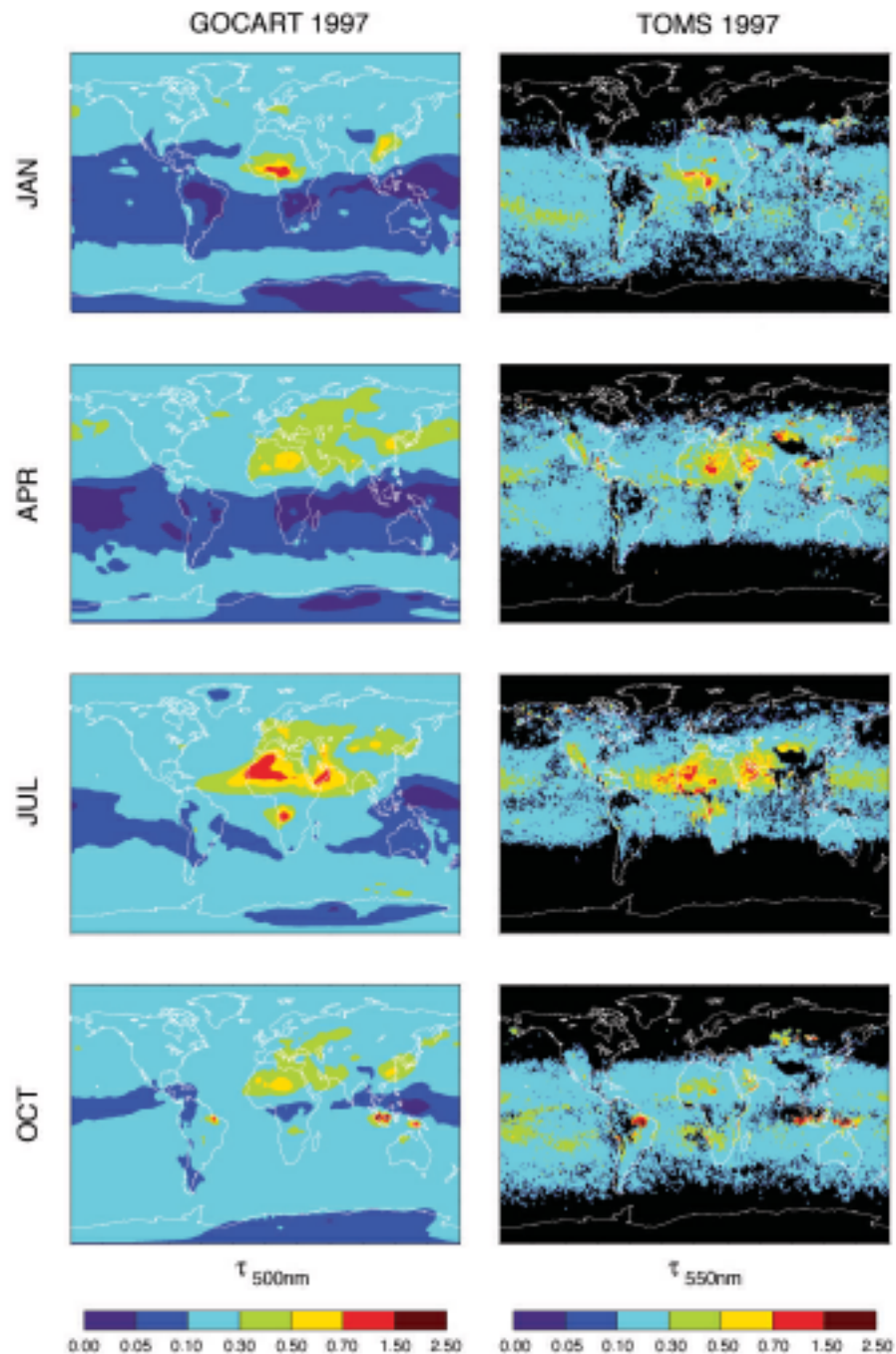
Outside these areas, interpreting model results is still difficult. For example, the model shows a sharp latitudinal drop-off in AOT over the oceans. In other words, the farther north or south from the Equator, the lower the AOT gets. However, this drop-off is not registered in the observation records.

Furthermore, the AERONET readings suggest that the model's set background level of dust is

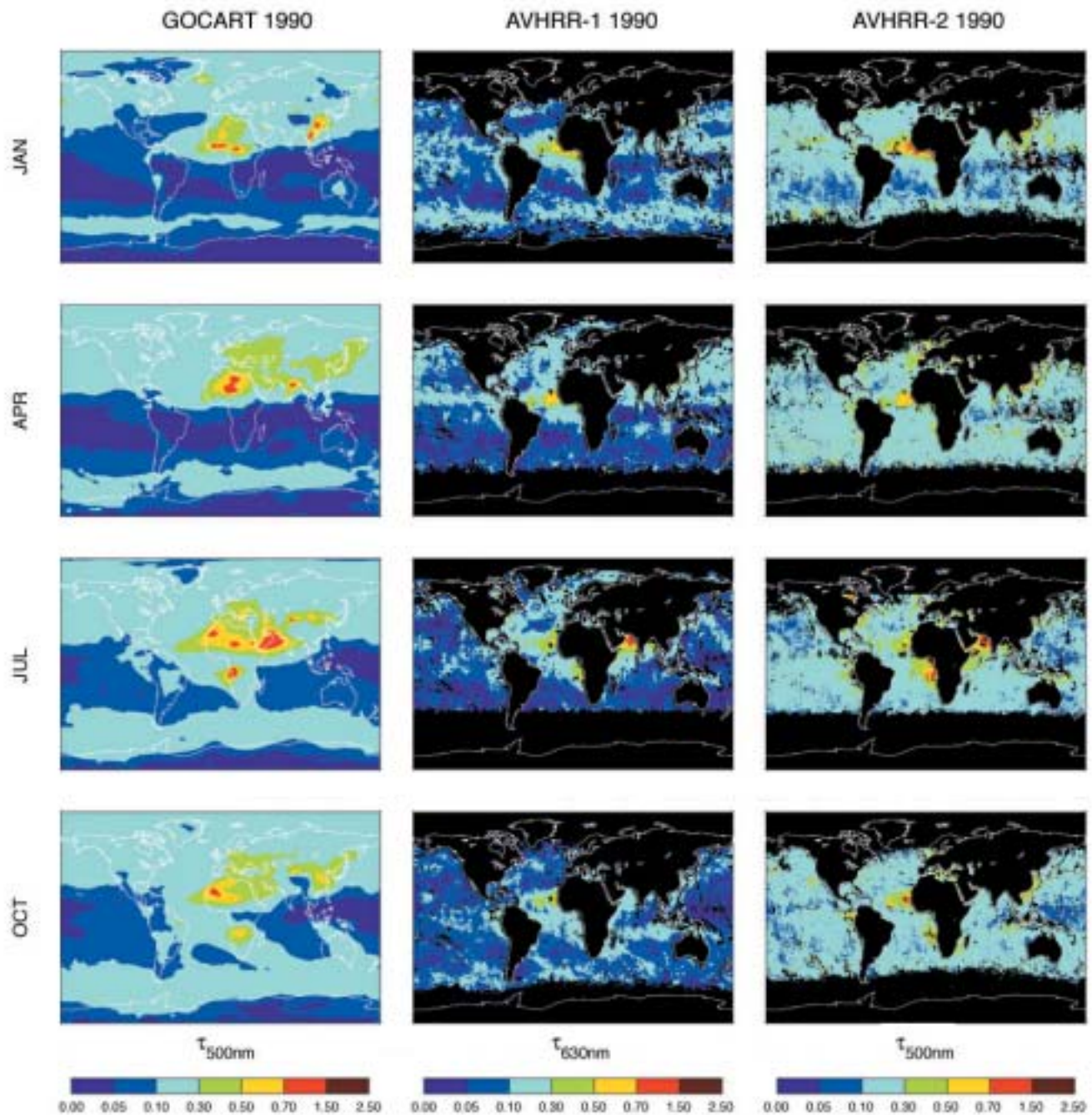
inaccurate. According to this comparison, the model may overestimate the AOT in areas with little aerosol matter and underestimate the AOT in areas with large amounts of aerosol matter.

One complication in this comparison stems from the manner in which the model or the satellite retrieval quantifies the physical properties of the aerosol types. The formulae that represent these properties are based on a limited number of measurements. For example, a constant value is assigned to the refractive index of dust, regardless of the kind of mineral that actually composes the dust.

In the end, the researchers concluded that more closely coordinated investigations among modeling, field experiments, and satellite retrieval would reduce the uncertainties in AOT modeling.



These data maps show the monthly composites of AOT measurements throughout 1997. The left column shows the calculations of the Georgia Tech/Goddard GOCART model; the right column displays the satellite retrievals from the TOMS. Both results place the highest AOT values over Africa, where vegetation is burned in the latter half of the year and desert dust blows over the Atlantic Ocean.



The GOCART calculations for AOT are compared to the measurements of the AVHRR for the year 1990. Researchers used two different techniques to retrieve measurements from the raw AVHRR data: one-channel and two-channel. Neither AVHRR retrieval produced readings over landmasses because the visible wavelengths that AVHRR measures are not reflected evenly by land.

A satellite image showing ocean chlorophyll concentrations. The image displays a large, dark blue area on the left, transitioning into a broad, light green band that curves along the coast of a landmass. The landmass itself is visible in shades of tan and brown on the right side of the image. The text "The Ocean's Carbon Factory" is overlaid in white on the upper left portion of the image.

The Ocean's Carbon Factory

Ocean chlorophyll is a vital part of the Earth's carbon cycle



According to biological data recorded by the Sea-Viewing Wide Field-of-View Sensor (SeaWiFS) satellite, the ocean contains nearly half of all the Earth's photosynthesis activity. Through photosynthesis, plant life forms use carbon from the atmosphere, and in return, plants produce the oxygen that life requires. In effect, ocean chlorophyll works like a factory, taking carbon and “manufacturing” the air we breathe.

Most ocean-bound photosynthesis is performed by single-celled plants called phytoplankton. “These things are so small,” according to Michael Behrenfeld, a researcher at NASA Goddard Space Flight Center, “that if you take hundreds of them and stack them end-to-end, the length of that stack is only the thickness of a penny.”

The humble phytoplankton species plays a vital role in balancing the amounts of oxygen and carbon dioxide in the atmosphere. Therefore, understanding exactly how phytoplankton growth works is important.

Major types of phytoplankton

Thousands of phytoplankton breeds exist. They differ in several ways:

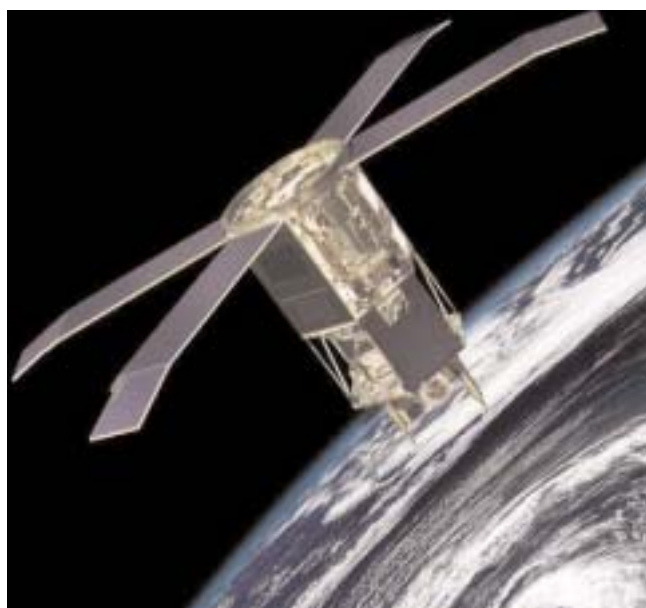
- Color
- Rate of growth
- What they feed on

- The portion of the light spectrum that they absorb most readily
- How quickly they sink after dying

Scientists use observations of these characteristics to distinguish phytoplankton in satellite recordings.

Common phytoplankton species include diatoms, picoplankton, and chlorophytes.

Diatoms grow quickly and, therefore, tend to dominate other phytoplankton species in areas with plentiful nutrients. On the other hand, they sink relatively quickly, so diatoms may link up in chains to slow their rate of descent. Diatoms require silica as well as nitrogen nutrients, and



The SeaWiFS satellite tracks the rate of photosynthesis across both land and ocean by measuring the color of light reflected off the Earth's surface. *Image Credit: SeaWiFS Project, NASA Goddard Space Flight Center, and ORBIMAGE*



the amount of iron in the ocean may also limit their growth.

Picoplankton are small, even compared to other phytoplankton. Because of their small size, they are nearly buoyant. Although they grow slowly, they recycle nutrients efficiently. Therefore, they tend to grow mostly in still waters that do not contain enough nutrients for other species to flourish.

Chlorophytes are the happy medium between diatoms and picoplankton, in terms of growth rate and nutrient requirements. The many distinct species of chlorophytes are commonly known as *green algae*.

Measuring the seasonal cycle

Scientists can determine the amount of phytoplankton in a particular area by measuring the chlorophyll that the phytoplankton produce. However, this amount changes according to the seasons and the differing levels of sunlight exposure.

At first, ocean chlorophyll was determined by in situ (at-the-site) observations. People onboard ships would draw water from different locations, and scientists would measure the chlorophyll in these samples. However, gathering samples from all over the ocean at any particular time was logistically too difficult.

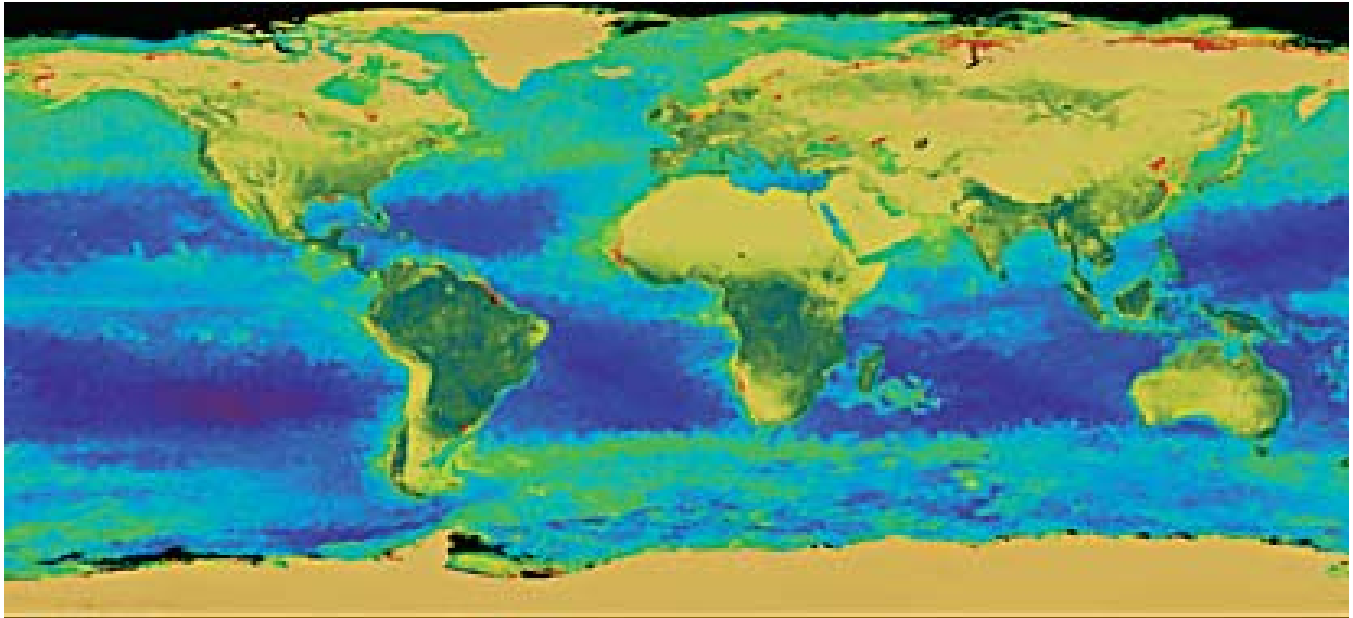
Remote observation from satellites provides a much more feasible method for measuring the

global coverage of ocean chlorophyll. Using instruments to quantify the color of the waters, scientists can determine the concentration of plant pigments near the ocean surface. Although this method is an improvement over the older method of collecting data, it has its own challenges. For example, cloud cover blocks a satellite's view and obscures data readings.

After readings are taken over a number of years, seasonal patterns emerge. For example, at different times, phytoplankton grow rapidly in different areas. These occasions of rapid plant growth are called *blooms*. Scientists now search for broader patterns in the manifestation of phytoplankton blooms across the years.

The following are some of the environmental factors that influence the growth of phytoplankton:

- **Sunlight exposure**—Phytoplankton reside near the ocean surface, where they are exposed to sunlight. This region is known as the *euphotic zone*, defined as the depth at which only 1 percent of the surface light survives. Although all phytoplankton require solar radiation, different species derive energy from different portions of the light spectrum.
- **Nutrients**—Besides sunlight, all phytoplankton require nitrogen, in the form of nitrate or ammonium. Some species also need other types of nutri-



The SeaWiFS instrument provides the first full record of photosynthetic productivity in the oceans. The color coding of this SeaWiFS data map is based on the rainbow spectrum: red and orange represent a high level of photosynthesis; green and yellow indicate a moderate amount of photosynthetic activity; and blue and purple show low levels of photosynthesis. *Image credit: SeaWiFS Project, NASA Goddard Space Flight Center, and ORBIMAGE*

ents, for example, the mineral iron. Most of the iron found in the oceans comes from soil dust blown into the waters by wind currents. Scientists hypothesize that some phytoplankton species require small amounts of iron to aid in photosynthesis. Even if an area of the ocean is rich in other nutrients, some phytoplankton may not survive without enough iron.

- Ocean currents—The movement of the ocean waters determines the distribution of phytoplankton and how close to the surface they can reside. Currents from the depths can bring

rich nutrients up to the surface, where phytoplankton can feed on them and grow.

References

- Lalli, C. M., and Parsons, T. R., *Biological oceanography: An introduction*, Butterworth-Heinemann, 1997
- Vernick, E. L., Scripps Institute of Oceanography, "Oceanic chlorophyll," *Encyclopedia of Earth System Science*, Vol. 3, Academic Press, 1992



Research Profile: The Growth Patterns of Phytoplankton Species

Investigator:

Watson Gregg, NASA Goddard Space Flight Center, Laboratory for Hydrospheric Processes

Watson Gregg developed a computerized model to simulate the growth of ocean chlorophyll throughout the seasons. He intended to compare the model results with real-world observations to see if the rules under which ocean chlorophyll are presumed to work are accurate.

A standard global run of this simulation works through approximately 4.25 GB of data. According to Gregg, working with a model of this size “just couldn’t be done without the NCCS” because the model requires such intense computing.

In fact, Gregg estimates that the recent upgrades at the NCCS to the Cray SV1 processors cut his computation time by a factor of about 2.5. The time required to process a year of phytoplankton growth dropped from 4 days to less than a day and a half. “Considering we need about 20 years to spin up to steady state,” Gregg says, “this makes a huge difference.” (See the NASA Center for Computational Sciences section for more information on this upgrade.)

Unlike previous models of chlorophyll distribution, Gregg’s model did not develop separate systems for different regions. To fully understand the growth of phytoplankton, Gregg devised a single three-dimensional system to cover the entire globe. The system boosted the

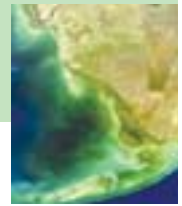
level of detail by calculating for three types of phytoplankton separately:

- Diatoms
- Picoplankton, which include cyanobacteria and prochlorophytes
- Chlorophytes, which include flagellates

Gregg used four governing equations to calculate the abundance of the following:

- Chlorophyll carried by diatoms, chlorophytes, and picoplankton
- Nutrients in the ocean (nitrate, ammonium, and silicate)
- Sea creatures that feed on phytoplankton
- Detritus left behind by dead phytoplankton

The numerical data plugged into these governing equations was generated by three distinct models: the Poseidon ocean general circulation model (OGCM), the biogeochemical model, and the general radiative transfer model. These coupled models ensured that the single system of governing equations remained accurate throughout the entire global region.



The Poseidon OGCM determines the horizontal and vertical currents that carry and move organisms and nutrients. The grid of this reduced-gravity model is nearly global in scale and has a resolution of approximately 0.8 degrees. The OCGM requires monthly averages of observed wind currents, changes in air temperature, and sea surface temperatures. Poseidon was developed by Paul Schopf at the George Mason University Center for Ocean-Land-Atmospheres.

The biogeochemical model uses Poseidon ocean current results to predict the amount of phytoplankton, herbivores, and detritus throughout the ocean. The biogeochemical model bases the growth of phytoplankton on temperature as well as the availability of sunlight and nutrients.

Phytoplankton consume nutrients, only to be consumed in turn by herbivores. The herbivores produce ammonium in the process of excretion. Phytoplankton that die naturally and rot also produce ammonium. All this ammonium feeds the remaining phytoplankton, and so the cycle continues.

The biogeochemical model also calculates the rate at which phytoplankton sink. This information is important because the faster phytoplankton sink, the less light they get to fuel photosynthesis. The speed at which plant life moves down the ocean depths is governed by plant size and Stokes' Law, which determines the drag on a spherical body in motion.

A general radiative transfer model calculates the amount of sunlight available for absorption by phytoplankton at any given time. The model uses observation data for the presence and thickness of clouds to determine how much sunlight reaches the oceans. This model also uses precipitation records to account for the ability of airborne moisture to block solar energy from the ocean surface. Other required observation data include surface pressure, wind speeds, and relative humidity.

To start the simulation, Gregg used annual climatology data from the National Oceanographic Data Center archives to set the initial values for the nutrients nitrate and silicate. The values for the phytoplankton groups were set at an equal, arbitrary amount. Once the model began calculating throughout time, phytoplankton distributions changed according to the model's rules.

As the model calculations progressed, the phytoplankton distributions grew more stable, changing less and less between time steps. In the 20th year of simulation time, the biogeochemical constituents (phytoplankton groups and nutrients) reached a steady state. In other words, the distributions in the 20th year were nearly identical to those of the 19th year.

At this point, Gregg was able to compare the results to existing observation data. The seasonal distribution of the three phytoplankton groups in the simulation mostly matched real-world distributions.



For further verification, Gregg checked the total ocean surface chlorophyll amounts against remote measurements from the satellites Coastal Zone Color Scanner (CZCS) and SeaWiFS. For this test, the ocean was divided into 12 basin regions for comparison. The simulation achieved a 95-percent confidence match with SeaWiFS for all 12 basins and with CZCS for 9 of the 12 basins.

Although the results were encouraging, such disagreements between the simulation and observation data might indicate the need for improvement in the simulation.

One notable improvement could be the inclusion of iron as a variable in the coupled model. That factor might explain why the simulation rated

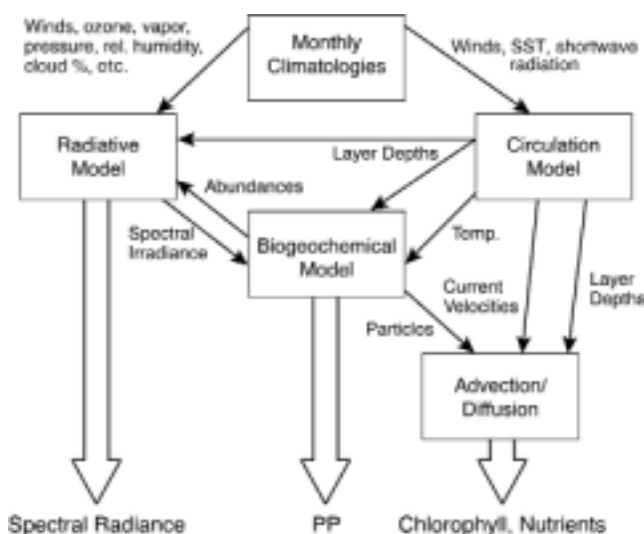
high diatom growth in areas that are observed to be dominated by other forms of phytoplankton.

These ocean areas are high in nutrients and normally would be conducive to diatom growth; however, they are also known to have low amounts of iron. According to the iron limitation theory, a low amount of iron in the oceans prevents some types of phytoplankton, such as diatoms, from flourishing.

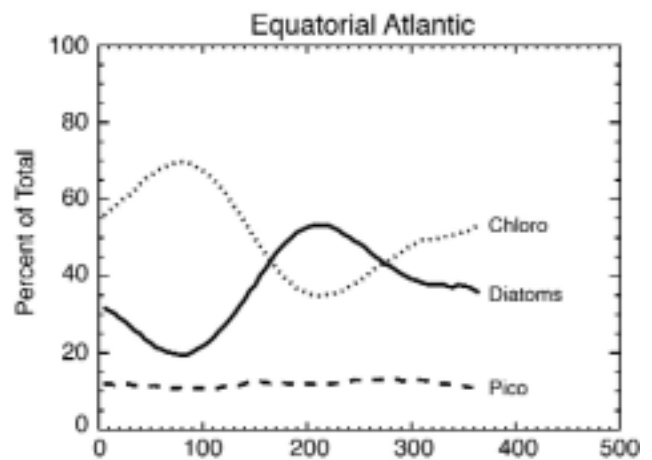
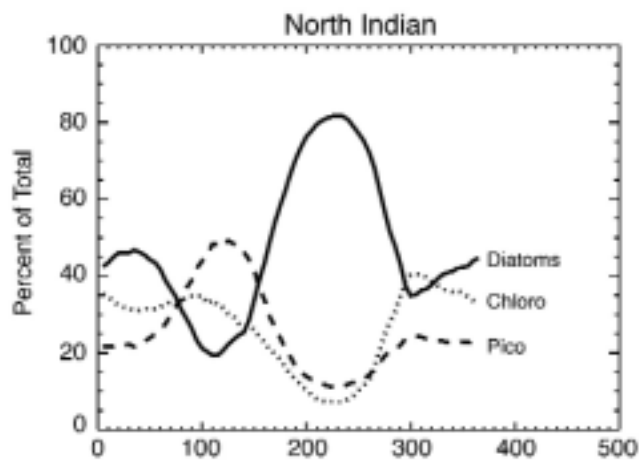
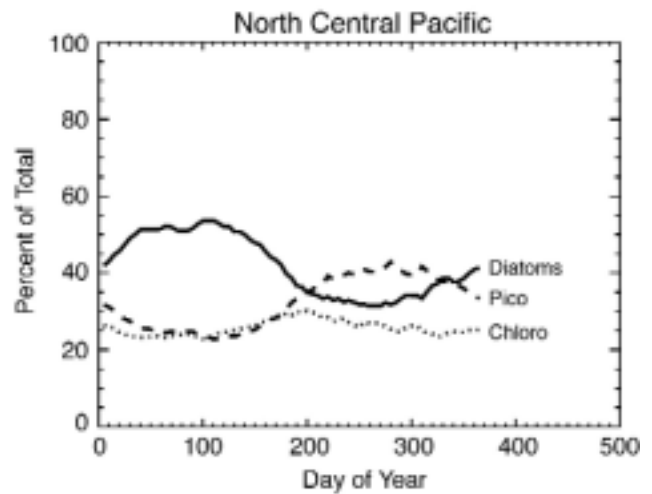
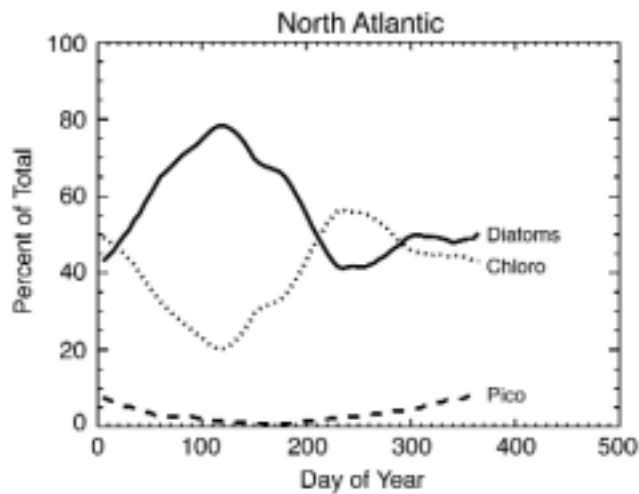
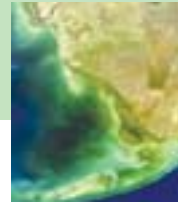
Gregg plans to explore the iron limitation theory in a research proposal with Paul Ginoux, a scientist from the Atmospheric Chemistry Dynamics Branch at NASA Goddard. They would modify the ocean chlorophyll modeling system to account for the effect of iron content on phytoplankton growth.

Several other factors might have contributed to inaccuracies in the simulation:

- Poor sampling in CZCS data, which does not show seasonal variability
- Inaccurate representation of vertical movement in ocean currents because of the reduced-gravity nature of the OGCM
- No simulation of the ability of ocean ice to cool water and limit phytoplankton growth
- No accounting for the effect of the ocean floor and coasts on circulation



Numerous data fields feed the coupled ocean general circulation, biogeochemical, and radiative models that calculate phytoplankton distributions.



This study charted the seasonal variability of diatoms, chlorophytes, and picoplankton in four ocean regions. These areas represent the range of most ocean conditions.

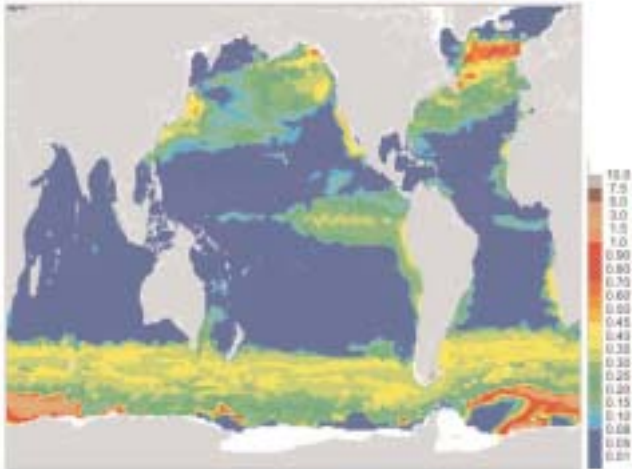
Despite these disparities, the accuracy of the model results indicate that current knowledge of

phytoplankton, on which the model equations were based, is largely accurate.

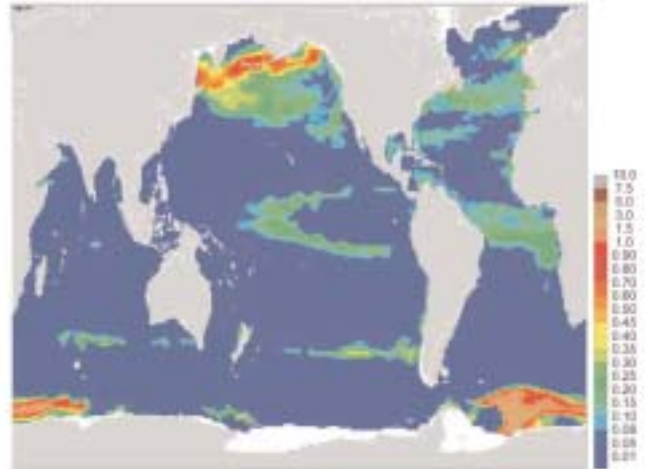


April

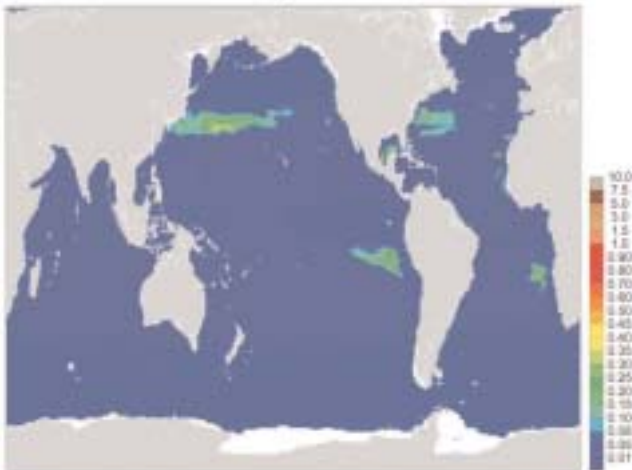
Diatoms



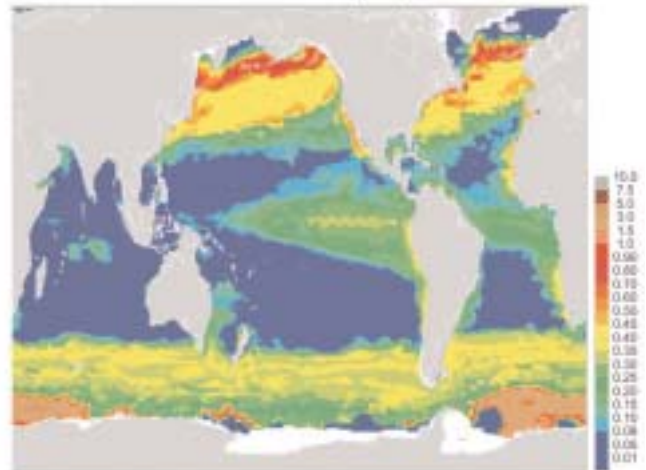
Chlorophytes



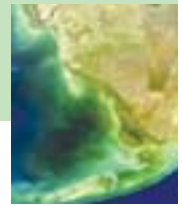
Picoplankton



Total Chlorophyll

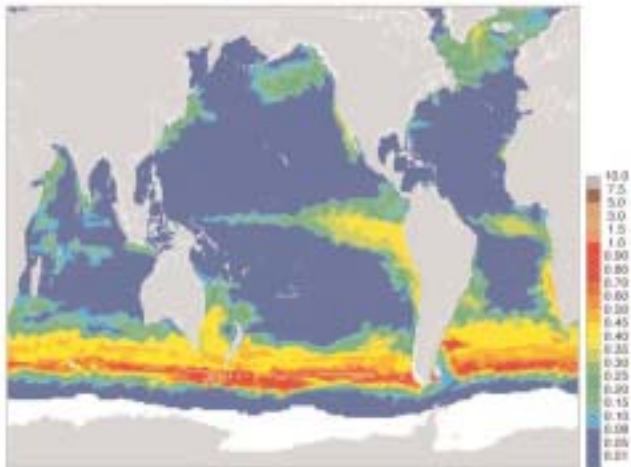


The phytoplankton growth model generated these distribution charts for the month of April after 4 years of simulation. The results generally conformed to expectations.

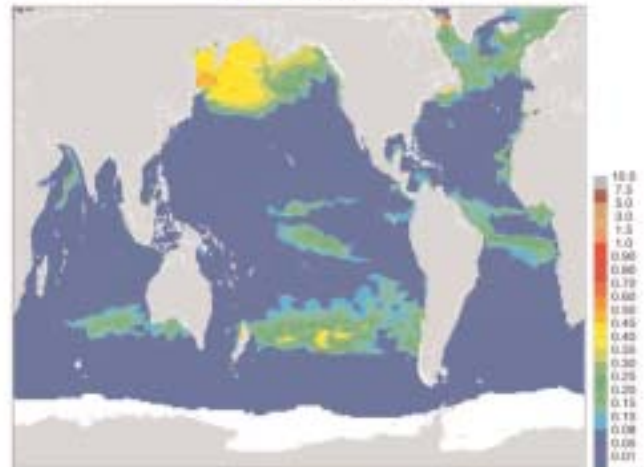


October

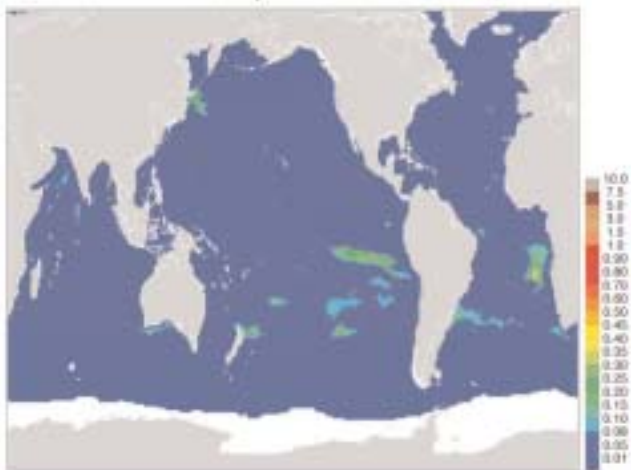
Diatoms



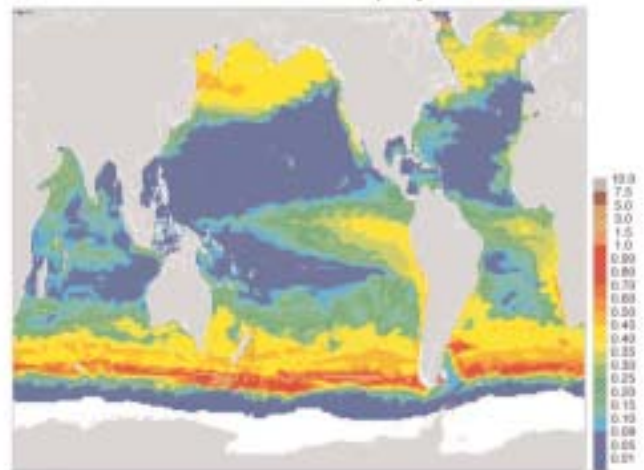
Chlorophytes



Picoplankton



Total Chlorophyll

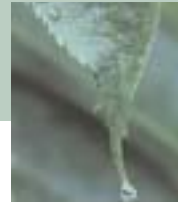


Group distributions of phytoplankton were computed for the month of October after 4 years of simulation. These maps represent totals for a single day near the beginning of the month, rather than monthly averages. The remnants of a monsoon in the Arabian Sea are visible, with a dominance of diatoms in the area. Diatoms also thrive in the southern oceans.



Rainfall Across the Globe

Precipitation plays an important role in many environmental phenomena



The numerical simulation of precipitation helps scientists understand the complex mechanisms that determine how and why rainfall is distributed across the globe.

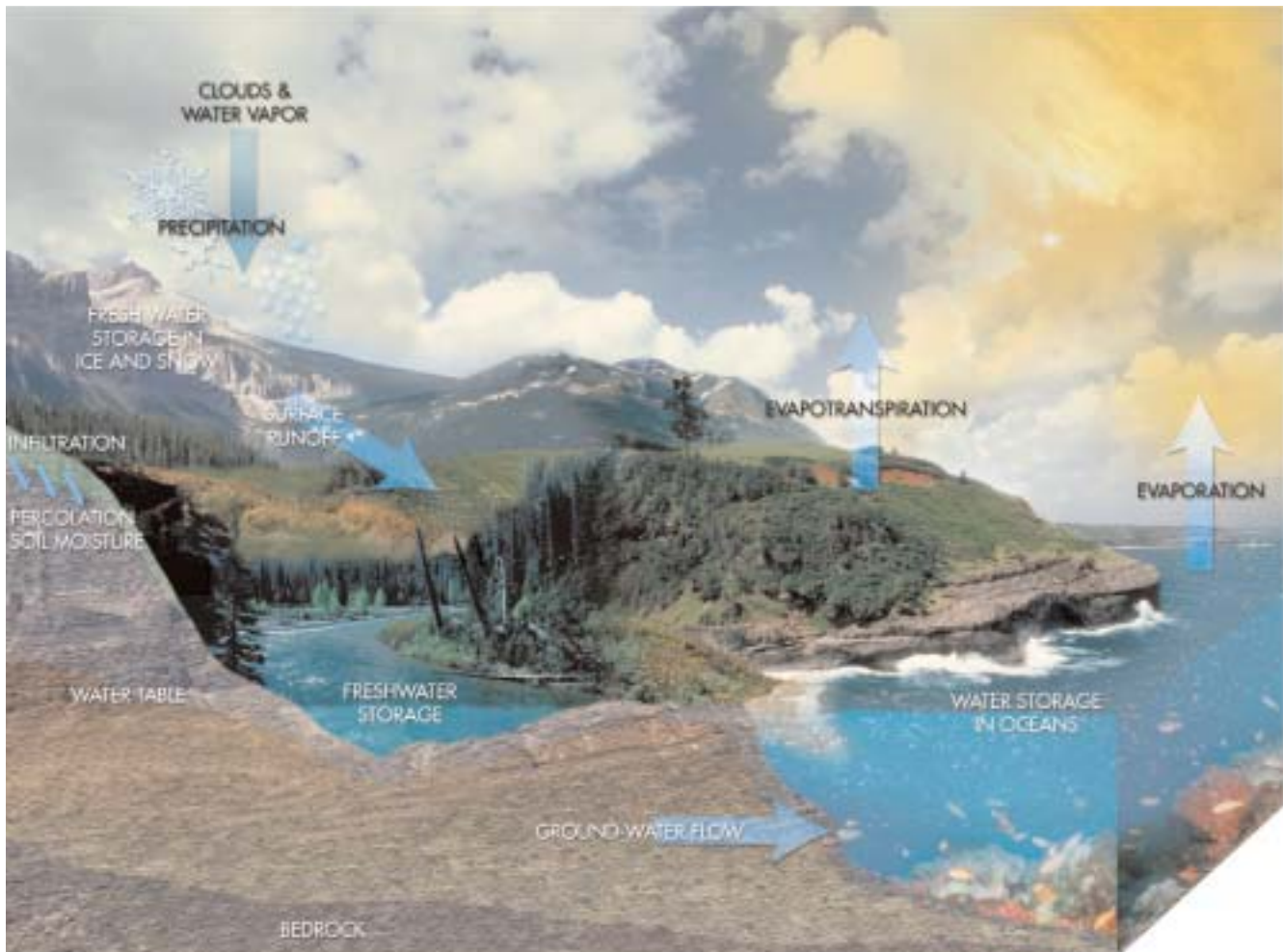
Simulation aids in the development of forecasting efforts that inform policies regarding the management of water resources. Precipitation modeling also provides short-term warnings for emergencies such as flash floods and mudslides.

Just as precipitation modeling can warn of an impending abundance of rainfall, it can help anticipate the absence of rainfall in drought. What constitutes a drought?

- A *meteorological drought* simply means that an area is getting a significantly lower amount of rain than usual over a prolonged period of time.
- An *agricultural drought* is based on the level of soil moisture.



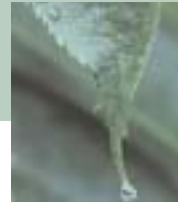
As we learn more about what drives precipitation, we can anticipate extreme fluctuations in rainfall, leading to droughts and floods.



Precipitation is a vital link in the hydrological cycle that moves water through land, sea, and air.

- A *hydrological drought* focuses on lower precipitation levels that reduce bodies of water on the surface, such as lakes and streams.
- A *socioeconomic drought* takes into account human activities, such as the construction of dams and terrain shaping, that alter the distribution of surface water.

A numerical model for drought prediction is shaped by the drought criteria that are selected. The meteorological definition of drought focuses primarily on the amount of precipitation. The agricultural and hydrological definitions require model components not only for precipitation but also for soil moisture absorption and evaporation of water. The socioeconomic view of



Monsoons

For people who live in the Pacific Ocean's monsoon region, the arrival of monsoon rainfall in July and August means the end of the long dry season. A monsoon that is either too strong or too weak may lead to flooding or drought. To help predict monsoon strength and to understand the interaction between monsoon and other atmospheric phenomena, we must understand why monsoons exist, what accounts for the circulation field of a monsoon, and why monsoon onset is abrupt.

The two types of monsoon are summer and winter. Despite their names, both monsoons take place during the July-August season. The main difference is in their location. The summer monsoon takes place more than 10 degrees north of the Equator, where the season is summer. Likewise, the winter monsoon is located south of the Equator, where July is in the middle of winter.

The summer monsoon is a continental-size convective system, characterized by a large precipitation region. This region is identified as an off-equatorial *intertropical convergence zone* (ITCZ). The strongest summer monsoons occur near southern Asia. Monsoons also occur near Australia, North and South America, and Africa.

In a northern summer monsoon, the prevailing winds at the low levels are from the southwest. At high levels, the wind direction reverses. This configuration produces a large vertical wind shear that does not occur elsewhere in the tropics.

Just as low-level winds run southwesterly in the northern summer monsoon, they run southeasterly in the southern winter monsoon. Ancient mariners depended on this seasonal change of prevailing wind to sail between India and Africa.

In the monsoon onset process, the ITCZ shifts from near the Equator to more than 10 degrees away in days. Compared with the movement of the Earth's tilt toward the Sun, this change is rapid.

Like any large-scale circulation, the monsoon is highly influenced by the Coriolis force. This force, which is created by the Earth's rotation, moves toward the right of wind direction in the Northern Hemisphere and toward the left of wind direction in the Southern Hemisphere. At the low levels, the air mass flows toward an ITCZ in the Northern Hemisphere from the other side of the Equator. The wind direction, which is influenced by the Coriolis force, enters the northern hemisphere from the southeast. After the air mass crosses the Equator, the direction changes to a southwesterly flow. Wind flow also comes from the north of the ITCZ, but its strength is much weaker.

At upper levels, the airflow must return in the opposite direction. The circulation field and the convective heating in the ITCZ precipitation region interact; yet, neither causes the other.



drought, with its dependence on human action, may be the most difficult version to quantify in a simulation.

Accurate precipitation modeling can also improve understanding of other environmental issues. For example, rain droplets absorb certain airborne pollutants and remove them from the atmosphere when they fall to the ground. Therefore, models of atmospheric composition can benefit by incorporating a precipitation component.

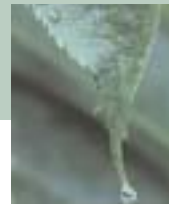
As scientists studied global precipitation, they noted a correlation between the amount of rainfall in particular areas of the world and other weather conditions. For example, in certain regions, droughts are strongly associated with the warm or cold phase of the El Niño-Southern Oscillation cycle. Indeed, evidence links global patterns of sea surface temperature (SST) to regional precipitation patterns across the decades. However, as evidenced in the second research profiles that follows, SST explains only a portion of precipitation variability.

Precipitation simulations are usually compared to actual rainfall measurements to test their accuracy. These measurements can be derived from

rain gauges at specific points on the ground. Remote sensors based on radar and satellite instruments are a more practical means of collecting data to estimate rainfall over larger regions.

References

- Browning, K. A., and Gurney, R. J. (Eds.), *Global Energy and Water Cycles*, Cambridge University Press, 1999
- Collier, C. G., World Meteorological Organization Operational Hydrology Report No. 46: *Precipitation Estimation and Forecasting*, 2000
- Linacre, E., and Geerts, B., *Climates and Weather Explained*, Routledge, 1997
- Sorooshian, S., "Hydrologic forecasting," *Encyclopedia of Earth System Sciences*, Vol. 2, Academic Press, 1992
- Trenberth, K. E. (Ed.), *Climate System Modeling*, Cambridge University Press, 1992
- Wilhite, D. A. (Ed.), *Drought Volume 1: A Global Assessment*, Routledge, 2000



Research Profile: The Role of Landmass in Monsoon Development

Investigator:

Winston Chao, NASA Goddard Space Flight Center, Climate and Radiation Branch

Since the 17th century, a fundamental belief has prevailed that the basic cause of a monsoon is the contrast in surface temperatures between the continents and the oceans. Research using general circulation model (GCM) experiments demonstrated that this belief should be changed.

In an experiment in which the researchers replaced the landmasses of Asia and Australia with ocean, the simulated Asian and Australian monsoons remained largely intact. The figures on page 62 show the monsoon precipitation averaged for the month of August in a 4-year model integration. The upper panel shows the control experiment with the continents intact. For the lower panel results, ocean replaced the continents.

Further experiments showed that in the Asian monsoon, the change resulting from the replacement of continents with ocean was caused more by the removal of topography than by the removal of land-sea contrast. Whereas land-sea contrast played a minor modifying role in the Asian summer monsoon, it played an important role in the African and South American summer monsoons. However, that role was not irreplaceable. If an ocean with a high enough SST replaced Africa or South America, the monsoon

remained, even without the presence of a continent.

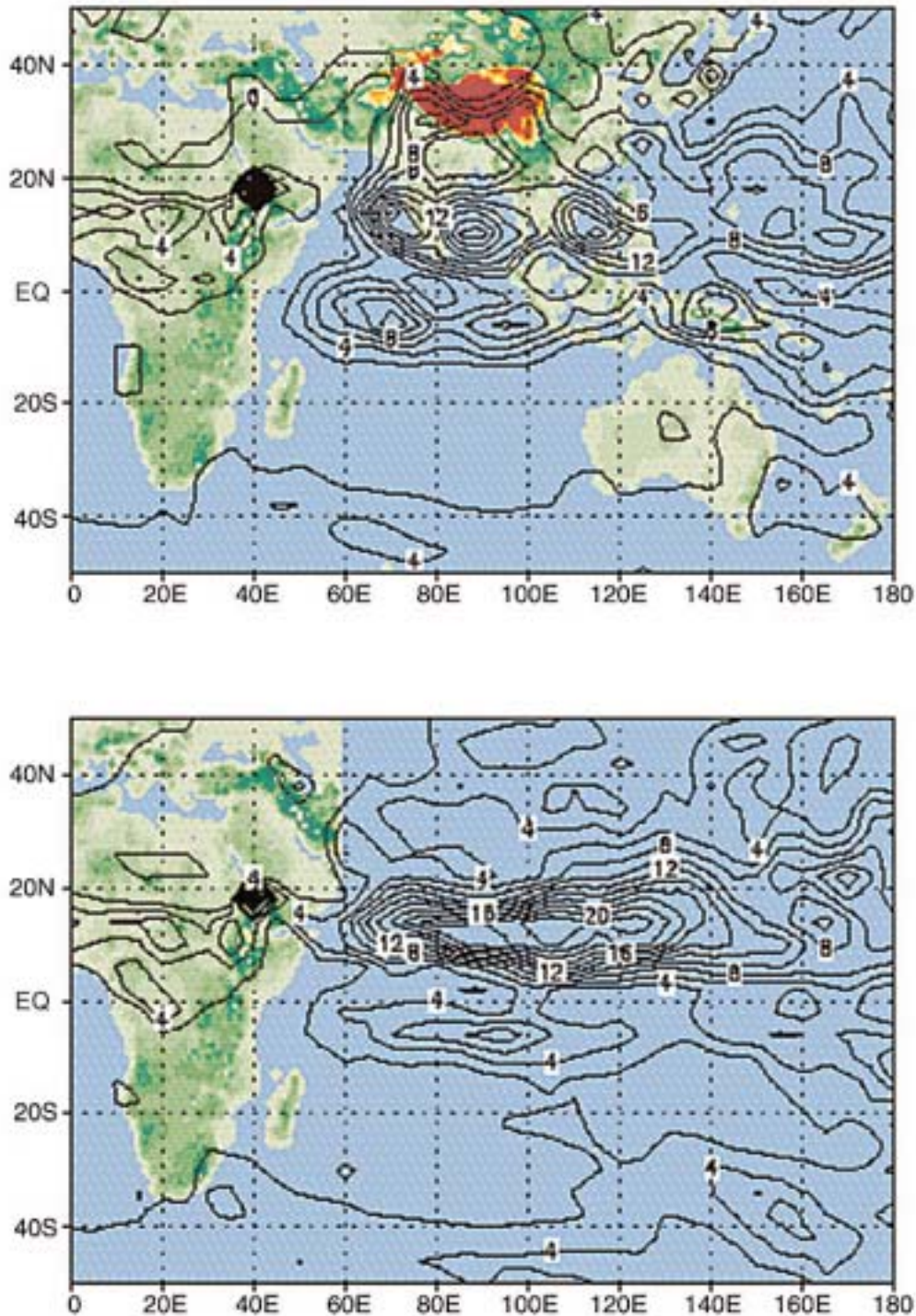
To understand why monsoons exist is to understand why the ITCZ exists in particular off-Equator regions during the summer. In an aqua-planet model with zonally uniform SST, the ITCZ is zonally uniform and located at the tropical latitudes where SST is high. The solar energy absorbed by the surface at these areas heats the air above and controls the location of convective precipitation.

The SST is only one factor that determines the location of the ITCZ. Another influencing factor is the Earth's rotation, which pulls the ITCZ toward two different latitudes at around 13 degrees north and south of the Equator. Therefore, ITCZ is often observed at both locations.

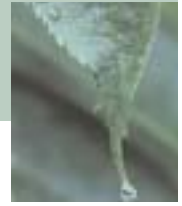
When researchers varied the distribution of SST in the simulation, the ITCZ was no longer zonally uniform but concentrated somewhat to the west of the longitudes where SST was highest. The model then gave a precipitation and circulation field that was very close to real-world observations. Therefore, researchers concluded that landmass is not a necessary condition for monsoons.



Precipitation



Monsoon mean precipitation levels for August were calculated for two drastically different environments. In one simulation (top), the land remained in place. In the other (bottom), the landmasses of Asia, Australia, and the Pacific Islands were replaced by ocean. When the land was removed from the model, the Asian and Australian monsoon regions still existed. However, monsoons did not extend into the southern China region.



The research project also showed that the monsoon process is similar to the flipping of a light switch. When a switch is pushed gently and persistently, it flips from one stable state to another very quickly. Likewise, the ITCZ is pushed toward the poles by the seasonal meridional movement of the peak of the SST. This movement is countered by another force that is produced by the Earth's rotation. When the latter force finally gives way, the ITCZ suddenly jumps away from near the Equator, and monsoon onset occurs.

Chao's numerical experiments with an atmospheric GCM have demonstrated the monsoon onset process. The circulation field associated with the ITCZ determines the equatorial surface winds that, in turn, determine SST near the equator. Therefore, study of monsoons or the ITCZ is highly relevant to the study of El Niño. The experiments used the Goddard Earth Observing System (GEOS) atmospheric GCM, running on the NCCS Cray SV1 supercomputer.



Research Profile: The Relationship Between Precipitation and Sea Surface Temperature on Decadal Time Scales

Investigators:

Siegfried Schubert, Max Suarez, and Philip Pegion, NASA Goddard Space Flight Center, Data Assimilation Office

This research project examined the possibility of a connection between SST and precipitation on multiyear time scales. In particular, the research focused on rainfall over the Great Plains region of the United States during the summer months.

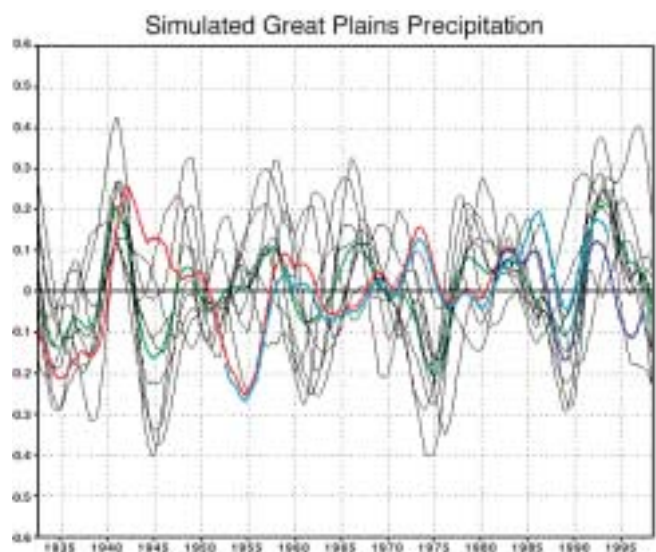
The researchers ran nine simulations of precipitation, spanning the years 1930 through 1999, using the NASA Seasonal-to-Interannual Prediction Project (NSIPP) atmospheric GCM. They used 64 of the NCCS Cray T3E computer's 1,360 processors to conduct these 70-year runs. The associated data was stored on the NCCS's Sun E10000 UniTree storage system.

A Cray support member from the NCCS helped speed up the progress of this effort. He located a default setting that prevented the model code from running at full speed. He also showed the researchers how to buffer the data output and speed up run times even further. These efforts reduced run times by 13 percent. Overall, the Cray T3E calculated more than 225,000 days of model simulation in only 700 days of computing time, spread across the 64 processors devoted to this project.

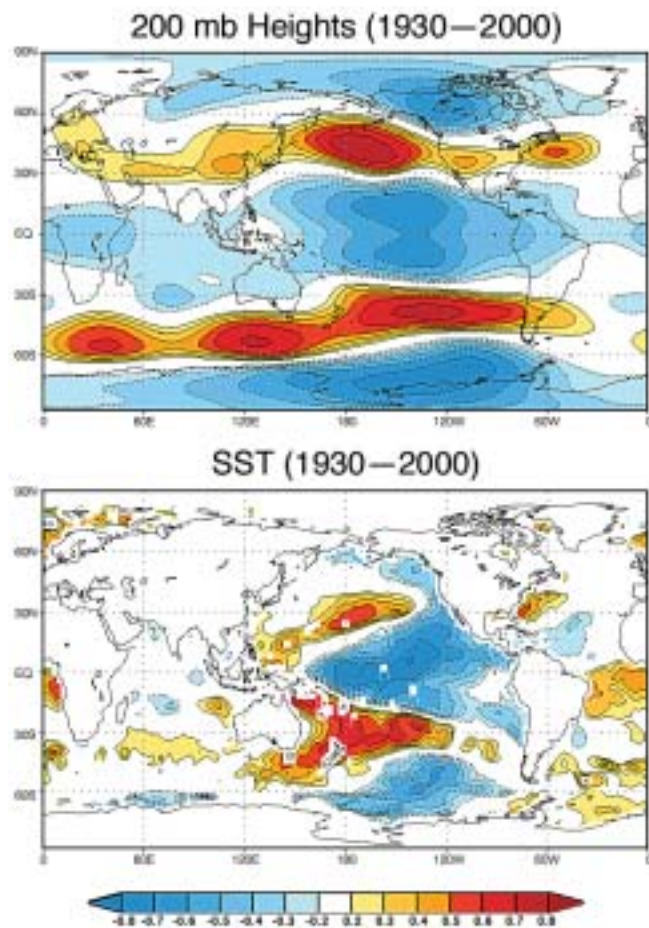
Each simulation run was forced with the same set of observed SST measurements. However,

initial atmospheric conditions were different. If the same SST data produced similar patterns of precipitation over the Great Plains, even with different atmospheric conditions, the results would demonstrate a link of predictability between SST and precipitation.

The nine runs showed different levels of rainfall; therefore, overall this experiment did not indicate a strong link between SST and precipitation. However, the simulated results did share similarities with actual rainfall records. Nearly all the



This graph lays out nine simulations of Great Plains rainfall. The black lines represent the individual simulation runs, and the green line is the ensemble mean. The red and blue lines represent various observational estimates.



These color maps indicate the negative correlation between certain meteorological measurements and calculations for precipitation over the Great Plains region. The bottom map shows SST correlation, and the top map shows the correlation for the altitude at which air pressure reaches a measurement of 200 millibars (mb). Because this project is concerned with the absence of precipitation, negative correlations are mapped.

runs indicated dry conditions during the 1930s, followed by wet conditions in the next decade. This result matches the infamous “Dust Bowl” drought of the Great Depression era.

In contrast, only one of the nine simulations replicated conditions similar to another major Great Plains drought that took place in the 1950s. In fact, some simulation runs produced multi-year droughts even when no anomalies in SST levels were present.

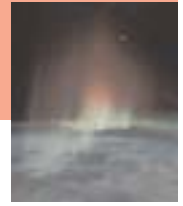
After they completed the simulation runs, the researchers mapped the correlation between Great Plains precipitation and SST. The correlation revealed a decades-spanning SST pattern across the Pacific Ocean that is linked to rainfall variations in the Great Plains region. When the Pacific pattern is in its warm phase, the Great Plains region gets more precipitation than usual. Conversely, drought conditions tend to occur in this area when the Pacific SST pattern is in a cold phase. Several additional atmospheric GCM runs confirmed this correlation.

Overall, the project results suggested that the ability to predict Great Plains droughts depends in part on the ability to predict the long-term behavior of the Pacific SST pattern.



Under the Weather

Supercomputers can track and analyze the movement of potentially damaging solar winds



Normally, only people in the far north can enjoy the dancing beauty of the aurora borealis; however, an intense collision of charged solar particles with the Earth's magnetic field can magnify the Northern Lights so much that they are visible in the southern United States. Behind the light show lies enough flux of energetic particles carried by solar wind to render our planet uninhabitable. The Earth's magnetic field, also known as the *magnetosphere*, is the only thing that shields us from the Sun.

Even the magnetosphere cannot fully guard us from the wrath of the Sun. In March 1989, a powerful solar flare hit Earth with such energy that it burned out transformers in Quebec's electrical grid, plunging Quebec and the eastern United States into darkness for more than 9 hours.

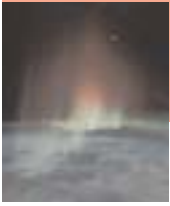
Northern lights and energy grid overloads are not the only ways that a solar wind can affect us. A solar storm in July 1999 interrupted radio broadcasts. Solar activity can disorient radars and satellite sensors, break up cell phone connections, and threaten the safety of astronauts. A large bombardment of solar particles can even reduce the amount of ozone in the upper atmosphere. *Magnetohydrodynamics* (MHD), the study of magnetic fields in magnetized plasmas, can help scientists predict, and therefore prepare for, the harmful side effects of solar weather in the magnetosphere.

From the Sun to the Earth

Eruptions in the outer atmosphere of the Sun are the usual source of “space weather” phenomena. These eruptions, called *coronal mass ejections* (CMEs), are related to the changes in magnetic fields that the Sun produces. This activity is cyclical. Every 11 years, the frequency of eruptions spikes at what is known as a *solar maximum*.

CMEs propel *plasmas*, or superheated ionized gases, into space through the background solar wind plasma. The solar wind plasma mostly consists of hydrogen atoms that have been fully ionized into protons and electrons. As the electrically charged particles move through space, they generate their own magnetic field. During a CME, the wind drags solar magnetic field lines into space to form the heliosphere. Because of the rotation of the Sun, the radially flowing solar wind produces spiral magnetic field lines known as the *Parker spiral*.

Rushing at speeds approaching 3 million miles per hour, a CME takes roughly 2 to 3 days to hit the Earth. The bombardment of Earth with solar protons is called a *solar proton event*. When the magnetic fields from the solar wind collide with the Earth's magnetosphere, the fields constantly twist and turn. Occasionally, they break apart and reform rapidly. This process of *magnetic reconnection* transfers large amounts of heat and energy from the solar wind to the magnetosphere.



Eye on the solar wind

For the past 35 years, the Space Environment Center in Boulder, Colorado, has been the United States' official space weather forecasting center. The organization collects images of the surface of the Sun, issues space weather advisory bulletins, and develops mathematical models for the activity of ions in outer space. The National Oceanic and Atmospheric Administration (NOAA) and the U.S. Air Force operate the Center jointly. Other major centers of space weather study in the United States include the NASA Goddard Space Flight Center and educational institutions such as UCLA, Dartmouth College, the University of Maryland at College Park, Rice University, and the University of Michigan.

The United States has also joined international efforts to study the Sun-Earth space environment. NASA, the European Space Agency (ESA), and Japan's Institute of Space and Astronautical

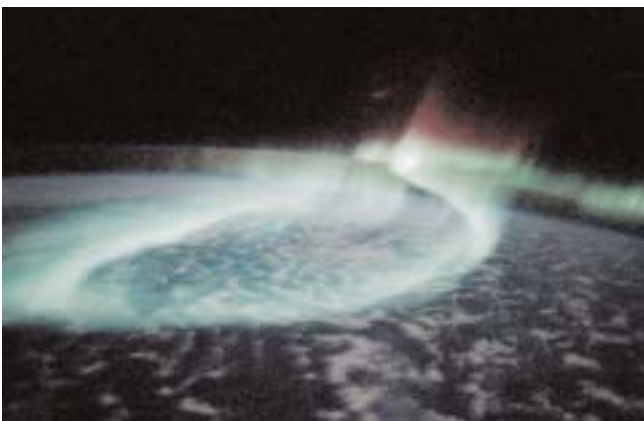
Sciences (ISAS) formed the International Solar Terrestrial Physics (ISTP) project in the 1980s. The ISTP has launched several missions to study solar wind and its interaction with the Earth.

A number of satellites can detect disturbances on the Sun's surface up to 3 days before a CME hits the Earth:

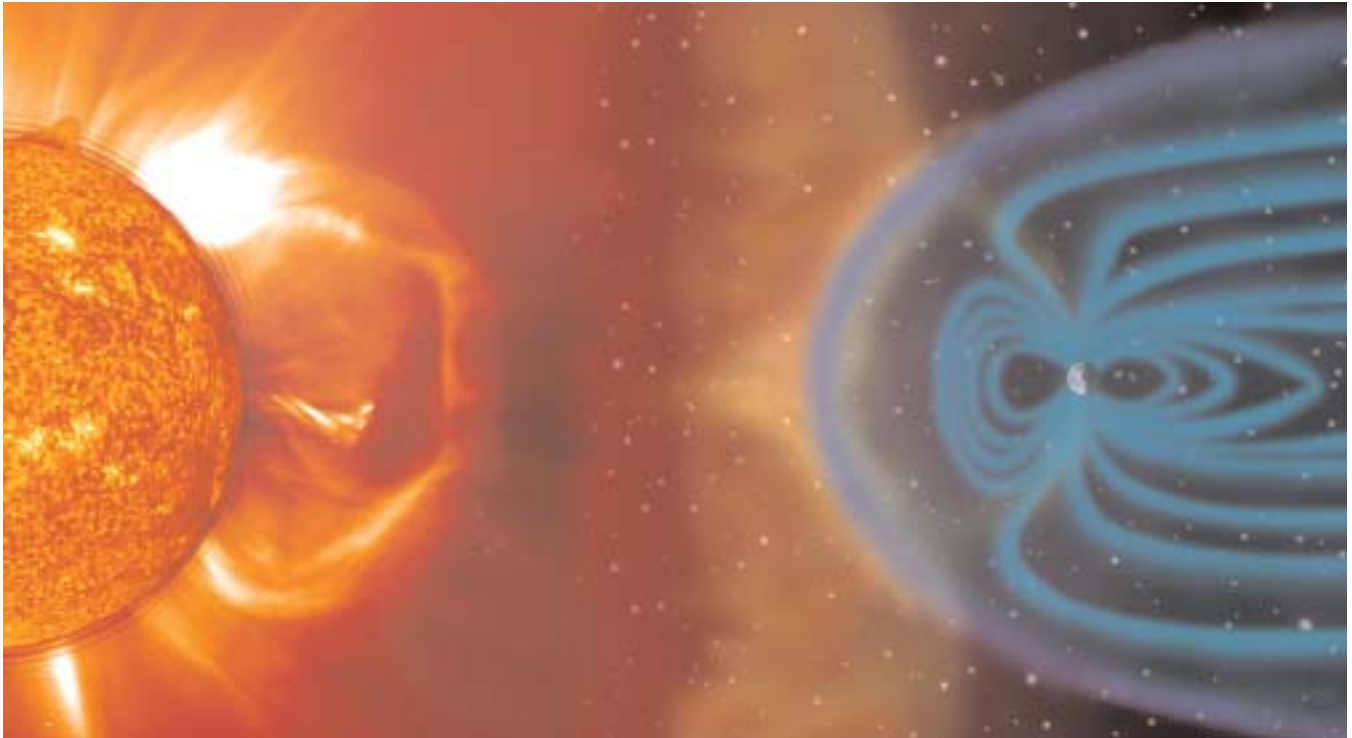
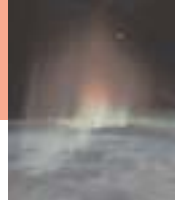
- Both the Solar and Heliospheric Observatory (SOHO) and the Advanced Composition Explorer (ACE) satellites are positioned 1.5 million miles away, in an orbit that keeps them at a constant position between the Earth and the Sun.
- The ISAS launched the Yohkoh satellite in 1991. Yohkoh carries x-ray telescopes and other sensors that were contributed by the United States and Great Britain.

In addition, a large fleet of spacecraft measures the effects of the solar wind and CMEs on the magnetosphere:

- NASA's Imager for Magnetopause-to-Aurora Global Exploration (IMAGE), launched in 2000, is the first satellite dedicated to obtaining global images of the magnetosphere.
- The ISTP launched GEOTAIL to measure global energy flow and transformation in the magnetic field lines that spread out from Earth's



The aurora australis shines over the Southern Hemisphere.



This illustration shows the Earth's magnetosphere deflecting a CME cloud. A CME takes 2 to 4 days to leave the Sun and reach Earth.
Image credit: The SOHO project

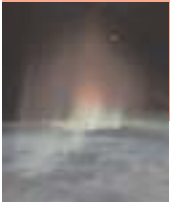
polar caps. Other ISTP spacecraft include WIND, POLAR, and Cluster II.

- The Los Alamos National Laboratory (LANL) created a series of satellites that analyze magnetospheric plasma and measure spaceborne electrons.
- NOAA and NASA developed the Geostationary Operational Environmental Satellites (GOES). Among the many instruments on GOES satellites are a magnetometer, an x-ray sensor, and other sensors

that monitor the development of space weather.

References

- Burch, J. L., "The fury of space storms," *Scientific American*, Vol. 284, No. 4, April 2001
- Glanz, J., "Unlocking secrets of magnetic fields' power," *New York Times*, October 24, 2000
- Seuss, S. T., and Tsurutani, B. T. (Eds.), *From the Sun*, American Geophysical Union, 1998



Research Profile: The Magnetic Field of the Heliosphere

Investigators:

Aaron Roberts and Melvyn Goldstein, NASA Goddard Space Flight Center, Interplanetary Physics Branch

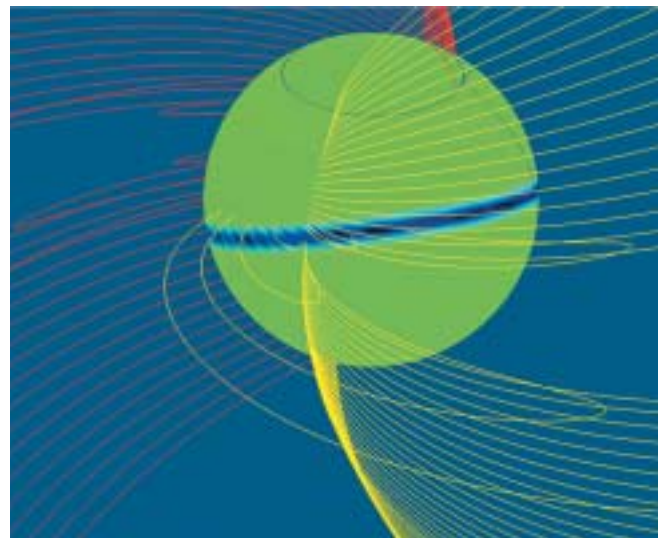
This research project simulated the dynamics of magnetic field lines and plasmas in the heliosphere to deepen our understanding of the approach of solar winds toward Earth. The study focused on various sources of field line distortions.

The researchers calculated solar wind conditions with a Flux-Corrected Transport MHD code. The code used a spherical-coordinate grid with general boundary conditions. A comparison with data from the Helios deep space probe showed that the code results were realistic.

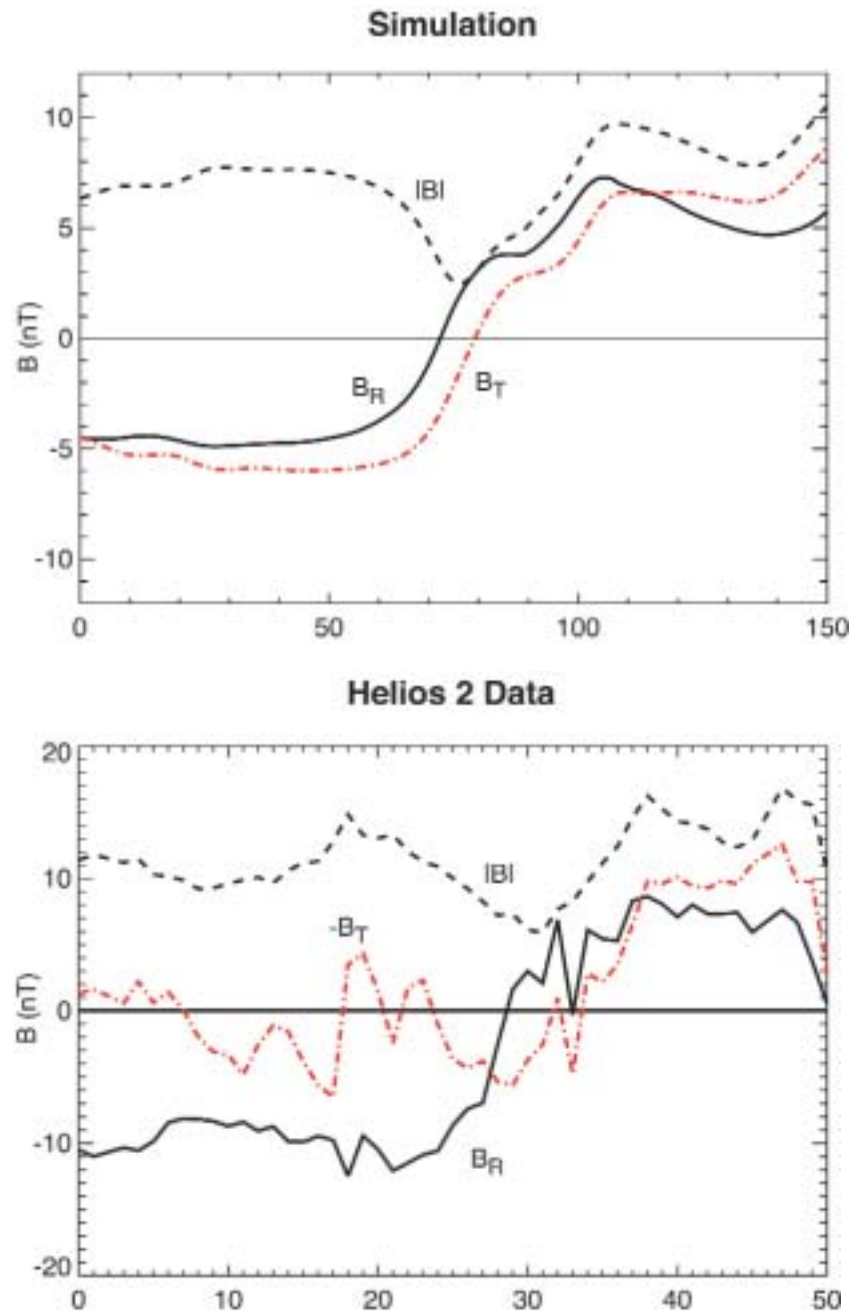
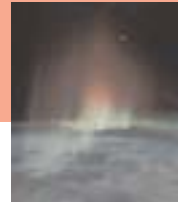
The simulations showed that the ideal Parker spiral field lines are easily modified, even in uniform flow conditions. In particular, the magnetic field deviates from the Parker spiral at a *sector boundary*, that is, the location near the ecliptic at which the field changes polarity. Here, loops of field form where the two polarities connect.

Another project simulated the presence of Alfvén waves in the heliosphere. An *Alfvén wave* is the movement of particles in a direction perpendicular to a magnetic field that bends the field lines. The simulation introduced Alfvén waves into a standard heliospheric flow, in which a high-speed solar wind surrounds a low-speed wind.

The results indicate that the simulations provide a valid description of the evolution of Alfvénic fluctuations in the solar wind. Therefore, scientists can use the simulation code to study realistic field configurations and their important effects on the propagation of potentially damaging energetic particles coming from the Sun. The investigators are currently optimizing the MHD code for a higher resolution and greater realism than before.



The yellow and red lines in this illustration represent simulated magnetic field lines from the Sun. The blue region on the green sphere indicates the sector boundary that separates magnetic polarities. Image credit: Interplanetary Physics Branch, NASA Goddard Space Flight Center



The top figure shows magnetic field values for the solar wind, calculated in this research project's simulation. For comparison, the bottom figure shows magnetic field recordings from the Helios 2 satellite, which was developed by NASA and the Federal Republic of Germany.

Burning in Outer Space

A lit matchstick is positioned vertically in the center of the frame. The matchstick is a light brown color. The flame is a bright yellow-orange, elongated into a teardrop shape, and extends upwards. The background is a deep blue space filled with numerous small, white stars of varying brightness.

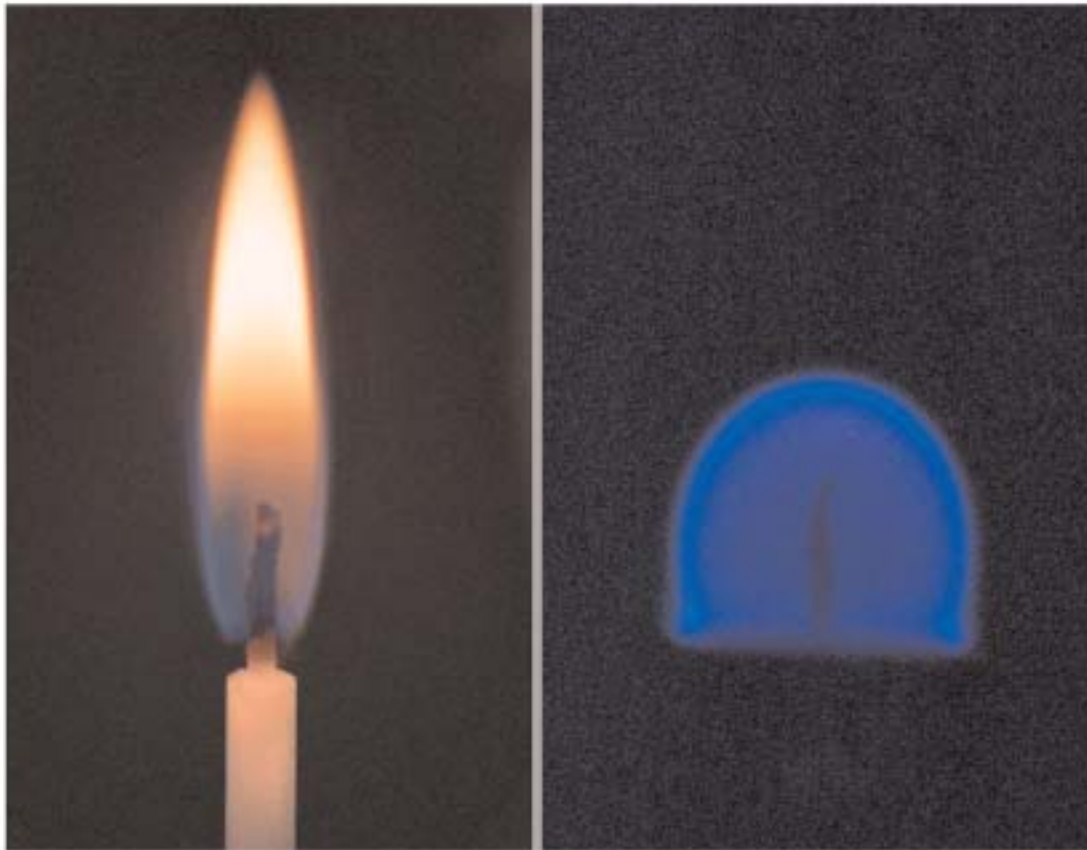
The study of
combustion in a low-
gravity environment
can improve both
material production
and fire safety in
Earth's orbit



A better understanding of combustion can lead to significant technological advances, such as less polluting, more fuel-efficient vehicles. Unfortunately, gravity can interfere with the study of combustion. Gravity drags down gases that are cooler—and, therefore, denser—than heated gases. This movement mixes the fuel and the oxidizer substance that promotes burning. Because of this mixing, an observer cannot necessarily distinguish what is happening as a result of the natural combustion

process and what is caused by the pull of gravity.

To remove this uncertainty, scientists can conduct experiments that simulate the negation of gravity through freefall. This condition is known as a *microgravity environment*. A microgravity experiment may take place in a chamber that is dropped down a hole or from a high-speed drop tower. The experiment can also be conducted in an airplane or a rocket during



The absence of gravity has a visible effect on combustion, as seen in these images of burning candles. *Image credit: Microgravity Science Division, NASA Glenn Research Center*



freefall in a parabolic flight path. This method provides less than a minute of microgravity at most.

An experiment that requires the prolonged absence of gravity may necessitate the use of an orbiting spacecraft as a venue. However, access to an orbital laboratory is difficult to acquire. High-end computing centers such as the NCCS can provide a practical alternative to operating in microgravity. Scientists can model phenomena such as combustion without gravity's observational interference.

The study of microgravity combustion produces important benefits beyond increased observational accuracy. Certain valuable materials that

are produced through combustion can be formed with a more uniform crystal structure—and, therefore, improved structural quality—when the pull of gravity is removed. Furthermore, understanding how fires propagate in the absence of gravity can improve fire safety aboard spacecraft.

Reference

Rogers, M., Vogt, G., and Wargo, M., *Microgravity—A Teacher's Guide with Activities in Science, Mathematics, and Technology*, NASA Office of Life and Microgravity Sciences and Applications - Microgravity Research Division; NASA Office of Human Resources and Education - Education Division



Research Profile: Simulation of Combustion in a Microgravity Environment

Investigators:

Bernard Matkowsky, Northwestern University, Department of Engineering Sciences and Applied Mathematics; Anatoly Aldushin, Russian Academy of Science, Institute for Structural Macrokinetics

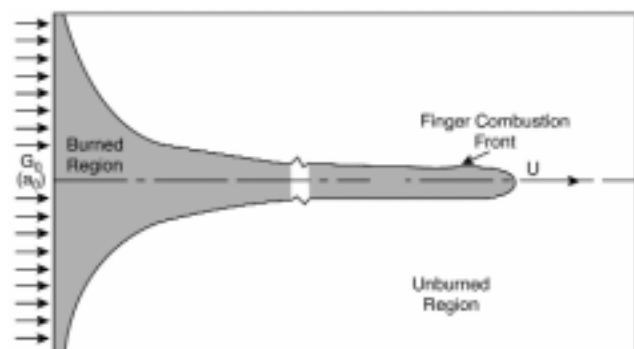
These researchers used the computational facilities of the NCCS to develop a model to analyze *filtration combustion*, the burning that takes place as a gaseous oxidizer flows through a porous solid fuel powder. In this situation, the gas and the solid both contain combustible and noncombustible, or *inert*, elements.

The scientific understanding has been that when filtration combustion takes place, the oxidizer flows slowly enough through the solid fuel that both substances increase in temperature at the same rate. However, this new research found that when the speed of the oxidizer is sufficiently high, the gas and the solid will experience different rates of temperature change. Because of this difference, Matkowsky estimates the speed increase at a factor of at least 3 or 4, and possibly even higher. This method of combustion may enable scientists to synthesize certain materials more quickly than before.

This research also helps illuminate the phenomenon of *smoldering*, the slow combustion of an oxidizer gas and a porous solid fuel, such as a lit cigarette. The gasified fuel that gradually accumulates during smoldering may react suddenly, producing sudden and dangerous fires.

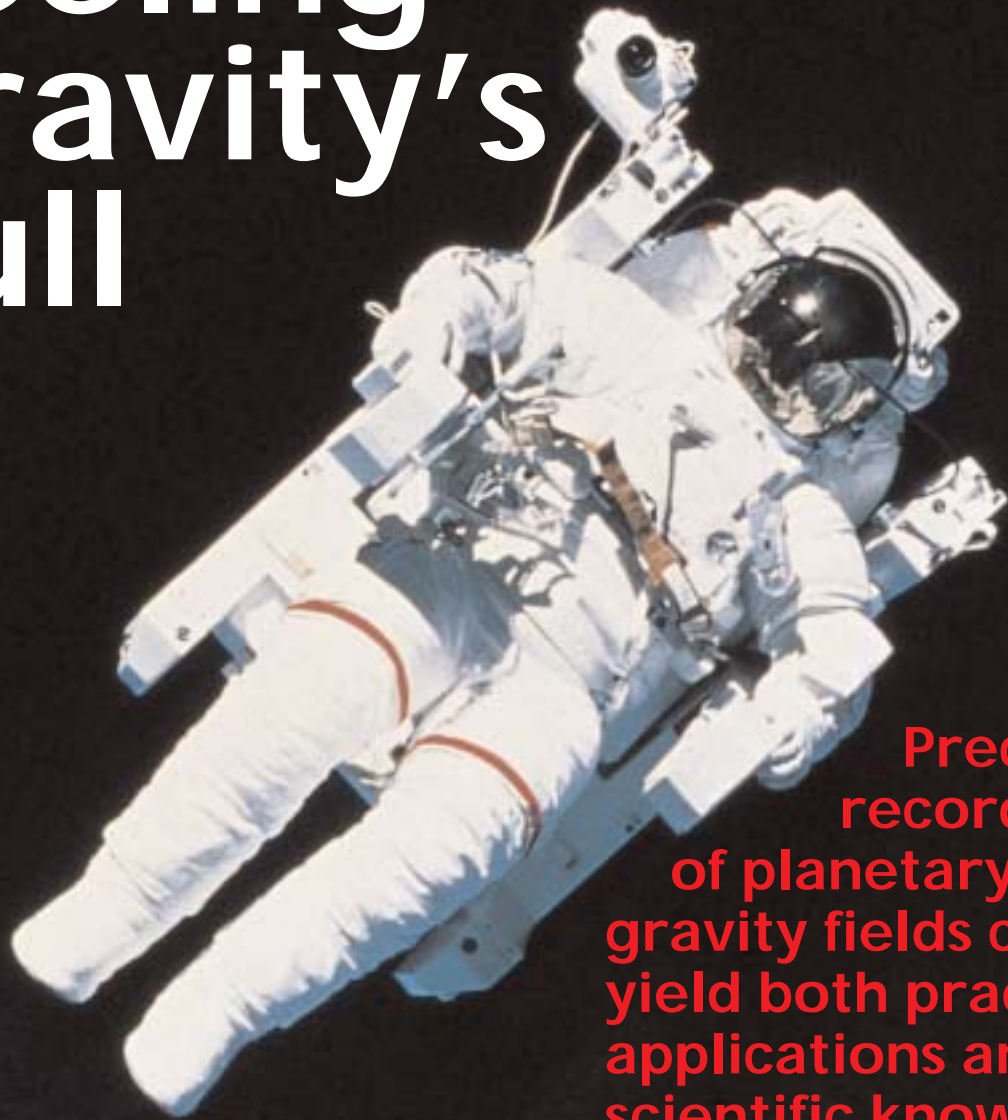
The simulation analyzed how the combustion starts and how it grows in both normal-gravity and microgravity situations. The study found significant differences in the progress of combustion at different gravity levels. Therefore, conventional knowledge of how fires spread on Earth does not necessarily apply to how a fire may react within an orbiting spacecraft.

Researchers also explored a combustion effect known as a *fingering instability*. This effect occurs when combustion spreads through the interior of a fuel in a path that resembles a finger, while the surface remains intact. A fingering instability can be dangerous because the burning is, for the most part, not visible.



In the process of filtration combustion, a gaseous oxidizer flows through a solid fuel substance. A model of this process proposes that a "finger region" of the oxidizer naturally projects into the unburned fuel.

Feeling Gravity's Pull



Precise recordings of planetary gravity fields can yield both practical applications and scientific knowledge



Most people take the constant presence of gravity's pull for granted. However, the Earth's gravitational strength actually varies from location to location. This variation occurs because mass, which influences an object's gravitational pull, is not evenly distributed within the planet. Changes in topography, such as glacial movement, an earthquake, or a rise in the ocean level, can subtly affect the gravity field.

An accurate measurement of the Earth's gravity field helps us understand the distribution of mass beneath the surface. This insight can assist us in locating petroleum, mineral deposits, ground water, and other valuable substances. Gravity mapping can also help notice or verify changes in sea surface height and other ocean characteristics. Such changes may indicate climate change from polar ice melting and other phenomena. In addition, gravity mapping can indicate how land moves under the surface after earthquakes and other plate tectonic processes. Finally, changes in the Earth's gravity field might indicate a shift in water distribution that could affect agriculture, water supplies for population centers, and long-term weather prediction.

Scientists can map out the Earth's gravity field by watching satellite orbits. When a satellite shifts in vertical position, it might be passing over an area where gravity changes in strength. Gravity is only one factor that may shape a satellite's orbital path. To derive a gravity measurement from satellite movement, scientists must

remove other factors that might affect a satellite's position:

- Drag from atmospheric friction
- Pressure from solar radiation as it heads toward Earth and as it is reflected off the surface of the Earth
- Gravitational pull from the Sun, the Moon, and other planets in the Solar System
- The effect of tides
- Relativistic effects



Perturbations in the flight path of a satellite may indicate a change in the strength of the Earth's gravity field.



Scientists must also correct for the satellite tracking process. For example, the tracking signal must be corrected for refraction through the atmosphere of the Earth.

Supercomputers can calculate the effect of gravity for specific locations in space following a mathematical process known as *spherical harmonics*, which quantifies the gravity field of a planetary body. The process is based on Laplace's fundamental differential equation of gravity. The accuracy of a spherical harmonic solution is rated by its degree and order.

Minute variations in gravity are measured against the *geoid*, a surface of constant gravity acceleration at mean sea level. The geoid reference gravity model strength includes the central body gravitational attraction (9.8 m/s^2) and a geopotential variation in latitude partially caused by the rotation of the Earth. The rota-

tional effect modifies the shape of the geoid to be more like an ellipsoid, rather than a perfect circle. Variations of gravity strength from the ellipsoidal reference model are measured in units called *milli-Galileos* (mGals). One mGal equals 10^{-5} m/s^2 .

Research projects have also measured the gravity fields of other planetary bodies, as noted in the user profile that follows. From this information, we may make inferences about our own planet's internal structure and evolution. Moreover, mapping the gravity fields of other planets can help scientists plot the most fuel-efficient course for spacecraft expeditions to those planets.

Reference

National Research Council, *Satellite Gravity and the Geosphere*, National Academy Press, 1997



Research Profile: The Gravity Field of Mars

Investigators:

Frank Lemoine, David Smith, and David Rowlands, NASA Goddard Space Flight Center, Laboratory for Terrestrial Physics; Maria Zuber and G. Neumann, Massachusetts Institute of Technology, Department of Earth, Atmospheric, and Planetary Sciences; Douglas Chinn and D. Pavlis, Raytheon ITSS Corp.

This research project developed the Goddard Mars Model 2B (GMM-2B), the first global spherical harmonic solution for the Mars gravity field. Scientists derived the GMM-2B by tracking the orbit of the Mars Global Surveyor (MGS) between October 1997 and February 2000.

The solution has a degree and order of 80. In comparison, the first Mars gravity solution, which was based only on Mariner 9 data,

had a degree and order of 6. According to Frank Lemoine, the equations of the GMM-2B included roughly 6,600 parameters for modeling the gravity field and another 5,000 for modeling the individual orbits of the MGS.

The orbital path of the MGS was lower, more complete, and more stable than the previous Mariner and Viking crafts, enabling improvements in the geopotential calculation. In addi-



Topographical features such as the Olympus Mons crater may vary the distributions of land mass and create variations in the gravity field of Mars. *Image credit: NASA*

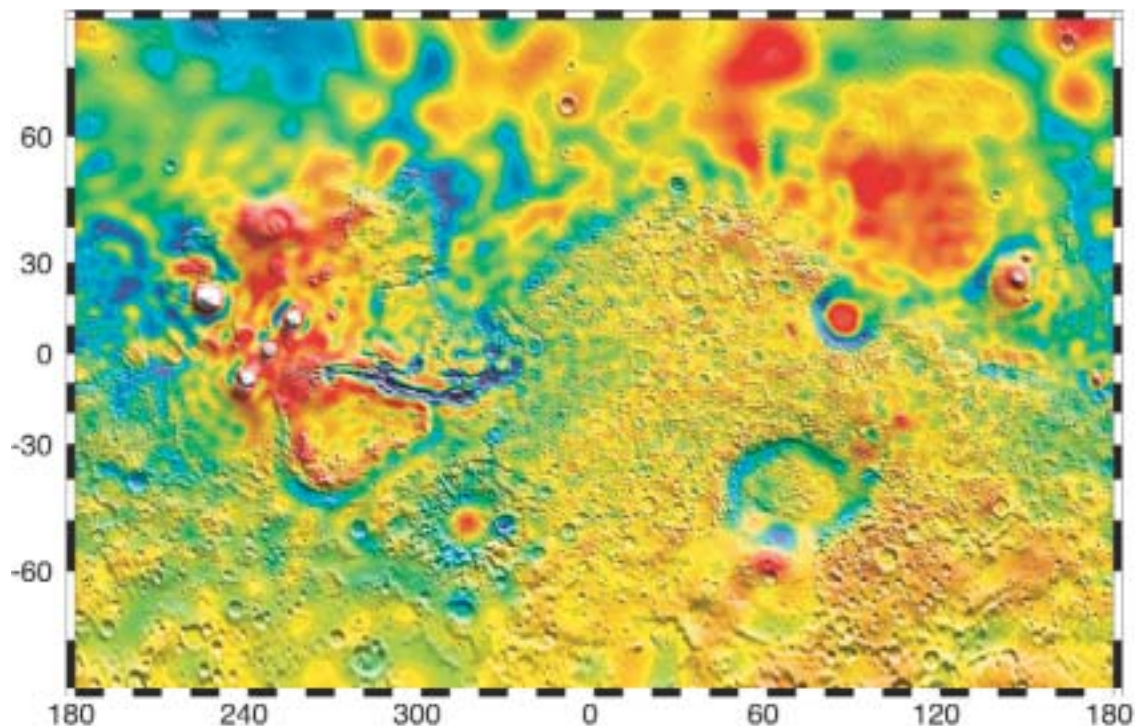


tion, the MGS had radio equipment that was less sensitive to disturbances caused by solar plasma. This equipment improved data quality by a factor of 10 over previous Mars mission data.

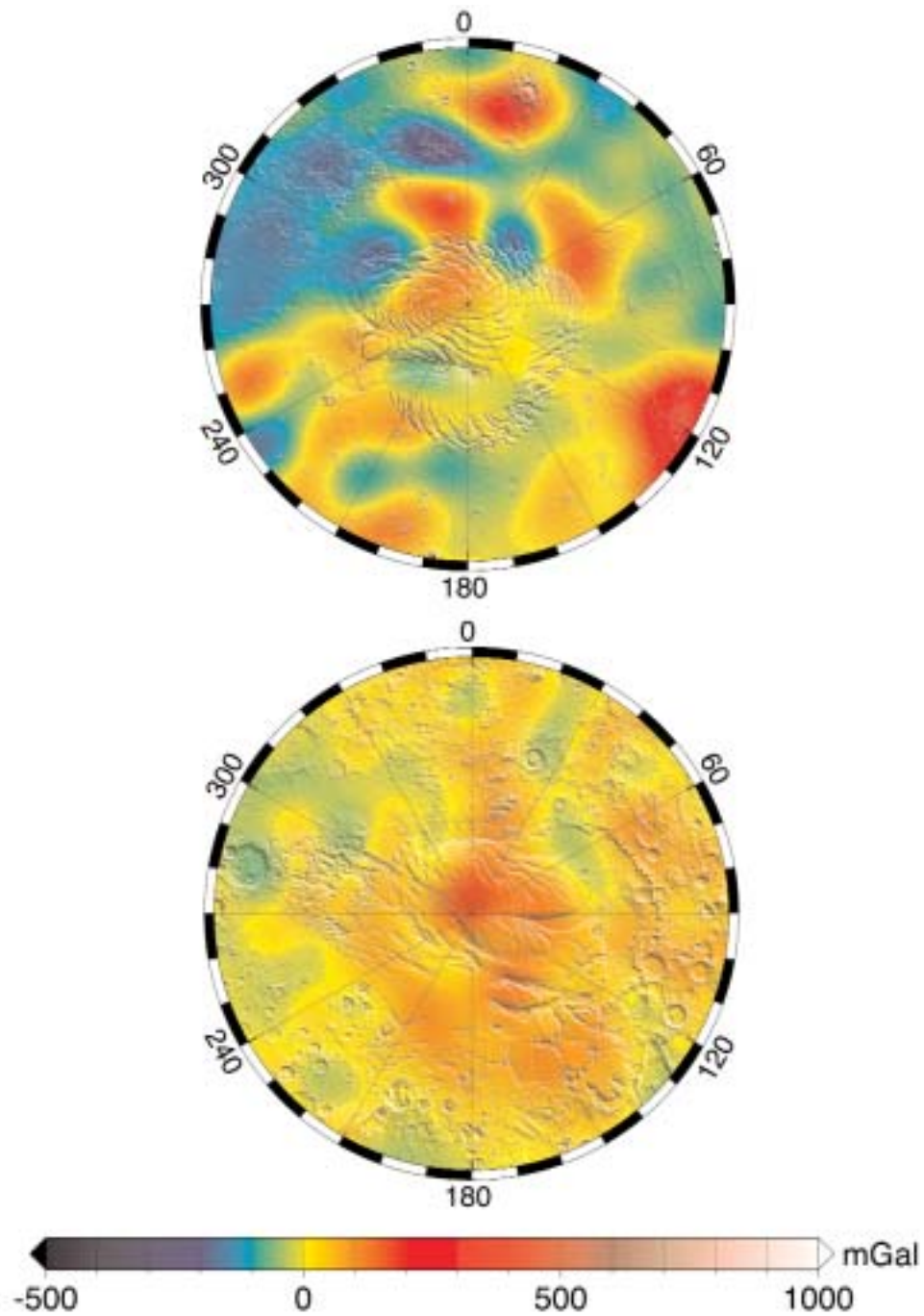
The researchers processed the spacecraft's orbital path data in individual arcs, each covering 5 days of movement. In each arc, factors such as atmospheric drag, solar radiation pressure, and the thrust maneuvers of the MGS were modeled. To process all this data, the researchers developed 150 equations, each of which consumed 298 megabytes of storage space on the NCCS's UniTree storage system.

Researchers compared the degree variances for the GMM-2B solutions to the GMM-1 model developed in 1993. Below degree 20, the field accuracy of GMM-2B showed an improvement of two to three orders of magnitude. Beyond degree 20, GMM-1 lacked the global coverage to provide a meaningful comparison.

The research project also mapped out gravity anomalies that GMM-2B had located. The gravity model displayed an improved resolution of the anomalies related to classic geographical features such as the Olympus Mons crater, Tharsis Montes, Elysium, and Isidis.



This map shows gravity anomalies of the planet Mars, as calculated by the GMM-2B. The features now appear with greater power than in the previous Global Mars Model. The anomalies are overlaid on a shaded relief map from the readings of the Mars Orbital Laser Altimeter. *Image credit: NASA*



These circular maps portray gravity anomalies for the northern (top) and southern (bottom) polar regions of Mars. *Image credit: NASA*

NCCS FY2000 Research Projects and Principal Investigators

3-D Chemical Modeling

Ronald Prinn
Massachusetts Institute of Technology

3-D Chemistry and Transport

Richard Rood
GSFC Data Assimilation Office

3-D Chemistry and Transport Model

Anne Douglass
GSFC Atmospheric Chemistry and Dynamics
Branch

4-D Data Assimilation/TOVS Pathfinder

George Serafino
GSFC Global Change Data Center

5-Year Analysis Production

Richard Rood
GSFC Data Assimilation Office

AMIP Experiment

Richard Rood
GSFC Data Assimilation Office

Absolute and Convective Instability and Splitting of a Liquid

Sung Lin
Clarkson University

Aircraft Impact Assessment

Richard Rood
GSFC Data Assimilation Office

Aircraft Winds in GLA Analysis

Joel Tenenbaum
State University of New York, Purchase

Analysis Diagnostics

Siegfried Schubert
GSFC Data Assimilation Office

Analysis Verification and Experimentation

Richard Rood
GSFC Data Assimilation Office

Analysis and Interpretation of Satellite Magnetic Data

Coerte Voorhies
GSFC Geodynamics Branch

Analysis for the Climatology and Short-Term Variability of the Atmospheric General Circulation With the GLA GEOS Data: Global Hydrological and Energy Cycles

Tsing-Chan Chen
Iowa State University

Biosphere-Atmosphere Interactions

George Collatz
GSFC Biospheric Sciences Branch

Bubbles and Drops

Ram Subramanian
Clarkson University

Chinks in the Solar Dynamo Theory

Edward DeLuca
Smithsonian Astrophysical Observatory

Climate Change

Donald Johnson
University of Wisconsin

Climate Diagnostics

Siegfried Schubert
GSFC Data Assimilation Office

Climate Modeling and Simulation

Jagadish Shukla
George Mason University and IGES/COLA

Climatic Effects of Volcanic Eruptions

Alan Robock
Rutgers University

Computation and Data Analysis

Edward Sullivan
GSFC Laboratory for Astronomy and Solar
Physics

Coupled DRB Model

Watson Gregg
GSFC Oceans And Ice Branch

Crustal Dynamics

David Smith
GSFC Laboratory for Terrestrial Physics

Crustal Geomagnetic Fields

Herbert Frey
GSFC Geodynamics Branch

Cumulus Cloud Modeling

Wei-Kuo Tao
GSFC Mesoscale Atmospheric Processes Branch

DOSE and LAGEOS Investigations

Ronald Kolenkiewicz
GSFC Space Geodesy Branch

Data Analysis and Distribution

Richard Rood
GSFC Data Assimilation Office

Data Preprocessing-Preparation

Arlindo da Silva
GSFC Data Assimilation Office

Decadal and ENSO Variability and Mass Pathways in the Pacific

Gary Mitchum
University of South Florida

Development of New Metrics for DAO Data Verification

Man-Li Wu
GSFC Data Assimilation Office

Diabatic Dynamic Initialization

Michael Fox-Rabinovitz
GSFC Data Assimilation Office

Diurnal Response of Boundary

David Randall
Colorado State University

Drop Collision and Coalescence

Gretar Tryggvason
University of Michigan

Dynamical Stratospheric Model

Richard Rood
GSFC Data Assimilation Office

EGRET Data Analysis

Teresa Sheets
GSFC Data Management and Programming Office

EOS Hydrologic Processes

William Lau
GSFC Climate and Radiation Branch

Ecosystem Simulation Analysis

John Walsh
University of South Florida

Effect of Variations in Pacific Heat and Fresh Water Fluxes on the Indian Ocean

Roxana Wajsowicz
University of Maryland

Effects of Gravity on Sheared and Nonsheared Turbulent Nonpremixed Flames

Said Elghobashi
University of California, Irvine

Effects of Gravity on Sheared Turbulence Laden With Droplets or Bubbles

Said Elghobashi
University of California, Irvine

Energy Diagnostics

Donald Johnson
University of Wisconsin

Erosional Processes on Mars

Alan Howard
University of Virginia

Estimate Ocean/Air Fluxes

Shu-Hsien Chou
GSFC Mesoscale Atmospheric Processes Branch

Extra-Solar Planet Modeling

Daniel Gezari
GSFC Infrared Astrophysics Branch

**Filtration for Microgravity Applications:
1) Smoldering, 2) Combustion Synthesis of
Advanced Material**

Bernard Matkowsky
Northwestern University

Flame Spread in Non-uniform Mixtures

Fletcher Miller
NASA, John H. Glenn Research Center

Flame Spread on Liquid Surface

William Sirignano
University of California, Irvine

Forecast Error Variance Model

Yong Li
GSFC Data Assimilation Office

Fractal Cloud Structure

Robert Cahalan
GSFC Climate and Radiation Branch

GEODYN Software Development

David Rowlands
GSFC Space Geodesy Branch

**GLA TOVS Satellite Data-Development,
Processing, Validation, and Scientific Research**

Joel Susskind
GSFC Laboratory for Atmospheres

GMAS Hydrology Parameterization

Michael Jasinski
GSFC Hydrological Sciences Branch

GPS Analysis

Braulio Sanchez
GSFC Space Geodesy Branch

GSFC Cumulus Cloud Modeling

Joanne Simpson
GSFC Earth Sciences Directorate

**GSFC Earth Science Data and Information
Systems (ESDIS) Program**

Christopher Bock
GSFC Science Data Systems Branch

**Gas-Phase Combustion Synthesis of Metal and
Ceramic Nano-Particles**

Richard Axelbaum
Washington University of St. Louis, Missouri

General Analysis

Franklin Ottens
GSFC Laboratory for Extraterrestrial Physics

Geomagnetic Field Studies

Herbert Frey
GSFC Geodynamics Branch

**Geopotential Determination Using Satellite,
Gravity, and Ocean Model Data**

Byron Tapley
University of Texas at Austin

**Global Inventory Mapping and Monitoring
(GIMMS)**

Compton Tucker
GSFC Biospheric Sciences Branch

Global Model Studies

George Emmitt
Simpson Weather Associates

Global Modeling of Tropospheric Chemistry

Daniel Jacob
Harvard University

Gravity Model Development

Frank Lemoine
GSFC Space Geodesy Branch

HST Phase Retrieval

Mark Turczyn
GSFC HST Flight Systems & Servicing Project

High Performance Computing

Richard Rood
GSFC Data Assimilation Office

IAU and Model/Analysis Interface

Richard Rood
GSFC Data Assimilation Office

IMP-J Magnetic Field Experiment

Ronald Lepping
GSFC Electrodynamics Branch

ISEE-1 VES Data Analysis

Keith Ogilvie
GSFC Laboratory for Extraterrestrial Physics

ISEE-OGH Data Analysis

Keith Ogilvie
GSFC Laboratory for Extraterrestrial Physics

Imaged EUV Spectra from SERTS

Roger Thomas
GSFC Solar Physics Branch

Improving Land Hydrologic Processes

Yogesh Sud
GSFC Climate and Radiation Branch

Improving Radiation Codes

Albert Arking
Johns Hopkins University

Inference of Global Warming from Satellite Data

Prabhakara Cuddapah
GSFC Climate and Radiation Branch

Influence of Land Surface Processes/Land Cover Changes in Amazon

Regional Hydrometeorology
Yongkang Xue
University of California, Los Angeles

Instability of Alfvén Wave

Adolfo Viñas
GSFC Interplanetary Physics Branch

Investigation of GRXE Production

Teresa Sheets
GSFC Data Management and Programming Office

Kalman Filtering

Richard Rood
GSFC Data Assimilation Office

Lidar

James Spinhirne
GSFC Mesoscale Atmospheric Processes Branch

Land Climatology

Yogesh Sud
GSFC Climate and Radiation Branch

Land Surface Component of the Climate System

Randal Koster
GSFC Hydrological Sciences Branch

Liquid He Heat Studies

Efstratios Manousakis
Florida State University

Low-Frequency Phenomenon Modeling

William Lau
GSFC Climate and Radiation Branch

MAGSAT Crustal Anomalies

Patrick Taylor
GSFC Geodynamics Branch

MHD Turbulence

Melvyn Goldstein
GSFC Interplanetary Physics Branch

Magnetic Wave-Particle Interaction

Richard Denton
Dartmouth College

Magnetospheric Simulation

Steven Curtis
GSFC Planetary Magnetospheres Branch

Mars Observer Gamma Ray Spectrometer

Jacob Trombka
GSFC Astrochemistry Branch

Mars Observer Laser Altimeter

David Smith
GSFC Laboratory for Terrestrial Physics

Mesoscale Dynamics

Wei-Kuo Tao
GSFC Mesoscale Atmospheric Processes Branch

Mid-Latitude Ocean Circulation

David Adamec
GSFC Oceans And Ice Branch

Miscellaneous Analysis Production

Richard Rood
GSFC Data Assimilation Office

Model Diagnostics

Siegfried Schubert
GSFC Data Assimilation Office

Model Production

Richard Rood
GSFC Data Assimilation Office

Model Research

Mark Helfand
GSFC Data Assimilation Office

Model and STRATAN Analysis

Richard Rood
GSFC Data Assimilation Office

Modeling Studies of LFV

Randall Dole
National Oceanic and Atmospheric
Administration

Modeling of Decadal Variability in the Tropical Atlantic Climate

Vikram Mehta
GSFC Climate and Radiation Branch

Molecular Dynamics II

Joel Koplik
City College of the City University of New York

Momentum and Energy Budgets in Models

David Salstein
AER, Inc.

NAOS Studies

Stephen Lord
National Oceanic and Atmospheric
Administration

Nimbus SMMR Data

Milton Halem
GSFC Earth and Space Data Computing Division

Non-local Coupling by Magnetospheric Currents

Keith Siebert
Mission Research Corporation

North Pacific Circulation Modeling

Michele Rienecker
GSFC Oceans and Ice Branch

Numerical Study of Large-Scale Tropical Circulations

Winston Chao
GSFC Climate and Radiation Branch

Objective Analysis Methods

Grace Wahba
University of Wisconsin

Ocean Surface Wind Analysis

Robert Atlas
GSFC Data Assimilation Office

Oceans and Ice Branch General Access

Michele Rienecker
GSFC Oceans and Ice Branch

Pioneer/Helios Data Analysis

Teresa Sheets
GSFC Data Management and Programming
Office

Planetary Scale Interactions

William Lau
GSFC Climate and Radiation Branch

Polar Ocean Modeling Studies

Sirpa Häkkinen
GSFC Oceans and Ice Branch

Radiation Budget

Man-Li Wu
GSFC Data Assimilation Office

Radiation Budgets/Aerosol Radiative Forcing

Ming-Dah Chou
GSFC Climate and Radiation Branch

Rain Retrieval Studies

Prabhakara Cuddapah
GSFC Climate and Radiation Branch

Rainfall Assimilation Studies

Vijaya Karyampud
GSFC Mesoscale Atmospheric Processes Branch

Rainfall from TRMM

James Weinman
GSFC Microwave Sensors Branch

Reduction & Analysis of LEO Satellite**Magnetic Field Data**

Joseph Cain
Florida State University

Regional Validation Centers

Patrick Coronado
GSFC Applied Information Sciences Branch

Remote Sensing of Clouds

Si-Chee Tsay
GSFC Climate and Radiation Branch

Resonances

Anand Bhatia
GSFC Solar Physics Branch

STIS GTO Research Support Using UniTree**Archival Data**

Sara Heap
GSFC UV Optical Astronomy Branch

Satellite Data Evaluation

Richard Rood
GSFC Data Assimilation Office

Science Network Office

J. Patrick Gary
GSFC Earth and Space Data Computing Division

Search and Rescue SAR Research

David Affens
GSFC Microwave Systems Branch

Seasonal-to-Interannual Climate Variability

Michael Ghil
University of California, Los Angeles

Seasonal-to-Interannual Collaboration

Michele Rienecker
GSFC Oceans and Ice Branch

Seasonal-to-Interannual Prediction

Michele Rienecker
GSFC Oceans and Ice Branch

Semi-LaGrangian GCM Development

Yong Li
GSFC Data Assimilation Office

Signatures at Magnetopause Reconnection

George Siscoe
Boston University

Simulation Studies

Robert Atlas
GSFC Data Assimilation Office

Solar Activity

Gordon Holman
GSFC Solar Physics Branch

Solar System and Milankovitch Cycles

David Rubincam
GSFC Geodynamics Branch

Space and Solar Plasmas Simulations

Ken-Ichi Nishikawa
Rutgers University

Stratosphere Analysis Production

Richard Rood
GSFC Data Assimilation Office

Stratospheric Analysis Research

Richard Rood
GSFC Data Assimilation Office

Structural Chemistry

Jerome Karle
Naval Research Laboratory

TOGA/COARE Atmospheric Circulation

Winston Chao
GSFC Climate and Radiation Branch

TOPEX Software Development and Operations

Benjamin Chao
GSFC Space Geodesy Branch

TRMM Rain Climatology, Errors and Models

Thomas Bell
GSFC Climate and Radiation Branch

Time Variable Gravity

Frank Lemoine
GSFC Space Geodesy Branch

Tropical Climate Variability

William Lau
GSFC Climate and Radiation Branch

Tropical Cyclone Rainfall

Edward Rodgers
GSFC Mesoscale Atmospheric Processes Branch

Tropical Ocean Circulation

Antonio Busalacchi
GSFC Laboratory for Hydrospheric Processes

Tropical Rainfall and Climate

William Lau
GSFC Climate and Radiation Branch

Tropospheric Chemistry Aerosol Model

Mian Chin
GSFC Atmospheric Chemistry and Dynamics
Branch

**Tropospheric Convection and Stratosphere-
Troposphere Exchange**

Kenneth Pickering
GSFC Atmospheric Chemistry and Dynamics
Branch

Tropospheric Photochemistry

Anne Thompson
GSFC Atmospheric Chemistry and Dynamics
Branch

Type III Solar Radio Bursts in the Corona

Iver Cairns
University of Sydney

UIT Data Reduction Pipeline

Theodore Stecher
GSFC UV Optical Astronomy Branch

U.S. Coastal Carbon Flux Study

John Moisan
GSFC Observational Science Branch

**Using NASA Full Physics Adjoint of the
GEOS-1 GCM for Retrospective Analysis**

Ionel Navon
Florida State University

Venus Gravity Modeling

Frank Lemoine
GSFC Space Geodesy Branch

Version 1 Research and Development

Arlindo da Silva
GSFC Data Assimilation Office

**Version 2 Research and Development (Global
OI)**

Arlindo da Silva
GSFC Data Assimilation Office

Voyager Magnetometer Data

Mario Acuña
GSFC Planetary Magnetospheres Branch

Voyager Neptune Atmosphere Composition

William Maguire
GSFC Planetary Systems Branch

Voyager Plasma Data Analysis

Keith Ogilvie
GSFC Laboratory for Extraterrestrial Physics

Water Vapor and Cloud Feedback

Albert Arking
Johns Hopkins University

X-Ray Data Analysis

Teresa Sheets
GSFC Data Management and Programming
Office

X-Ray Study of 1E1740

Joseph Dolan
GSFC UV Optical Astronomy Branch

Acronym List

ACE	Advanced Composition Explorer
AERONET	Aerosol Robotic Network
AGCM	atmospheric general circulation model
AOT	aerosol optical thickness
ASTG	Advanced Software Technology Group
AVHRR	Advanced Very High Resolution Radiometer
BC	black carbon
ccNUMA	cache-coherent Non Uniform Memory Access
CME	coronal mass ejection
COADS	Comprehensive Ocean Atmosphere Data Set
CUC	Computer Users Committee
CZCS	Coastal Zone Color Scanner
DAO	Data Assimilation Office
ECMWF	European Centre for Medium-Range Weather Forecasts
EDGAR	Emission Database for Global Atmospheric Research
ENSO	El Niño-Southern Oscillation
ESSIC	Earth System Science Interdisciplinary Center
FLOPS	floating-point operations per second
GB	gigabyte
GCM	general circulation model
GEOS	Goddard Earth Observing System
GMM-2B	Goddard Mars Model 2B
GOCART	Global Ozone Chemistry Aerosol Radiation and Transport
GOES	Geostationary Operational Environmental Satellite
IMAGE	Imager for Magnetopause-to-Aurora Global Exploration
IRD	Institute for Research and Development
ISAS	Institute of Space and Astronautical Sciences
ISTP	International Solar Terrestrial Physics project
ITCZ	intertropical convergence zone
JCE	Joint Center for Earth Systems Technology
LANL	Los Alamos National Laboratory
LEGOS	Laboratory for the Space-Based Study of Geophysics and Oceanography

mb	millibar
MEOF	multivariate empirical orthogonal function
MGal	milli-Galileo
MGS	Mars Global Surveyor
MHD	magnetohydrodynamics
NASA	National Aeronautics and Space Administration
NCAR	National Center for Atmospheric Research
NCCS	NASA Center for Computational Sciences
NCEP	National Centers for Environmental Prediction
nm	nanometer
NOAA	National Oceanic and Atmospheric Administration
NSIPP-1	NASA's Seasonal-to-Interannual Prediction Project
OC	organic carbon
OGCM	ocean general circulation model
PMEL	Pacific Marine Environmental Laboratory
SeaWiFS	Sea-Viewing Wide Field-of-View Sensor
SI	seasonal-to-interannual
SOHO	Solar and Heliospheric Observatory
SSH	sea surface height
SSM/I	Special Sensor Microwave/Imager
SST	sea surface temperature
STK	StorageTek
TAG	Technical Assistance Group
TAO	Tropical Atmosphere Ocean
TB	terabyte
TIROS	Television and Infrared Observation Satellite
TOGA	Tropical Ocean Global Atmosphere
TOMS	Total Ozone Mapping Spectrometer
TOPEX	Ocean Topography Experiment
WWW	World Wide Web

Acknowledgments

Planning and production

Michael Mendoza
Audrey Hopkins

Carole Long
Lara Clemence

Management

Carol Boquist

Richard Glassbrook

Special thanks

David Adamec
Joseph Ardizzone
Michael Behrenfeld
Christopher Bock
Timothy Burch
Anthony Busalacchi
Winston Chao
Mian Chin
Harold Domchick
Gene Feldman
Michael Fox-Rabinovitz
Watson Gregg
Eric Hackert
Sirpa Häkkinen

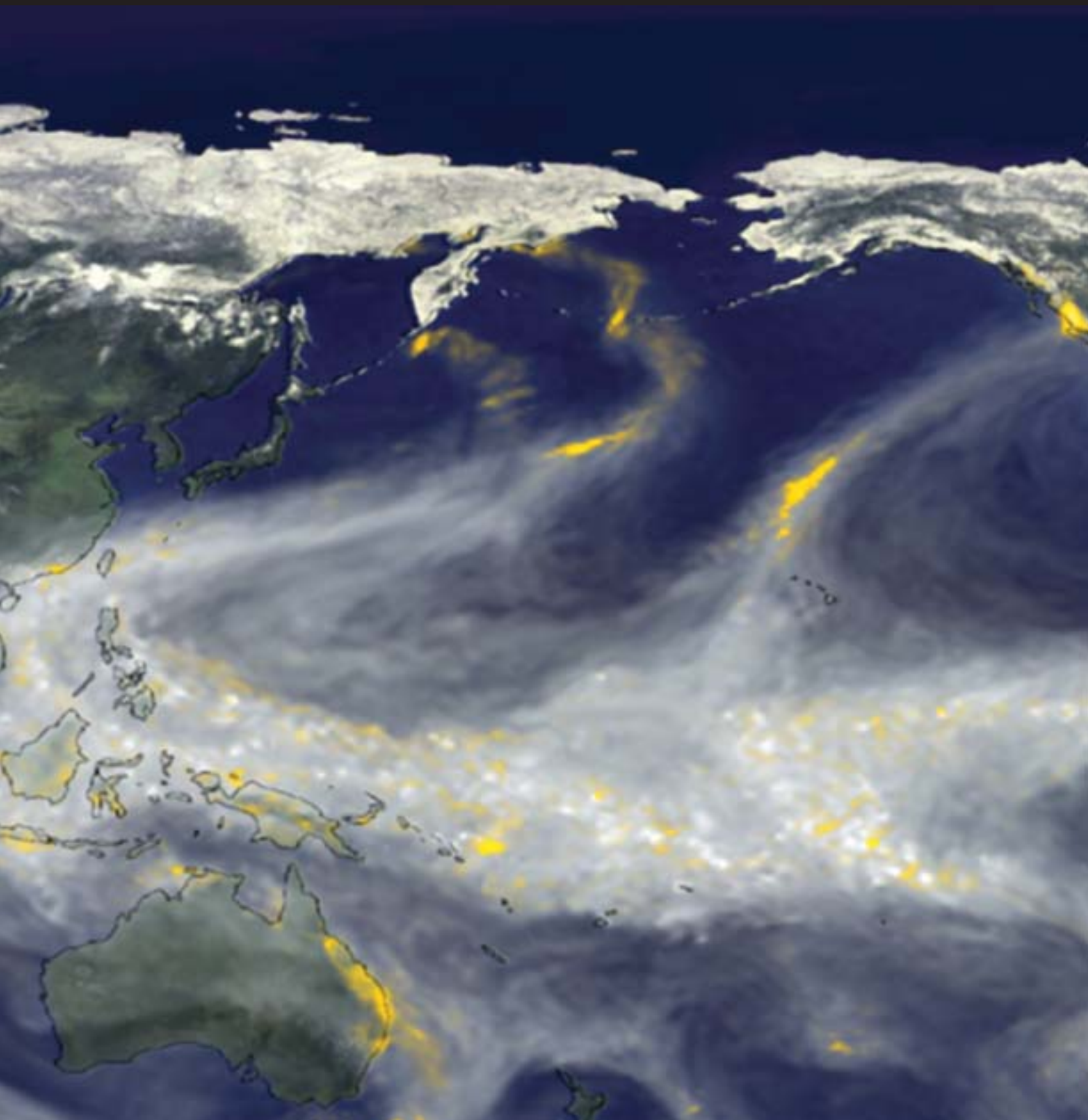
Carol Ladd
Judy Laue
Frank Lemoine
Bernard Matkowsky
Kevin McMahon
Sherri Panciera
Phil Pegion
Michele Rienecker
Aaron Roberts
Siegfried Schubert
Fred Shaffer
Gregory Shirah
Janis Thomas
The personnel of the NCCS

Additional image credits

IBM 7090, page 3, *IBM Archive*
IBM 360 console, page 5, *IBM Archive*
Images, pages 14, 46, 56, 66, 72, and 77,
Copyright © 1996 PhotoDisc
Image, page 18, *Corbis*

To Contact Us

If you would like more information about the NCCS or
would like to obtain a copy of this document, please



National Aeronautics and
Space Administration

Goddard Space Flight Center
Greenbelt, Maryland

NP-2002-8-491-GSFC